PhD Thesis

Linear and Nonlinear Aspects of Interactive Boundary Layer Transition

Deborah Jane Savin[1]
Department of Mathematics
University College London
Gower Street
London WC1E 6BT

1996

[1]Supported by a grant from EPSRC

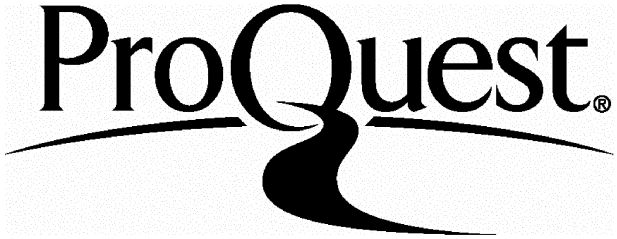

Abstract

Linear and nonlinear investigations into the early stages of transition to turbulence within interactive boundary layer flows are described. The behaviour of linear disturbances downstream of the point of breakaway separation of a high Reynolds number boundary layer away from a smooth wall is investigated first, emphasis being placed on the structure and scales at each stage of the investigation. Neutral eigensolutions of the Rayleigh equation are considered and the wavenumber obtained to leading order. A critical distance downstream of separation is found at which the disturbance characteristics alter rapidly. Moving upstream, next, Rayleigh instability which can occur within locally separating two- and three-dimensional triple-deck boundary layer flows is considered, demonstrating that the existence, locally, of a point of inflection is not a sufficient condition for such instability to occur. Finally, nonlinear vortex/Rayleigh-wave interactions are studied for small wavenumbers and a new wave-pressure amplitude (integro-differential) equation is obtained which further generalizes the application of vortex/wave interactions in interactive boundary layer flows. The inclusion of temporal effects at the onset of inflectional instability leads to a new initial-value problem for weakly nonlinear input holding there. To conclude, nonlinear forced vortex/wave interaction solution properties are discussed and numerical solutions of the corresponding receptivity problem are presented.

Contents

List of Figures

Chapter 1

Introduction

1.1 Classical boundary layer theory

The foundations of classical boundary layer theory were laid by Prandtl (1904) who addressed the flow of a fluid with small viscosity past a solid surface. In his paper on this subject, presented in 1904 at the Third International Congress of Mathematicians, Prandtl postulates the existence, between the main body of the flow and the solid surface, of a relatively thin viscous layer, the motion of which is regulated by the pressure gradient in the inviscid mainstream flow. Within this *boundary layer* the velocity increases smoothly but steeply from zero at the solid surface to the inviscid slip-velocity at the edge of the layer.

The physical problem resulting from these postulates gave rise to one of the original, and now classical, solutions of boundary layer theory, the Blasius (1908) similarity solution. Here Blasius shows that the attached flow strategy can work in the case of an aligned flat plate immersed in a uniform stream.

The continuation of the Blasius solution into the wake behind the aligned flat plate was verified by Goldstein (1930) who showed that the viscous wake solution has a two-tiered structure just downstream of the trailing edge. Although Goldstein (1948)

went on to demonstrate the existence of the separation singularity, a realization which heralded the collapse of the attached flow strategy, it was his two-tiered structure which, in part, motivated the search for an alternative strategy which would produce regular separation.

The attached flow strategy of classical boundary layer theory is thus based on the following main assumptions:

1. The viscous effects are confined mainly to a thin boundary layer lying close to the solid surface of a body and to a thin viscous wake.

2. The mainstream flow is supposed unaffected by the presence of the boundary layer and the boundary layer solution is constructed to correspond with the undisturbed mainstream, in particular the pressure at any point in the boundary layer is that of the mainstream at the same section.

Experience suggests that for most thick bodies these assumptions are unrealistic and that separation occurs, the boundary layer breaking away from the solid surface and forming a shear-layer downstream significantly detached from the body.

At the onset of separation, accurate numerical solutions (Brown and Stewartson (1969)) of the boundary layer problem for flows with prescribed pressure gradients generally indicate the occurrence of the Goldstein (1948) separation singularity at the point of zero skin friction. This separation singularity, when encountered, cannot be sensibly removed using a shorter-scale analysis, as is shown by Stewartson (1970). Thus, with the exception of a few notable cases of which Blasius (1908) is one, the classical scheme described above never works.

What is needed therefore, is an extension of classical boundary layer theory which produces regular separation by incorporating into its scheme the interaction between the mainstream pressure gradient and the separating boundary layer. Such a theory emerged in the late sixties and early seventies, see Stewartson and Williams (1969),

Neiland (1969), Messiter (1970), and predicts a *triple-deck* structure which holds on a shorter lengthscale $O(Re^{-3/8})$ in the neighbourhood of the point of separation and is described in §1.2. See, for example, the reviews by Smith (1982) and (1986a), and the subsequent demonstration of its application to instability theory, Smith (1979a,b).

We note here that there are two types of separation which can occur in boundary layer flows. The first is *breakaway separation (or free separation)* which is observed in flow past a bluff body. The second type may be described as local separation and occurs in flows past small humps, corners, injection slots, trailing edges, etc. The two types of separation are related, e.g. by the triple-deck structure (as described below), and are interactive with relative pressure unknown, hence avoiding the Goldstein singularity.

1.2 The triple-deck structure

On a lengthscale $O(Re^{-3/8})$ about the point of separation the adverse pressure gradient induced by the flow outside the boundary layer drives a reversed flow in a sublayer, or lower deck, close to the solid surface and of thickness $O(Re^{-5/8})$. This causes a shear layer, or main deck, of thickness $O(Re^{-1/2})$ to be pushed out into the mainstream flow, which in turn modifies the adverse pressure gradient. A third region, or upper deck, is needed, but in the potential flow outside the boundary layer, to relate the induced pressure to the local displacement. Because potential flow is expected in this third region its thickness is comparable with its streamwise lengthscale $O(Re^{-3/8})$.

The viscous-inviscid triple-deck form is controlled mainly by the lower deck equations, which in scaled terms are

$$\frac{\partial U}{\partial X} + \frac{\partial V}{\partial Y} = 0, \tag{1.1}$$

$$U\frac{\partial U}{\partial X} + V\frac{\partial U}{\partial Y} = -P'(X) + \frac{\partial^2 U}{\partial Y^2}, \tag{1.2}$$

with

$$\begin{aligned} U = V = O \quad &\text{at} \quad Y = 0, \\ U \sim Y + A(X) \quad &\text{as} \quad Y \to \infty, \\ (U, V, P', A') \to (Y, 0, 0, 0) \quad &\text{as} \quad X \to -\infty. \end{aligned}$$

The unknown displacement increment $-A(X)$ is linked to the unknown induced pressure P by Ackeret's law

$$P(X) = -A'(X)$$

in the case of *supersonic* motion, and by the Cauchy-Hilbert integral

$$P(X) = \frac{1}{\pi} \int_{-\infty}^{\infty} \frac{dA}{d\xi}(\xi) \frac{d\xi}{(x - \xi)}$$

in the case of *subsonic* motion.

However, triple-deck flows are observed to be often unstable in practice, see again Smith (1979a,b), and yield transition to turbulence; see following sections. It is this observation which forms part of the motivation for the following study.

In overall terms this thesis is concerned with separating or near-separating two-dimensional basic flows, although the three-dimensional basic flow is touched upon in Chapter 4.

1.3 Hydrodynamic stability

For over a century hydrodynamic stability has been recognized as one of the fundamental problems within the field of fluid mechanics, rightly so in view of its practical

importance with regard to engineering, meteorology and oceanography, and astrophysics and geophysics. It is concerned with when and how laminar flows break down, their subsequent development and their eventual transition to turbulent flow.

Few authors on this subject have been able to introduce the concept of hydrodynamic stability without seeking the assistance of Reynolds (1883) and his own description of his classic series of experiments on the instability of flow in a pipe.

> The ... experiments were made on three tubes .... The diameters of these were nearly 1 inch, $\frac{1}{2}$ inch and $\frac{1}{4}$ inch. They were all ... fitted with trumpet mouthpieces, so that water might enter without disturbance. The water was drawn through the tubes out of a large glass tank, in which the tubes were immersed, arrangements being made so that a streak or streaks of highly coloured water entered the tubes with the clear water.
>
> The general results were as follows:-
>
> 1. When the velocities were sufficiently low, the streaks of colour extended in a beautiful straight line through the tube.
> 2. If the water in the tank had not quite settled to rest, at sufficiently low velocities, the streak would shift about the tube, but there was no appearance of sinuosity.
> 3. As the velocity was increased by small stages, at some point in the tube, always a considerable distance from the trumpet or intake, the colour band would all at once mix up with the surrounding water, and fill the rest of the tube with a mass of coloured water. Any increase in the velocity caused the point of break down to approach the trumpet, but with no velocities tried did it reach this. On viewing the tube by the light of an electric spark, the mass of colour resolved itself into a mass of more or less distinct curls, showing eddies.

Leading on from this, Reynolds showed that the laminar flow, as described in (1.) above, breaks down when Ur/ν (now known as the Reynolds number) exceeds a certain critical value; U being the maximum velocity of the water in the tube, r the radius of the tube, and ν the kinematic viscosity of water at the appropriate temperature.

However,

the critical velocity was very sensitive to disturbance in the water before entering the tubes .... This at once suggested the idea that the condition might be one of instability for disturbances of a certain magnitude and stability for smaller disturbances.

At the critical velocity

another phenomenon ... was the intermittent character of the disturbance. The disturbance would suddenly come on through a certain length of tube and pass away and then come on again, giving the appearance of flashes, and these flashes would often commence successively at one point in the pipe.

These 'flashes' are now known as *turbulent spots*, see for example Smith (1995). Below the critical Reynolds number the flow was of a laminar Poiseuille form with a parabolic velocity profile. As the velocity was increased above its critical value Reynolds found that the flow became turbulent with a chaotic motion that strongly diffused the dye throughout the water in the tube.

Reynolds' description illustrates the aims of the study of hydrodynamic stability: to determine whether or not a given laminar flow is unstable and, if it is, to investigate how it breaks down into turbulent or some other laminar flow.

Since the subject of hydrodynamic stability is hugely varied in its application, and in the light of the work contained within this thesis, we restrict ourselves hereinafter to the subject of boundary layer stability and the subsequent transition to turbulence.

1.4 Boundary layer stability and transition to turbulence

Boundary layer stability and transition to turbulence are a major concern to experimentalists and theoreticians alike. On the experimental side see, for example,

Schubauer and Skramstad (1947), and the much later work of Dovgal *et al* (1986). On the theoretical side the processes of transition form three mathematically distinct levels or stages, namely linear disturbance theory, weakly nonlinear theory, and finally strongly nonlinear theory.

As is described in more detail in Chapter 2, the classical linear disturbance theory can be formulated by superimposing a disturbance on a given steady-state solution of the Navier-Stokes equations, resulting in the nonlinear Orr-Sommerfeld system of equations which governs the disturbance behaviour. Linearizing these equations for small disturbances, homogeneous equations are obtained which, when coupled with appropriate homogeneous boundary conditions, produce an eigenvalue problem for the growth-rate parameter and hence determine the effect, stabilizing or destabilizing, which the disturbance has on the basic flow.

Weakly nonlinear theory is usually based on the assumption that wave-like neutral solutions of the nonlinear Orr-Sommerfeld equations exist at leading order, see for example the work of Stuart and Watson (1960), Stewartson and Stuart (1971). In contrast, strongly nonlinear theory assumes that the mean flow is completely altered by the presence of the disturbance. There are three main strongly nonlinear theories for flat plate boundary layer-like flows at large Reynolds numbers, namely vortex/wave interaction theory, discussed below in detail, pressure-displacement interactive boundary layer theory, and high-frequency cum Euler-scale theory, corresponding basically to increasing amplitudes in turn, see Smith (1995). Alternatively, direct nonlinear simulations can be carried out at finite values of the Reynolds number Re, although such computations struggle at large Re due to resolution difficulties.

By way of an example, and in reference to Chapter 6, we note here that the condition

$$\int_0^\infty \frac{1}{(U_0 - c_0)^2} d\bar{y} = 0, \tag{1.3}$$

is a direct result of strongly nonlinear stability theory and is in accordance with Smith (1988), agreeing with experiments as shown in Smith and Bowles (1992).

Since the development of triple-deck theory (see §1.2) over two decades ago, interactive descriptions of boundary layer flows have become a valuable tool in obtaining a greater theoretical understanding of both the transition process and, it is hoped, ultimately a systematic account of turbulent flow and turbulence modeling.

Among those more widely used in the study of transition and turbulence in both incompressible and compressible boundary layers are, for example, viscous/inviscid, two-/three-dimensional, small-/large-scale, and vortex/wave interactions, see Smith (1993) for a detailed account of current research employing these interactions.

Our concern within the latter chapters of this thesis is with nonlinear vortex/wave interactions initiated within an interactive boundary layer, following on from a string of papers on vortex/wave interactions by Hall and Smith (1988, 1989, 1990, 1991), Brown *et al* (1993), Smith *et al* (1993) and more recently Timoshin and Smith (1995), Brown and Smith (1995); much of Chapters 5 and 6 is based upon Smith *et al* (1993). A separate and approximately simultaneous string of papers is by Benney and Chow (1989), Goldstein and Choi (1989), Wu (1993), Wu *et al* (1993) and Khokhlov (1994), including non-equilibrium critical layers which have an extra effect (time-dependence) acting in the critical layer but miss the nonparallel flow effect that is present in Smith *et al* (1993) [later referred to as SBB].

We now present a brief summary of vortex/wave interactions, what appears to be a promising candidate in providing an increased rational understanding of the early stages of transition to turbulence in boundary layers, or pipe or channel flows.

1.5 Vortex/wave interactions

Vortex/wave interactions arise in various forms, principally with either viscous-inviscid Tollmien-Schlichting waves or inviscid, inflectional Rayleigh-waves; see again Hall and Smith (1991), Brown *et al* (1993), Smith *et al* (1993). A feature common to all such interactions is that at high Reynolds numbers three-dimensional waves are coupled nonlinearly with the mean flow via its unknown longitudinal vortex component.

This coupling is termed weakly nonlinear if the vortex part is a small-amplitude perturbation of the mean flow. On the other hand, the coupling is strongly nonlinear if the mean flow comprises entirely the vortex contribution, as in the flow considered in the latter chapters of this thesis.

The work of Hall and Smith (1988, 1989, 1990, 1991) in particular highlights the ability of vortex/wave interactions to provoke strongly nonlinear effects even for extremely small three-dimensional input disturbances.

It has been noted in Brown and Smith (1995) that an obvious reason for the theoretical focus on vortex/wave interactions is the qualitative and quantitative links with experiments on transition described by Hall and Smith (1991), Walton and Smith (1992), Stewart and Smith (1992) and Smith and Bowles (1992) for a variety of input conditions. It is also noted that observations of the significant role of longitudinal vortices in the early stages of some transition paths are given experimentally by Klebanoff and Tidstrom (1959), Nishioka *et al* (1979) and others.

1.6 Description of subsequent chapters

Throughout this thesis the flows considered are of large Reynolds number, a range of much practical concern in aerodynamics, atmospheric dynamics, and internal engine dynamics. In Chapter 2 the growth of linear disturbances in a high Reynolds

number interactive boundary layer flow is investigated downstream of the point at which the boundary layer itself separates away from the wall. Initially the point of interest is sufficiently far downstream that we can ignore the presence of the wall, thus assuming the extent of the flow is infinite both above and below the separating boundary layer. In steps we move our point of interest upstream, always remaining outside the interactive triple-deck region, introducing the effects of the wall via appropriate boundary conditions. At each step the disturbances within the boundary layer are governed by the Rayleigh equation and we emphasize the structures and scales involved which, together with the solution obtained, determine the structures and scales of subsequent steps. Neutral eigensolutions are considered and the value of the wavenumber obtained to leading order. A critical distance downstream of separation is found at which the disturbance characteristics alter rapidly.

Continuing on from the work of Chapter 2, in Chapter 3 we consider the linear stability of the basic flow to long-wave inviscid perturbations. Here we also demonstrate, by comparison, the value of modeling the basic velocity profile using a piecewise-linear approximation which possesses some of the main features of the basic flow.

Chapter 4 provides a possible link between the linear studies of Chapters 2–3 and the nonlinear work to follow in Chapters 5–7. Here we are concerned with the Rayleigh instabilities which occur in separating two- and three-dimensional boundary layer flows as a result of inflectional velocity profiles produced locally, for example, flows past humps, corners, injection slots, trailing edges etc. Experimental studies of flow transition over various isolated or distributed roughnesses on solid surfaces are given in Acarlar and Smith (1987) and references therein, while computational studies include Mason and Morton (1987) and other works.

Smith and Bodonyi (1985) show, by means of an exact solution of the two-dimensional Rayleigh equation, that an order-one hump height h is required if inflectional instability, or its onset, is to occur, and therefore deduce that the existence of an

inflectional point in the local velocity profile is a necessary but not sufficient condition for Rayleigh instability. Based on this paper, we show that as the boundary layer undergoes increased separation, i.e. the inflectional point moves upwards in the positive y-direction, a cut-off point exists at which the flow ceases to be unstable. Moreover, this point occurs prior to the point at which the inflection point itself leaves the lower deck, re-iterating the findings of Smith and Bodonyi (1985).

A detailed description of the work of Smith *et al* (1993) [SBB] is presented in Chapter 5 in which the starting process of strongly nonlinear vortex/Rayleigh-wave interactions in a boundary layer is considered on a shorter lengthscale than that of Hall and Smith (1991), Brown *et al* (1993). On this new shorter lengthscale the abrupt starting of the interaction is smoothed out and the wave-pressure amplitude no longer satisfies the bifurcation equation of the previous works, now replaced by an integro-differential equation. Here, however, we restrict ourselves to a boundary layer of interactive triple-deck form, the scales involved proving significant in later chapters.

In the latter sections of this chapter, and in preparation for the following chapter, we introduce the additional influence of a slow time derivative ∂_{t_1} accompanying the slow spatial derivative ∂_{x_1}.

The starting point for Chapter 6 is the integro-differential equation obtained in SBB, and derived again in the previous chapter, in which the wavenumbers α and β are taken to be $O(1)$. Here we let $\alpha, \beta \to 0$ and consider the solution in the core region of the flow, deducing that

$$\gamma = 2 \int_0^\infty f(\bar{y}) \mathrm{I}(\bar{y}) d\bar{y}, \tag{1.4}$$

where

$$\gamma^2 = \alpha^2 + \beta^2,$$
$$f(\bar{y}) = \frac{d}{d\bar{y}}\left\{\frac{(U_1 - c_1)}{(U_0 - c_0)}\right\},$$
$$\mathrm{I}(\bar{y}) = \int_{\infty}^{\bar{y}} (U_0 - c_0)^{-2} d\bar{y}.$$

Given the wave speed and the basic velocity profile we may conclude that (1.4) fixes the value of γ at leading order before the wave-pressure amplitude (integro-differential) equation can come into play at second order. Fixing γ in turn fixes the input frequency Ω, thus restricting the range of frequencies to which the vortex/wave interaction theory of SBB applies.

By considering certain physical characteristics of the flow we set up an entirely new regime in which $\alpha = O(Re^{-1/12})$ and the streamwise lengthscale is shortened still further. The wave-pressure amplitude equation thus obtained comprises the integro-differential equation of Chapter 5 and (1.4), now acting together at leading order. This new equation holds for arbitrary input frequencies Ω, further generalizing the application of vortex/Rayleigh-wave interactions in interactive boundary layer flows. Alternative regimes are briefly discussed, highlighting their physical importance and mathematical consequences.

To conclude this chapter we formally generalize the fixed frequency approach adopted up until now in this work by interpreting the results in terms of a new spatio-temporal form. This theory has the makings of an initial-value problem for weakly nonlinear input in general at the onset of inflectional instability in boundary layer-like flows. Previous initial-value problems are found in Stewartson and Stuart (1971) (near the nose of the neutral curve at the critical Re) and in Smith (1986b) (at relatively high frequencies and large Re). However in both examples the problem is for slowly-varying wave packets, a big assumption to make in comparison with the work contained herein, which certainly works well in the linear case and for streamwise-periodic inputs.

Work is in progress with Professor F T Smith to investigate in more detail the impact of the initial-value problem on weakly nonlinear theory.

Chapter 7 presents numerical solutions of the integro-differential equation when the effects of forcing are taken into account, corresponding to a nonlinear receptivity problem. Comparisons are made with the numerical solutions of SBB, the case of no added forcing, to establish the effects of the forcing downstream of its point of application.

The main novel contributions of this thesis are perhaps threefold, namely:

1. The account in Chapters 2–3 of the behaviour of neutral wavenumbers in the separating boundary layer flow downstream as it detaches from the wall.

2. The inclusion of temporal effects in the nonlinear vortex/wave interactions at the onset of inflectional instability, leading to the new initial-value problem there (Chapters 5–6).

3. The nonlinear forced vortex/wave interaction solution properties of Chapter 7.

We note finally the existence of slightly related work by Vickers and Smith (1994) on two-dimensional nonlinear unsteady effects just downstream of breakaway separation. Here we cover a wider range of distances downstream, both shorter and longer, and connect both breakaway separation and local separation, finding that their transitions may be somewhat related too.

Chapter 2

Linear stability of a two-dimensional separating interactive boundary layer

2.1 Introduction

Because of the mathematical simplifications associated with linearization and the fact that linearized theory is able to provide the critical conditions for the occurrence of instability for infinitesimal disturbances, stability theory has largely been developed with this restriction. However, in recent years the role of nonlinearity in flow instability has received increasing study, see for example the work of Stewartson and Stuart (1971), Smith (1979b) and Hall and Smith (1991), consideration of which is the eventual aim with regard to the present thesis. Thus, the present work considers linear properties first, followed by certain nonlinear aspects in the later chapters.

The mathematical problem of hydrodynamic stability can be formulated by taking the given steady-state solution to the Navier-Stokes equations and superimposing a

disturbance of a suitable kind. The result is a set of nonlinear 'disturbance' equations governing the behaviour of the disturbance. If the disturbance ultimately decays to zero the flow is said to be stable. On the other hand, if the resulting disturbance is permanently nonzero the flow is said to have become unstable. On linearizing these equations for small disturbances homogeneous equations are obtained, allowing disturbances which contain an exponential time factor of the form e^{qt} to be considered, t denoting time. Along with homogeneous boundary conditions the result is an eigenvalue problem for the determination of q, the growth-rate parameter that indicates the effect, stabilizing or de-stabilizing, which the superimposed disturbance has on the basic flow.

In this chapter the growth of linear disturbances in a high Reynolds number interactive boundary layer flow is investigated, the flow being considered beyond the point at which the boundary layer separates away from a smooth wall. The disturbances within the boundary layer respond according to the Rayleigh equation, considered here for neutral-wave solutions, and in each case the structure and scales of the instability are presented. In considering the neutral-wave solution three regimes are examined. Initially the flow is examined far downstream of the point of separation where the effects of the wall are assumed negligible, the flow being taken to be infinite both above and below the separated boundary layer. Moving back towards the point of separation, a second regime is considered in which the presence of the wall becomes important. It is the results obtained here which lead the investigation into the final regime, just beyond the point at which separation occurs, where the typical y-scaling of the small disturbance is seen to increase.

The high Reynolds number flow under investigation is that of an incompressible fluid past a smooth wall just beyond the point at which breakaway separation occurs. Here the boundary layer progressing downstream undergoes a gradually increased shift away from the wall. The actual process of separation is governed by the triple-deck equations as described in §1.2. In what follows "just beyond the point of

separation" should be taken to mean just outside the $O(Re^{-3/8})$ triple-deck region.

The strategy adopted here is similar to that of Papageorgiou and Smith (1989) in which two-dimensional stability theory is applied to a wake formed just downstream of a flat plate. In §2.2 below the linear stability problem is formulated. In §2.3 the structure and scales are described and the Goldstein-type velocity profiles, which hold beyond the triple-deck region, are given. Neutral-wave solutions are found in §2.4 for each of the regimes outlined above and the changes in the disturbance structure and scales of the flow are set out accordingly. By way of a check, §2.5 presents and compares the results of a numerical calculation carried out in support of the analysis obtained in the third and final regime of §2.4. In §2.6 the neutral curve is presented in full and concluding remarks then follow.

Throughout this chapter in nondimensional terms the origin of the Cartesian coordinates is fixed at the point of separation x_0, with x, y the streamwise and transverse coordinates respectively. In addition u, v, p are the velocities in the x-direction, the y-direction and the pressure respectively, and ψ denotes the streamfunction for the two-dimensional flow.

2.2 Formulation of the linear stability problem

Beyond the point of separation the boundary layer experiences a gradual shift away from the smooth wall. The thickness of the boundary layer remains of order $Re^{-1/2}$ and the motion is governed downstream by the two-dimensional boundary layer equations.

Small unsteady perturbations in the flow quantities are supposed to be introduced just beyond the point of separation x_0 but still outside the triple-deck region, i.e. where $x - x_0 \gg Re^{-3/8}$. The disturbances which result are expected to evolve inviscidly and therefore their x and y scales are equal. From a physical point of view it is reasonable to first study fluctuations inside the separated boundary layer

and thus the prime scales are $x \sim y \sim Re^{-1/2}$. The two-dimensional unsteady Navier-Stokes equations form the basis of the problem and the basic flow at a fixed x-station is two-dimensional and quasi-parallel, written as $(\bar{u}(y), 0)$ to leading order. Linearization about the basic state reduces these equations to

$$\begin{aligned}
\frac{\partial u}{\partial t} + \bar{u}\frac{\partial u}{\partial x} + v\frac{d\bar{u}}{dy} &= -\frac{\partial p}{\partial x} + \frac{1}{Re}\left(\frac{\partial^2 u}{\partial x^2} + \frac{\partial^2 u}{\partial y^2}\right), \\
\frac{\partial v}{\partial t} + \bar{u}\frac{\partial v}{\partial x} &= -\frac{\partial p}{\partial y} + \frac{1}{Re}\left(\frac{\partial^2 v}{\partial x^2} + \frac{\partial^2 v}{\partial y^2}\right), \\
\frac{\partial u}{\partial x} + \frac{\partial v}{\partial y} &= 0.
\end{aligned}$$

However, assuming that the Reynolds number is asymptotically large the effects of viscosity are neglected and the Navier-Stokes equations become

$$\begin{aligned}
\frac{\partial u}{\partial t} + \bar{u}\frac{\partial u}{\partial x} + v\frac{d\bar{u}}{dy} &= -\frac{\partial p}{\partial x}, \\
\frac{\partial v}{\partial t} + \bar{u}\frac{\partial v}{\partial x} &= -\frac{\partial p}{\partial y}, \\
\frac{\partial u}{\partial x} + \frac{\partial v}{\partial y} &= 0
\end{aligned} \tag{2.1}$$

in the classical Rayleigh fashion (e.g. see Stuart (1963)).

It is convenient to define

$$u = \frac{\partial \phi}{\partial y}, \quad v = -\alpha\phi,$$

where the streamfunction ψ is given by $\psi(x, y, t) = \phi(y)\exp[i\alpha(x - ct)]$. The quantity α is real and is the wavenumber of the disturbance in the x-direction. On the other hand, c is complex; the real part, namely c_r, is the wave velocity and the imaginary part, namely c_i, represents the amplification or damping of the oscillation with time. If c_i is positive the disturbance amplifies and becomes unstable, while if it is negative the disturbance decays and is stable. The situation of neutral stability is governed by $c_i = 0$.

Substitution of the streamfunction into the scaled, linearized and inviscid Navier-Stokes equations (2.1) above yields the classical Rayleigh stability equation

$$(\bar{u} - c)(\phi'' - \alpha^2\phi) = \bar{u}''\phi,$$

with ϕ required to vanish at the wall and as $y \to \infty$ in the freestream.

An extremely important result obtained by Rayleigh (1880) is that a necessary condition for instability in an inviscid fluid is that the velocity profile $\bar{u}$ should contain a point of inflection. Tollmien (1935) has since shown that for symmetrical velocity profiles in a channel, and boundary layer velocity profiles, the condition $\bar{u}'' = 0$ is also a sufficient condition for instability. In some other contexts however it is not sufficient: see Chapter 4.

2.3 Structures and scales

In considering the possibility of neutral eigensolutions just beyond the point of separation x_0 the basic velocity profile must be examined more closely and its points of inflection found. If the given profile $\bar{u}$ has an inflection point at $y = y_s$ say, then for symmetrical profiles in a channel and boundary layer profiles there is a band of wavelengths α ($< \alpha_s$) for which $c_i > 0$, giving instability, and this band is bounded by the neutral state

$$\phi_s = \phi(y_s), \quad \alpha = \alpha_s > 0, \quad c = \bar{u}(y_s) = c_s, \quad c_i = 0. \tag{2.2}$$

The profile used is that just beyond the triple-deck region of the separation and is described below.

For $y = O(1)$ $\bar{u} = \bar{u}(y)$, where

$$\bar{u} \sim \lambda y - \lambda_2 y^2 + \epsilon\gamma \left(\frac{y}{\epsilon}\right)^{-\frac{1}{4}} e^{-\frac{4}{9}(y/\epsilon)^3} + \ldots \tag{2.3}$$

as $y \to 0^+$ and $\bar{u} \sim 0$ for $y < 0$.

For $y = \epsilon z$, $z = O(1)$, $\bar{u} = \epsilon F(z)$, where the Goldstein-like function $F(z)$ is such that

$$F(z) \sim \lambda z + A_G + \frac{\gamma}{z^4} e^{-\frac{\lambda}{9} z^3} + ... \tag{2.4}$$

as $z \to \infty$ and $F(z) \to 0$ as $z \to -\infty$.

Here $\epsilon = (x - x_0)^{1/3}$, γ is a positive constant and A_G is a Goldstein displacement constant. We may locate the inflection point by combining (2.3) and (2.4) and balancing their second derivatives. This yields an inflection point at $y = \epsilon L + O(\epsilon)$ where $L^3 = -(9/\lambda)\log\epsilon$. From (2.2), combined with (2.3), we see that the neutral wave speed has the expansion

$$c = \epsilon L \lambda + \epsilon^2 L^2 \hat{c} + \ldots, \tag{2.5}$$

and a balance of terms in the Rayleigh equation leads to the following expansion for α;

$$\alpha = \frac{\alpha_0}{\epsilon L} + \alpha_1 + \epsilon L \alpha_2 + \ldots. \tag{2.6}$$

Solutions must be found in each of the regions shown in Figure 2.1 and matched with those of neighbouring regions.

2.4 Neutral-wave solutions

Initially in what follows we consider the problem set out in §2.3 for the case in which the presence of the wall is ignored, i.e. the flow is considered far enough downstream of the point of separation x_0 for the effect of the wall to become negligible. Thus the extent of the flow is assumed infinite both above and below the separating boundary layer and boundary conditions are applied accordingly.

With the same structure and scales as those used in the case above we may then proceed to readily consider the same problem, this time taking into account the

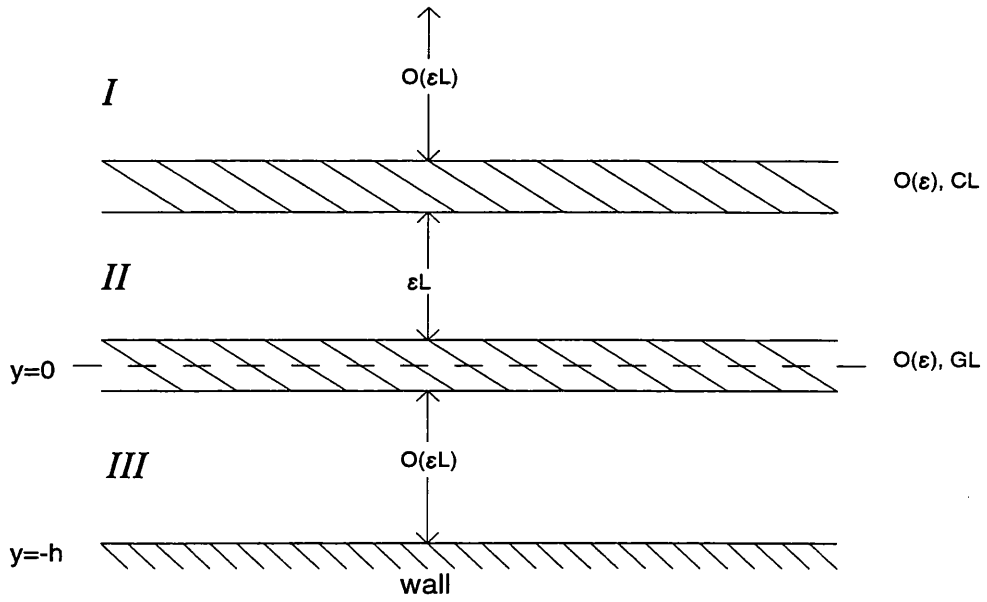

Figure 2.1: The various regions in which neutral waves develop. CL denotes the critical layer, GL the Goldstein layer.

presence of the wall. Thus, through the new boundary conditions, we introduce the separation distance h between the boundary layer and the wall. It is the results obtained for this case which lead us into the second and third regimes, moving our position of interest upstream towards the point of separation by reducing h gradually.

The aim of the work below is mostly to obtain the neutral curve for this particular separating boundary layer flow as a function of the separation distance (height) h. In each of the three regimes mentioned above we employ matched asymptotic expansions in the various regions of the flow, and in doing so obtain an expression for the wavenumber α to leading order.

2.4.1 Regime 1

Region I

We begin in region I in which $y = \epsilon L(1+Y)$, $0 < Y = O(1)$, and the expansions for $\bar{u}$ and ϕ are

$$\bar{u} = \epsilon L\lambda(1+Y) - \epsilon^2\lambda_2 L^2(1+Y)^2 + \epsilon\frac{\gamma}{L^4(1+Y)^4}E_I + \ldots, \tag{2.7}$$

$$\phi = \phi_0 + \epsilon L\phi_1 + \epsilon^2 L^2\phi_2 + \ldots, \tag{2.8}$$

where $E_I \equiv \exp[-(\lambda/9)L^3(1+Y)^3]$.

Substituting (2.5) – (2.8) into the Rayleigh equation and balancing successive powers of ϵL, we obtain the equations

$$\lambda Y(\phi_0'' - \alpha_0^2\phi_0) = 0, \tag{2.9}$$

$$\lambda Y(\phi_1'' - \alpha_0^2\phi_1 - 2\alpha_0\alpha_1\phi_0) = -2\lambda_2\phi_0, \tag{2.10}$$

subject to the boundary conditions $\phi_0 \to 0$ and $\phi_1 \to 0$ as $Y \to \infty$. It should be noted here that for (2.9) and (2.10) to hold true we require that $\epsilon^{-1}E_I L \overset{L}{=} \epsilon^{(1+Y)^3-1}$ be small compared with $\epsilon^{-1}L^{-1}$ and $\epsilon^{(1+Y)^3-1}$ be small compared with 1. Since $Y > 0$ in region I these requirements are met and therefore the first and second order terms in the expansion of ϕ have solutions

$$\phi_0 = A_0 e^{-\alpha_0 Y}, \tag{2.11}$$

$$\phi_1 = B_1 e^{-\alpha_0 Y} - \alpha_1 A_0 Y e^{-\alpha_0 Y} + \frac{\lambda_2 A_0}{\alpha_0\lambda}e^{-\alpha_0 Y}\log Y - \frac{\lambda_2 A_0}{\alpha_0\lambda}e^{\alpha_0 Y}\int_{\infty}^{Y} t^{-1}e^{-2\alpha_0 t}dt, \tag{2.12}$$

where A_0, B_1 are constants. In order to achieve our goal it is necessary only to obtain a solution for the first two terms in the expansion for ϕ in region I.

It can be shown that as $Y \to 0^+$

$$\phi_1 \sim D_0 + D_1 Y + D_2 Y\log Y + O(Y^2) \tag{2.13}$$

where D_0, D_1, D_2 are constants and $D_2 = -2\lambda_2 A_0/\lambda$.

We will use (2.13) to match the solution of region I with that of the critical layer, which we now proceed to obtain.

Critical layer

Here $y = \epsilon L + \epsilon z$ $(-\infty < z < \infty)$ and, since $Y = zL^{-1}$, the expansions for $\bar{u}$ and ϕ implied in the critical layer are

$$\bar{u} = \epsilon L\lambda + \epsilon\lambda z - \epsilon^2 L^2\lambda_2(1+zL^{-1})^2 + \epsilon L^{-4}\frac{\gamma}{(1+zL^{-1})^4}E_{CL} + \ldots, \quad (2.14)$$

$$\phi = \psi_0 + L^{-1}\psi_1 + L^{-2}\psi_2 + \ldots + \epsilon L\left\{\tilde{\psi}_0 + L^{-1}\tilde{\psi}_1 + \ldots\right\} + \ldots$$
$$+ L^{-4}\frac{\gamma}{(1+zL^{-1})^4}E_{CL}\left\{\hat{\psi}_0 + \ldots\right\} + \ldots, \quad (2.15)$$

where $E_{CL} \equiv \exp[-(\lambda/9)L^3(1+zL^{-1})^3]$.

Substituting expansions (2.5), (2.6), (2.14) and (2.15) into the Rayleigh equation we obtain the equations

$$\lambda z\psi_0'' = 0, \quad \lambda z\psi_1'' = 0, \quad \lambda z(\psi_2'' - \alpha_0^2\psi_0) = 0, \quad (2.16)$$

and

$$\lambda z\tilde{\psi}_0'' = 0, \quad \lambda z\tilde{\psi}_1'' = -2\lambda_2\psi_0. \quad (2.17)$$

The solutions of (2.16) consistent with those in region I are

$$\psi_0 = A_0, \quad \psi_1 = -\alpha_0 A_0 z, \quad \psi_2 = \tfrac{1}{2}\alpha_0^2 A_0 z^2.$$

In order to match with the solution in region I it follows from (2.17) that $\tilde{\psi}_0 = D_0$ while the equation for $\tilde{\psi}_1$ becomes

$$\tilde{\psi}_1'' = -\frac{2\lambda_2 A_0}{\lambda z}.$$

Again, on matching with the solution in region I we have

$$\tilde{\psi}_1 = -\frac{2\lambda_2 A_0}{\lambda}(z\log z - z) + b_1 z$$

where $b_1 = D_1 - 2\lambda_2 A_0/\lambda$. Finally the equation for $\hat{\psi}_0$ is obtained from a balance of terms $O(\epsilon^{-1}\gamma E_{CL})$ in the Rayleigh equation and is

$$\hat{\psi}_0 = \frac{A_0}{\lambda} z^{-1}.$$

Region II

Continuing into region II where $y = \epsilon L(1+Y)$, $-1 < Y < 0$, the effects of the exponential term in the basic velocity profile must be considered more closely. Here the expansions for $\bar{u}$ and ϕ are

$$\bar{u} = \epsilon L\lambda(1+Y) - \epsilon^2\lambda_2 L^2(1+Y)^2 + \epsilon\frac{\gamma}{L^4(1+Y)^4}E_{II} + \ldots, \tag{2.18}$$

$$\phi = \phi_0 + \epsilon L\phi_1 + \ldots + L^{-5}\frac{\gamma\epsilon^{(1+Y)^3}}{(1+Y)^4}\left\{\hat{\phi}_0 + L^{-1}\hat{\phi}_1 + \ldots\right\} + \ldots, \tag{2.19}$$

where $E_{II} \equiv \exp[-(\lambda/9)L^3(1+Y)^3]$.

In (2.19) ϕ_0 is given by (2.11) and ϕ_1 satisfies (2.10). We note here for future reference that at $O(\epsilon^{(1+Y)^3-1})$ the Rayleigh equation implies

$$\hat{\phi}_0 = \frac{A_0}{\lambda Y}e^{-\alpha_0 Y}$$

which matches with the contribution from $\hat{\psi}_0$ in the critical layer.

Goldstein layer

Moving into the Goldstein layer where $y = \epsilon z$, $z = O(1)$, and $\bar{u} = \epsilon F(z)$, ϕ has an expansion of the form

$$\phi = \Phi_0 + L^{-1}\Phi_1 + L^{-2}\Phi_2 + \ldots. \tag{2.20}$$

On substituting (2.5), (2.6) and (2.20) into the Rayleigh equation, along with the above expression for $\bar{u}$, we obtain

$$-\lambda\Phi_0'' = 0, \quad -\lambda\Phi_1'' = F''(z)\Phi_0. \tag{2.21}$$

In matching with region II it follows from (2.21) that $\Phi_0 = A_0 e^{\alpha_0}$ while the equation for Φ_1, along with its behaviour as $z \to \infty$, is

$$\Phi_1 = -\frac{A_0 e^{\alpha_0}}{\lambda} F(z) + a_0 z + b_0, \tag{2.22}$$

$$\Phi_1 \sim -\frac{A_0 e^{\alpha_0}}{\lambda}(\lambda z + A_G + \frac{\gamma}{z^4} e^{-\frac{\lambda}{9}z^3}) + a_0 z + b_0. \tag{2.23}$$

The exponential term in (2.23) matches with the contribution from $\hat{\phi}_0$ of region II as $Y \to -1^+$. As there is no constant term of order L^{-1} in the solution for ϕ obtained in region II, we may deduce that $b_0 = A_0 A_G \lambda^{-1} e^{\alpha_0}$. In order to determine the value of a_0, and hence α_0, it is necessary to match the solution across the Goldstein layer into region III.

Region III

In region III $y = \epsilon L Y$ for $Y < -1$ and the basic velocity profile $\bar{u}$ is approximated to zero. The expansion for ϕ is now

$$\phi = \phi_0 + L^{-1}\phi_{01} + \ldots + \epsilon L\{\phi_1 + \ldots\} + \ldots. \tag{2.24}$$

In (2.24) ϕ_0 satisfies (2.9) subject to the boundary condition that $\phi_0 \to 0$ as $Y \to -\infty$ and therefore $\phi_0 = \hat{A}_0 e^{\alpha_0 Y}$, where $\hat{A}_0$ is a constant to be determined. Similarly,

$$\phi_{01}'' - \alpha_0^2 \phi_{01} = 0 \tag{2.25}$$

and hence $\phi_{01} = \hat{A}_1 e^{\alpha_0 Y}$, where again $\hat{A}_1$ is a constant to be determined.

Matching into the Goldstein layer it follows that

$$\hat{A}_0 = A_0 e^{2\alpha_0}, \quad \hat{A}_1 = A_0 A_G \lambda^{-1} e^{2\alpha_0}, \quad a_0 = \alpha_0 A_0 e^{\alpha_0}. \tag{2.26}$$

Finally, matching the linear terms of order L^{-1} across the Goldstein layer, a value for α_0 is obtained, namely

$$\alpha_0 = \frac{1}{2}, \tag{2.27}$$

implying a neutral wave frequency $\omega = \alpha c = \frac{\lambda}{2} + O(\epsilon L)$. The results above indicate that when the the presence of the wall is ignored, typical wavelengths for neutral waves are $O(\epsilon L)$.

We must now introduce the effects of the wall on the flow as our position of interest x starts to move back upstream towards the point of separation, still remaining outside the triple-deck region. At this early stage these effects are seen only in region III in which the boundary condition to be satisfied by the streamfunction reduces to the requirement that $\phi = 0$ at $y = -h$. Matching similar to that above yields the result

$$\alpha_0 = 1 - \frac{\alpha_0}{\tanh \alpha_0 H} \tag{2.28}$$

where $h = \epsilon L H$. Notice that as $H \to \infty$, i.e. as the current position progresses downstream, (2.28) becomes $\alpha_0 \sim 1 - \alpha_0$ and so we regain the result (2.27) in which the value of H was effectively taken to be infinite.

With (2.28) as our starting point we now begin a closer examination of the separation distance H and its effects on the value of the resulting wavenumber α to leading order. If we let $H \to 0^+$ in such a way that $\alpha_0 H \to 0^+$ it follows that

$$\alpha_0 \sim 1 - H^{-1},$$

thus producing a critical value, $H_c \equiv 1$, of the separation distance H at which the wavenumber α vanishes to leading order. We proceed next by expanding H about its critical value H_c.

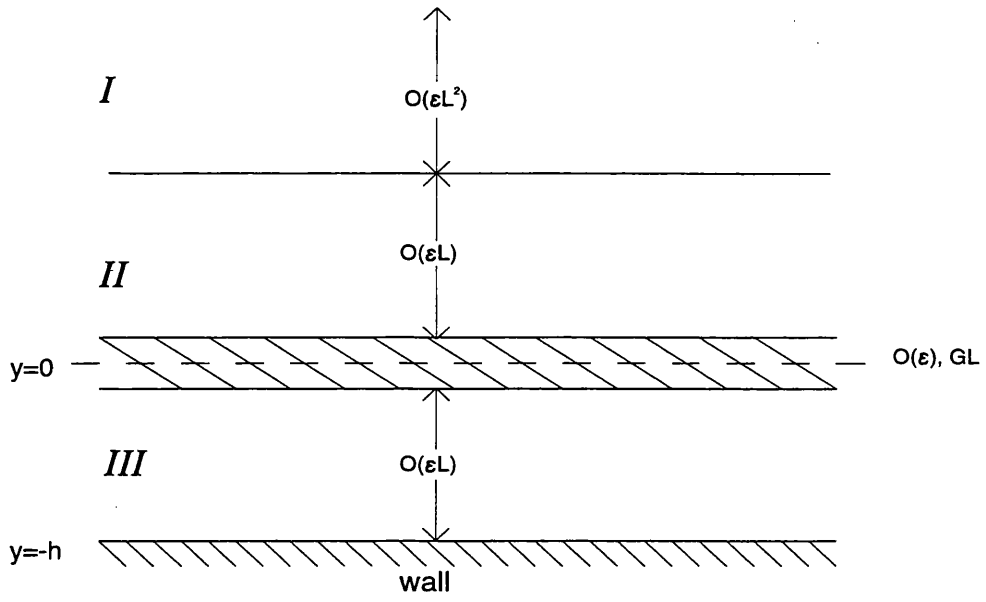

Figure 2.2: The flow structure at H-values close to the critical value H_c, $y = \epsilon LH$.

2.4.2 Regime 2

The analysis carried out in Regime 1 above indicates the need for a more detailed investigation into the effects of the separation distance h on the boundary layer flow under consideration, in particular on the wavenumber α, about the point at which the scaled separation distance H attains the critical value of 1. As mentioned above, at this value the wavenumber vanishes to leading order and so it is necessary to consider the behaviour at second order, achieved by expanding H about its critical value. We write

$$H = 1 + L^{-1}\hat{h} + \ldots$$

implying an expansion for the wavenumber α of the form

$$\alpha = \epsilon^{-1}L^{-2}\alpha_{00} + \epsilon^{-1}L^{-3}\alpha_{01} + \ldots + \alpha_{10} + L^{-1}\alpha_{11} + O(\epsilon L). \qquad (2.29)$$

In each of the regions II, III and the Goldstein layer (as described in Figure 2.2) we

will use matched asymptotic expansions to solve the Rayleigh equation, noting that in these regions it reduces to the equation

$$(\bar{u}-c)\frac{\partial^2\phi}{\partial y^2}=\frac{\partial^2\bar{u}}{\partial y^2}\phi \tag{2.30}$$

for the order of working considered, i.e. the $-\alpha^2\phi$ term may be neglected. If in (2.30) we write ϕ in the form

$$\phi=(\bar{u}-c)f(y) \tag{2.31}$$

for some function $f(y)$, we obtain the integral equation

$$\phi=D_1(\bar{u}-c)\int_{y_w}^{y}(\bar{u}-c)^{-2}dt \tag{2.32}$$

where $y_w=\epsilon Lq$, $q=-1-\tilde{L}^{-1}\hat{h}$, and D_1 is some constant to be determined. This can be rewritten in the form

$$\frac{\phi}{D_1}=(\bar{u}-c)\int_{y_w}^{y}\frac{1}{(\bar{u}-c)^2}-\frac{1}{(\lambda t-c)^2}dt-\frac{(\bar{u}-c)}{\lambda}\left\{\frac{1}{(\lambda y-c)}-\frac{1}{(\lambda y_w-c)}\right\}. \tag{2.33}$$

Solving (2.33) directly will provide us with an alternative form of the required solution and may be used to determine the value of arbitrary constants obtained using the matched-asymptotics approach.

In what follows, the process of solution begins in those regions closest to the smooth wall itself and proceeds in the 'upward' direction of y increasing, towards the mainstream flow.

Region III

Here $y=\epsilon LY$, $-H\leq Y<0$, the basic velocity profile $\bar{u}$ is approximated to zero and the expansion for ϕ takes the form

$$\phi=\phi_{00}+L^{-1}\phi_{01}+L^{-2}\phi_{02}+\ldots+\epsilon L\left\{\phi_{10}+L^{-1}\phi_{11}+\ldots\right\}+\ldots. \tag{2.34}$$

A balance of similarly-ordered terms in the Rayleigh equation yields

$$\begin{aligned}
-\lambda\phi_{00}'' &= 0, \\
-\lambda\phi_{01}'' &= 0, \\
-\lambda\phi_{02}'' + \lambda\alpha_{00}^2\phi_{00} &= 0, \\
-\lambda\phi_{03}'' + \lambda\alpha_{00}^2\phi_{01} + 2\lambda\alpha_{00}\alpha_{01}\phi_{00} &= 0,
\end{aligned}$$

and

$$\begin{aligned}
-\lambda\phi_{10}'' &= 0, \\
-\lambda\phi_{11}'' + 2\lambda\alpha_{00}\alpha_{10}\phi_{00} &= 0, \\
\phi_{12}'' + 2\lambda\left\{\alpha_{00}\alpha_{11} + \alpha_{01}\alpha_{10}\right\}\phi_{00} + 2\lambda\alpha_{00}\alpha_{10}\phi_{01} + \lambda\alpha_{00}^2\phi_{10} &= 0,
\end{aligned}$$

which have solutions of the form

$$\begin{aligned}
\phi_{00} &= A_0 Y + B_0, \\
\phi_{01} &= C_0 Y + D_0, \\
\phi_{02} &= \frac{1}{2}\alpha_{00}^2\left\{\frac{1}{3}A_0 Y^3 + B_0 Y^2\right\} + E_0 Y + F_0, \\
\phi_{03} &= \frac{1}{2}\alpha_{00}^2\left\{\frac{1}{3}C_0 Y^3 + D_0 Y^2\right\} + \alpha_{00}\alpha_{01}\left\{\frac{1}{3}A_0 Y^3 + B_0 Y^2\right\} + G_0 Y + H_0,
\end{aligned}$$

and

$$\begin{aligned}
\phi_{10} &= \hat{A}_0 Y + \hat{B}_0, \\
\phi_{11} &= 2\alpha_{00}\alpha_{10}\left\{\frac{1}{3}A_0 Y^3 + B_0 Y^2\right\} + \hat{C}_0 Y + \hat{D}_0,
\end{aligned}$$

where A_0, B_0, etc. are constants.

Applying the boundary condition $\phi = 0$ at the wall we find that

$$\begin{aligned} A_0 &= B_0, \\ D_0 &= C_0 + A_0\hat{h}, \\ C_0\hat{h} &= \alpha_{00}^2 A_0/3 - E_0 + F_0, \\ \hat{A}_0 &= \hat{B}_0, \\ \hat{D}_0 &= \hat{C}_0 + \hat{A}_0\hat{h} - 2\alpha_{00}\alpha_{10}A_0/3. \end{aligned}$$

Since $\bar{u} \sim 0$ in region III, it follows from (2.33) that the solution to the reduced Rayleigh equation taking the form of (2.31) is

$$\frac{\phi}{D_1} \sim -c\int_{-\epsilon L-\epsilon\hat{h}}^{\epsilon LY} \frac{1}{c^2} - \frac{1}{(\lambda t - c)^2}dt + \frac{c}{\lambda}\left\{\frac{1}{(\epsilon LY - c)} + \frac{1}{(\lambda\epsilon L + \epsilon^2 L^2\lambda\hat{h} + c)}\right\}, \tag{2.35}$$

where, as before, c is given by (2.5). Matching this solution with that obtained using the method of asymptotic expansions we deduce that $D_1 = -\lambda A_0$, $C_0 = 0$ and $\hat{A}_0 = -\hat{c}\lambda^{-1}A_0$, A_0 remaining arbitrary.

Goldstein layer

Inside the Goldstein layer $y = \epsilon z$, $\bar{u} = \epsilon F(z)$ and the following expansion is implied for ϕ;

$$\phi = \Phi_0 + L^{-1}\Phi_1 + \ldots + \epsilon L(\hat{\Phi}_0 + L^{-1}\hat{\Phi}_1 + \ldots) + \ldots. \tag{2.36}$$

In order to match with the solution in region III as $z \to -\infty$, we note here that in this limit the terms of (2.36) are such that

$$\begin{aligned} \Phi_0 &\sim A_0, \\ \Phi_1 &\sim A_0 z + A_0\hat{h}, \\ \Phi_2 &\sim F_0, \\ \Phi_3 &\sim (F_0 + \frac{1}{3}\alpha_{00}^2 A_0)z + H_0, \\ \Phi_4 &\sim \frac{1}{2}\alpha_{00}^2 A_0 z^2 + \frac{2}{3}A_0(\alpha_{00}^2\hat{h} + \alpha_{00}\alpha_{01})z + (H_0 - F_0\hat{h})z + K_0, \end{aligned} \tag{2.37}$$

and

$$\hat{\Phi}_0 \sim -\frac{\hat{c}A_0}{\lambda},$$
$$\hat{\Phi}_1 \sim -\frac{\hat{c}A_0}{\lambda}(z+\hat{h}) - \frac{2}{3}\alpha_{00}\alpha_{10}A_0 + \hat{C}_0. \tag{2.38}$$

Substituting (2.36) into the Rayleigh equation, with α given by (2.29), c given by (2.5) and $\bar{u} = \epsilon F(x)$, we obtain

$$\begin{aligned} -\lambda\Phi_0'' &= 0, \\ -\lambda\Phi_1'' &= F''(z)\Phi_0, \\ -\lambda\Phi_2'' + F(z)\Phi_1'' &= F''(z)\Phi_1, \\ -\lambda\Phi_3'' + F(z)\Phi_2'' &= F''(z)\Phi_2, \\ -\lambda\Phi_4'' + F(z)\Phi_3'' + \lambda\alpha_{00}^2\Phi_0 &= F''(z)\Phi_3. \end{aligned} \tag{2.39}$$

and

$$\begin{aligned} -\lambda\hat{\Phi}_0'' &= 0, \\ -\lambda\hat{\Phi}_1'' - \hat{c}\phi_1'' &= F''(z)\hat{\Phi}_0. \end{aligned} \tag{2.40}$$

The solutions of (2.39) which satisfy the conditions of matching with region III, as set out in (2.37), are

$$\begin{aligned} \Phi_0 &= A_0, \quad \Phi_1 = -\frac{A_0}{\lambda}F(z) + A_0(z+\hat{h}), \\ \Phi_2 &= -\frac{A_0}{\lambda}\{zF(z) - 2I_1(z)\} - \frac{A_0}{\lambda}F(z) + F_0, \\ \Phi_3 &= -\frac{2A_0}{\lambda^2}\left\{F(z)I_1(z) - \frac{3}{2}I_2(z)\right\} - \frac{F_0}{\lambda}F(z) + (F_0 + \frac{1}{3}\alpha_{00}^2A_0)z + H_0, \\ \Phi_4 &= -\frac{3A_0}{\lambda^3}\left\{F(z)I_2(z) - \frac{4}{3}I_3(z)\right\} - \frac{1}{\lambda}(F_0 + \frac{1}{3}\alpha_{00}^2A_0)\{zF(z) - 2I_1(z)\} \\ &\quad - \frac{H_0}{\lambda}F(z) + \frac{1}{2}\alpha_{00}^2A_0z^2 + \frac{2}{3}A_0(\alpha_{00}^2\hat{h} + \alpha_{00}\alpha_{01})z + (H_0 - F_0\hat{h})z + K_0, \end{aligned} \tag{2.41}$$

where

$$I_1(z) = \int_{-\infty}^{z} F(s)\,ds,$$

$$I_2(z) = \int_{-\infty}^{z} F(s)^2 ds,$$
$$I_3(z) = \int_{-\infty}^{z} F(s)^3 ds.$$

The solutions of (2.40), consistent with (2.38), are

$$\hat{\Phi}_0 = -\frac{\hat{c}A_0}{\lambda},$$
$$\hat{\Phi}_1 = \frac{2\hat{c}A_0}{\lambda}F(z) - \frac{\hat{c}A_0}{\lambda}(z+\hat{h}) - \frac{2}{3}\alpha_{00}\alpha_{10}A_0 + \hat{C}_0. \tag{2.42}$$

Although not outlined here, given that $D_1 = -\lambda A_0$ the alternative approach to solving the Rayleigh equation described in (2.30) – (2.33) also yields (2.41) and (2.42).

Region II

Here $y = \epsilon LY$, $Y > 0$, and the appropriate expansions for $\bar{u}$ and ϕ are

$$\bar{u} = \epsilon LY - \epsilon^2 L^2 \lambda_2 Y^2 + \epsilon A_G + \epsilon \frac{\gamma}{L^4 Y^4} e^{-\frac{\lambda}{9}L^3Y^3} + \ldots, \tag{2.43}$$
$$\phi = \phi_0 + L^{-1}\phi_1 + L^{-2}\phi_2 + \ldots + \epsilon L\left\{\hat{\phi}_0 + L^{-1}\hat{\phi}_1 + \ldots\right\} + \ldots$$
$$+ L^{-5}\gamma e^{-\frac{\lambda}{9}L^3Y^3}\left\{f_0 + L^{-1}f_1 + \ldots + \epsilon L\left\{\hat{f}_0 + L^{-1}\hat{f}_1 + \ldots\right\} + \ldots\right\} + \ldots. \tag{2.44}$$

From the Rayleigh equation we obtain as the equations for ϕ_0, ϕ_1 and ϕ_2

$$\lambda(Y-1)\phi_0'' = 0, \quad \lambda(Y-1)\phi_1'' = 0, \quad \lambda(Y-1)(\phi_2'' - \alpha_{00}^2\lambda\phi_0) = 0$$

which, in order to match with the Goldstein layer as $Y \to 0^+$, have solutions

$$\phi_0 = A_0, \quad \phi_1 = A_0\left(\frac{A_G}{\lambda} - \hat{h}\right)(Y-1),$$
$$\phi_2 = \frac{1}{2}\alpha_{00}^2 A_0 Y^2 + \frac{1}{3}\alpha_{00}^2 A_0 Y + \frac{A_0 A_G^2}{\lambda^2}Y - \frac{A_0 A_G}{\lambda}\hat{h} + F_0.$$

It can also be deduced from the Rayleigh equation that

$$
\begin{aligned}
Y^4 f_0 &= \frac{A_0}{\lambda(Y-1)}, \\
Y^4 f_1 &= \frac{A_0 A_G}{\lambda^2} - \frac{A_0 A_G}{\lambda^2 (Y-1)^2} - \frac{A_0 A_G}{\lambda}, \\
Y^4 f_2 &= \frac{A_0 A_G^2}{\lambda^3} + \frac{A_0 A_G^2}{\lambda^3 (Y-1)^3} + \frac{F_0}{\lambda(Y-1)} + \frac{\alpha_{00}^2 A_0 Y}{\lambda(Y-1)} \left\{ \frac{1}{2} Y + \frac{1}{3} \right\},
\end{aligned}
$$

matching with the solution in the Goldstein layer as $Y \to 0^+$. The governing equation for $\hat{\phi}_0$ is obtained from a balance of $O(1)$ terms in the Rayleigh equation and is, together with its solution which satisfies matching requirements with the Goldstein layer,

$$
\begin{aligned}
\hat{\phi}_0'' &= -\frac{2\lambda_2 \phi_0}{\lambda(Y-1)}, \\
\hat{\phi}_0 &= -\frac{2\lambda_2 A_0}{\lambda} \{(Y-1)\log|Y-1| - Y\} + \frac{\hat{c} A_0}{\lambda}(Y-1).
\end{aligned}
$$

We note here for future reference that as $Y \to \infty$

$$
\phi \sim A_0 + \frac{A_0}{L} \left\{ \frac{A_G}{\lambda} - \hat{h} \right\} (Y-1) + O(L^{-2}, \epsilon L), \tag{2.45}
$$

where only the terms given explicitly are necessary in matching region II with region I for the purpose of obtaining α_{00}.

Region I

In region I we introduce the new coordinate $\xi > 0$ such that

$$
y = \epsilon L^2 \xi
$$

with $\xi = O(1)$. Here it follows that $\bar{u}$ and ϕ have expansions of the form

$$
\bar{u} = \epsilon L^2 \lambda \xi - \lambda_2 \epsilon^2 L^4 \xi^2 + \frac{\epsilon \gamma}{L^{10} \xi^4} e^{-\frac{\lambda}{9} L^6 \xi^3} + \ldots, \tag{2.46}
$$

$$
\phi = \Psi_0 + L^{-1}\Psi_1 + \ldots + L^{-10} \gamma e^{-\frac{\lambda}{9} L^6 \xi^3} \left\{ g_0 + L^{-1} g_1 + \ldots \right\} + \ldots \tag{2.47}
$$

and, when balances between terms in the Rayleigh equation are set up, the equation obtained for the leading component of ϕ is

$$\lambda\xi(\Psi_0'' - \alpha_{00}^2\Psi_0) = 0.$$

Hence $\Psi_0 = A_1 e^{-\alpha_{00}\xi}$ where A_1 is a constant. Matching this solution with that obtained in region II leads us to the result that $A_1 = A_0$. We notice that as $\xi \to 0^+$

$$\Psi_0 \sim A_0\left\{1 - \alpha_{00}\xi + \frac{1}{2}\alpha_{00}^2\xi^2 - \ldots\right\} + \ldots \tag{2.48}$$

and, since $Y \sim L\xi$ for large Y and small ξ, on matching (2.45) with (2.48) we deduce that

$$\alpha_{00} = \hat{h} - \frac{A_G}{\lambda}.$$

The value obtained here for α_{00} provides the motivation for the third and final regime. By putting $\hat{h} = A_G\lambda^{-1}$ in the expansion for H of Regime 2 we are able to conduct an even closer examination of the behaviour of the wavenumber α_{00} about the point at which H attains its critical value of 1.

2.4.3 Regime 3

In the light of the results obtained in the working of Regime 2 we expand H in the form

$$H = 1 + \frac{A_G}{L\lambda} + \epsilon L\tilde{h} + \ldots$$

so that to leading order the wavenumber α is $O(1)$, thus indicating the possibility of neutral waves of wavelength $O(1)$ close to the point of separation. We write

$$\alpha = \bar{\alpha} + L^{-1}\alpha_1 + L^{-2}\alpha_2 + \ldots + \epsilon L(\hat{\alpha}_0 + L^{-1}\hat{\alpha}_1 + \ldots) + \ldots,$$

producing an upper region I of $O(1)$.

Similar matching of the solutions in each of the flow regions I, II, III and the Goldstein layer leads to the eigenvalue problem

$$\bar{u}(\phi_0'' - \bar{\alpha}^2\phi_0) = \bar{u}''\phi_0 \tag{2.49}$$

for $\bar{\alpha}$, the $O(1)$ equation obtained from the Rayleigh equation in region I, where as $y \to 0^+$

$$\begin{aligned}\bar{u} &\sim \lambda y - \lambda_2 y^2 + O(y^3),\\ \phi_0 &\sim A_0 - A_0(\tilde{h} - \frac{\hat{c}}{\lambda})y - \frac{2A_0\lambda_2}{\lambda}(y\log y - y) + \frac{1}{2}\bar{\alpha}^2 A_0 y^2\\ &+ \frac{A_0\lambda_2}{\lambda}(\tilde{h} - \frac{\hat{c}}{\lambda})y^2 + \frac{2A_0\lambda_2^2}{\lambda^2}(y^2\log y - 3y^2) + \ldots\end{aligned} \tag{2.50}$$

in order to match with the solution obtained in region II.

We consider the problem presented in (2.49) and (2.50) for small wavenumbers and approach it both analytically and numerically, the analytical method being described below.

The flow is considered in an outer region I_0 in which $y = \bar{\alpha}^{-1}\bar{y}$, $\bar{y} = O(1)$ and $\bar{u} \sim 1$. The expansion for ϕ_0 takes the form

$$\phi_0 = \bar{\alpha}^{-1}\Phi_0 \quad + \quad \Phi_1 + \bar{\alpha} \quad \Phi_2 + \ldots,$$

and on substituting this into (2.49) we find that for $i = 0, 1, 2, \ldots$

$$\Phi_i'' - \Phi_i = 0, \quad \Phi_i = a_i e^{-\bar{y}}, \tag{2.51}$$

where each a_i is a constant.

Moving into region I in which $y = O(1)$, the behaviour of $\bar{u}$ is such that

$$\begin{cases} \bar{u} \sim 1 & \text{as } y \to \infty, \\ \bar{u} \sim \lambda y - \lambda_2 y^2 + O(y^3) & \text{as } y \to 0^+, \end{cases} \tag{2.52}$$

and it emerges that the expansion for ϕ_0 takes the form

$$\phi_0 = \bar{\alpha}^{-1}\tilde{\phi}_0 + \tilde{\phi}_1 + \bar{\alpha}\tilde{\phi}_2 + \bar{\alpha}^2\tilde{\phi}_3 + \ldots.$$

Substituting this expansion into (2.49) and equating powers of $\bar{\alpha}$ yields the following equations for the four leading terms in ϕ_0;

$$\bar{u}\tilde{\phi}_0'' = \bar{u}''\tilde{\phi}_0, \tag{2.53}$$

$$\bar{u}\tilde{\phi}_1'' = \bar{u}''\tilde{\phi}_1, \tag{2.54}$$

$$\bar{u}\tilde{\phi}_2'' - \bar{u}\tilde{\phi}_0 = \bar{u}''\tilde{\phi}_2, \tag{2.55}$$

$$\bar{u}\tilde{\phi}_3'' - \bar{u}\tilde{\phi}_1 = \bar{u}''\tilde{\phi}_3. \tag{2.56}$$

Considering equation (2.54) first, a possible solution for $\tilde{\phi}_1$ is

$$\tilde{\phi}_1 = b_1\bar{u} + b_0\bar{u}\int_1^y \bar{u}^{-2}dy_1, \tag{2.57}$$

where b_0 and b_1 are constants to be determined.

As $y \to \infty$, $\tilde{\phi}_1$ behaves linearly with

$$\tilde{\phi}_1 \sim b_1 + b_0\kappa + b_0 y,$$
$$\kappa = \int_1^\infty \bar{u}^{-2}dy.$$

Matching with the solution obtained in region I_0 as $\bar{y} \to 0$ we may deduce that

$$b_0 = -a_0, \quad b_1 \propto b_0. \tag{2.58}$$

As $y \to 0^+$ it can be shown that

$$\tilde{\phi}_1 \sim -\frac{b_0}{\lambda} + \frac{2b_0\lambda_2}{\lambda^2}y\log y + O(y)$$

and therefore, to match with region II, it follows from (2.50) that $b_0 = -A_0\lambda$, i.e. $a_0 = \lambda A_0$.

The solution to (2.53) which matches with that of region I_0 is

$$\tilde{\phi}_0 = a_0\bar{u} = \lambda A_0\bar{u}.$$

To conclude we note that, in matching the solutions between regions I and II,

$$\tilde{\phi}_0 \sim \lambda A_0\left\{\lambda y - \lambda_2 y^2 + \ldots\right\} \tag{2.59}$$

as $y \to 0$.
If we assume that $\tilde{h} - \hat{c}\lambda^{-1}$ is $O(\bar{\alpha}^{-1})$ then in matching with region II it follows from (2.59) that

$$\tilde{h} - \hat{c}\lambda^{-1} = -\lambda^2\bar{\alpha}^{-1}.$$

Thus, to complete the neutral curve for the separating interactive boundary layer flow under consideration, all that remains is for us to reinforce the assumption made above, namely

$$\tilde{h} - \frac{\hat{c}}{\lambda} = O(\bar{\alpha}^{-1}). \tag{2.60}$$

To do this we now solve numerically the eigenvalue problem set out in (2.49) and (2.50) for small wavenumbers.

2.5 Numerical solution of Regime 3

As mentioned towards the end of the previous section, the aim in this section is to solve numerically the problem set out in (2.49) and (2.50) in order to verify the assumptions made in the analytical working of Regime 3.

The numerical problem is thus. For a given wavenumber, $\bar{\alpha}$ to leading, the value of the constant A_1 is to be found such that

$$\phi_0'(0) = A_1,$$

subject to the boundary condition that $\phi_0 \to 0$ as $y \to \infty$.

The undisturbed flow $\bar{u}(y)$ is assumed to have exponential decay as $y \to \infty$; more precisely $\bar{u} \sim 1 - e^{-y}$. For clarity, this model, rather than the full Blasius profile, has been assumed to apply over all y since the effect of the decay is qualitatively the same.

The numerical method of integration employed is the classical Runge-Kutta method of order four generalized to solve a system of first order differential equations, in this case a system of two.

The second order differential equation which arises from (2.49) and (2.50) is

$$(1 - e^{-y})(\phi_0'' - \bar{\alpha}^2\phi_0) = -e^{-y}\phi_0, \tag{2.61}$$

subject to the initial and boundary conditions

$$\begin{aligned} \phi_0(0) &= A_0, \\ \phi_0'(0) &= A_1, \\ \phi_0(\infty) &= 0. \end{aligned}$$

With $v(y) = \phi_0'(y)$ and $w(y) = \phi_0(y)$, (2.61) is transformed into the system

$$v' = \bar{\alpha}^2 w + (1 - e^{y})^{-1} w, \tag{2.62}$$

$$w' = v, \tag{2.63}$$

and upon normalization, owing to the singularity at $y = 0$ in equation (2.62), the initial conditions are replaced by the boundary conditions $w \to 1$ (i.e. $A_0 = 1$) and $v \to v_0$ as $y \to 0^+$, where the constant v_0 is to be found.

The range of dependence is taken to be $y \in (0, y_\infty]$, y_∞ a suitably large number. We then map this range onto the interval $(0,1]$ using the transformation $y = f(\bar{y})$ for $\bar{y} \in (0,1]$ where

$$f(\bar{y}) = \frac{\bar{y} + 8\bar{y}^2}{1 + (\bar{\alpha} - 1)\bar{y}}. \tag{2.64}$$

If $\bar{y}$ is taken over the range $[\bar{y}_0, 1]$, where $0 < \bar{y}_0 \ll 1$, the system of first order differential equations in (2.62) – (2.63) becomes

$$\frac{dw}{d\bar{y}} = \frac{df}{d\bar{y}} v, \tag{2.65}$$

$$\frac{dv}{d\bar{y}} = \bar{\alpha}^2 \frac{df}{d\bar{y}} w + \frac{df}{d\bar{y}} (1 - e^{f(\bar{y})})^{-1} w, \tag{2.66}$$

with initial conditions $w(\bar{y}_0) = 1$, $v(\bar{y}_0) = v_0$.

The interval $[\bar{y}_0, 1]$ is divided into N equal subintervals, the transformation $y = f(\bar{y})$ therefore concentrating the mesh points in the lower half of the interval $[f(\bar{y}_0), f(1)]$ in which the streamfunction varies more dramatically. The differential equations (2.65) and (2.66) are used to obtain the value v_0 for different values of the parameter $\bar{\alpha}$, the true value taken to be that which results in the solution for ϕ_0 satisfying the appropriate boundary condition at y_∞; namely that $\phi_0(y_\infty) = 0$ where $y_\infty = f(1)$.

In the model described above the constants A_0, λ and λ_2 take the values 1, 1, 0.5 respectively and therefore from equation (2.50) it follows that as $y \to 0^+$

$$\phi_0 \sim 1 - A_h y - (y \log y - y) + \ldots, \tag{2.67}$$

$$\phi_0' \sim -A_h - \log y + \ldots, \tag{2.68}$$

where $A_h = \tilde{h} - \hat{c}\lambda^{-1}$.

Figures 2.3–2.6 show the variation of ϕ_0 with the scaled variable $\bar{y}$ for $\bar{\alpha} = 0.25$, 0.125, 0.0625, 0.03125 respectively, and the values for v_0 are given. Values of A_h are calculated for each value of $\bar{\alpha}$ using (2.68) and the transformation equation (2.64)

and are presented in Table 2.1. As $\bar{\alpha} \to 0$ it can be seen from these results that $\bar{\alpha}A_h \to -1$, thus reinforcing the assumption (2.60) made in §2.4.3.

$\bar{\alpha}$	A_h	$\bar{\alpha}A_h$
0.25	-2.8169	-0.704
0.125	-7.1173	-0.890
0.0625	-15.2531	-0.953
0.03125	-31.2355	-0.976

Table 2.1: Values of A_h and $\bar{\alpha}A_h$ for $\bar{\alpha} \ll 1$

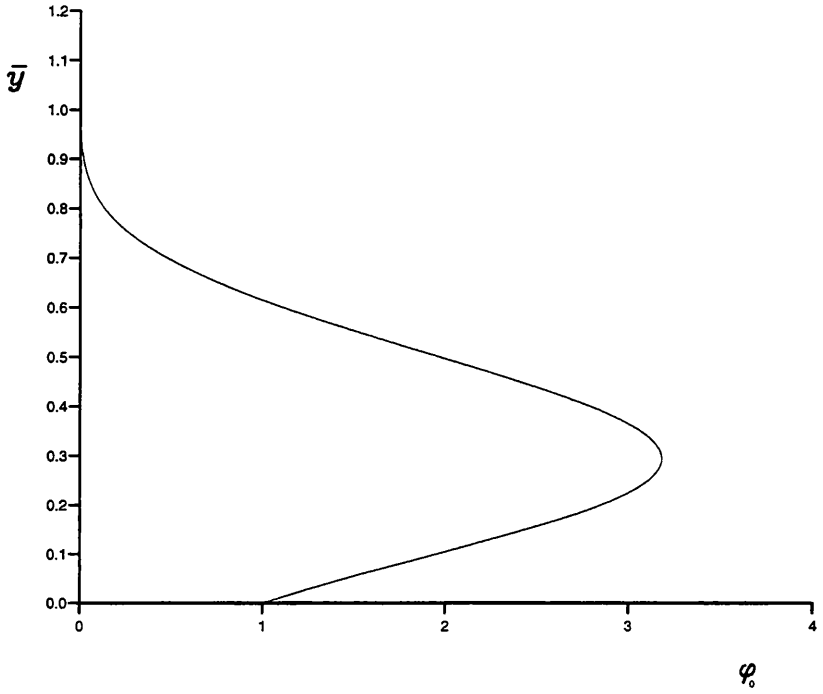

Figure 2.3: Plot of $\bar{y}$ against ϕ_0 for $\bar{\alpha} = 0.25$; $v_0 = 12.0263$.

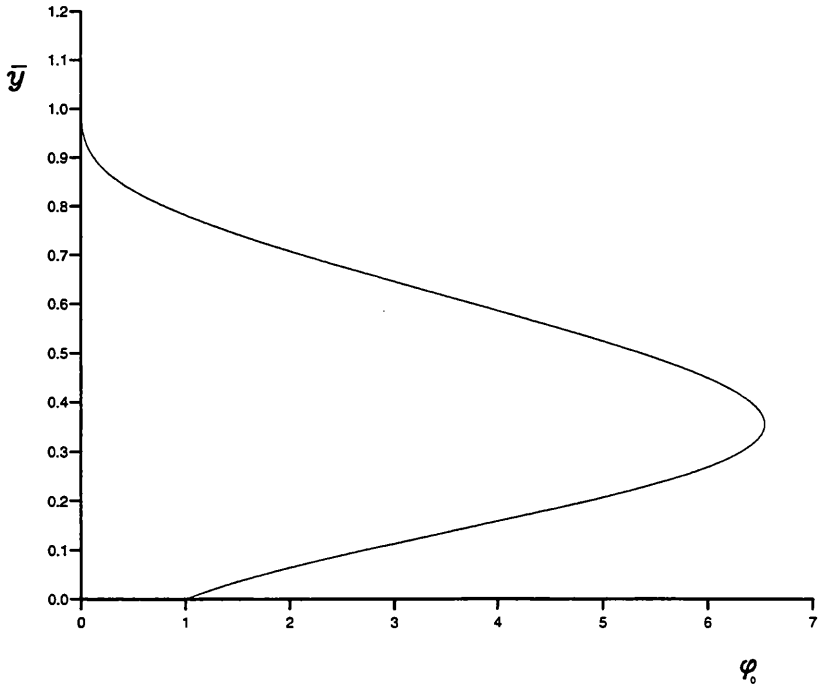

Figure 2.4: Plot of $\bar{y}$ against ϕ_0 for $\bar{\alpha} = 0.125$; $v_0 = 16.3267$.

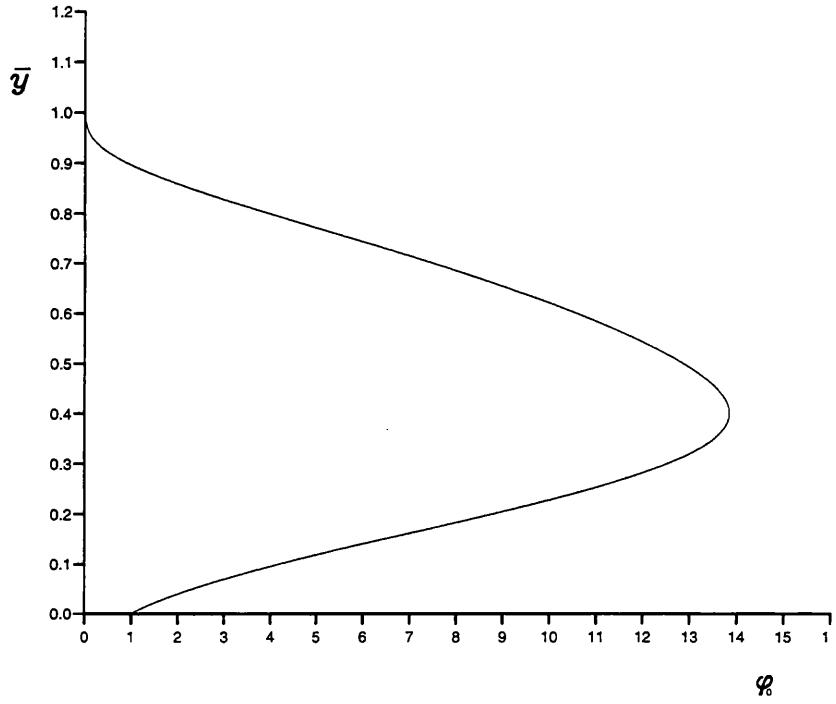

Figure 2.5: Plot of $\bar{y}$ against ϕ_0 for $\bar{\alpha} = 0.0625$; $v_0 = 24.4627$.

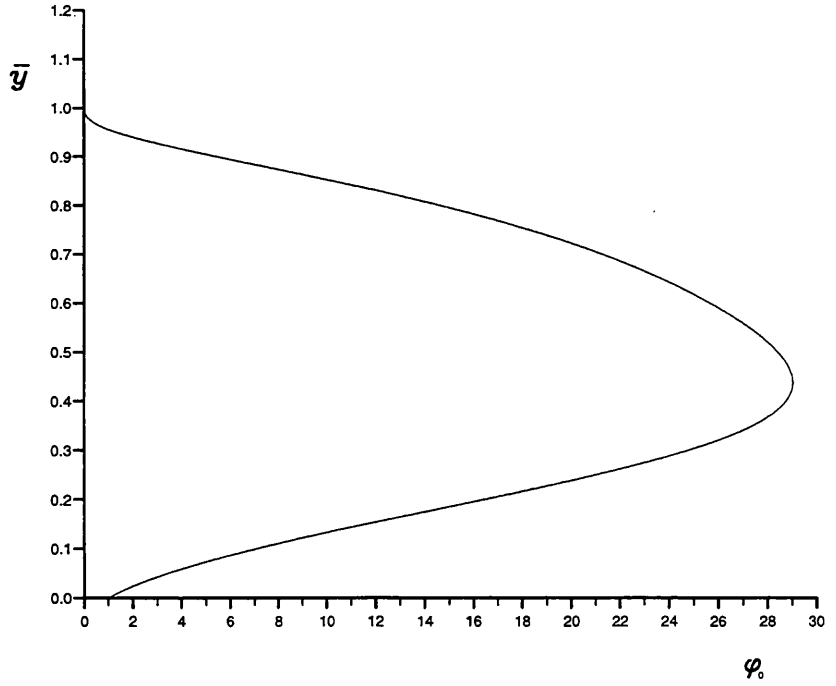

Figure 2.6: Plot of $\bar{y}$ against ϕ_0 for $\bar{\alpha} = 0.03125$; $v_0 = 40.4450$.

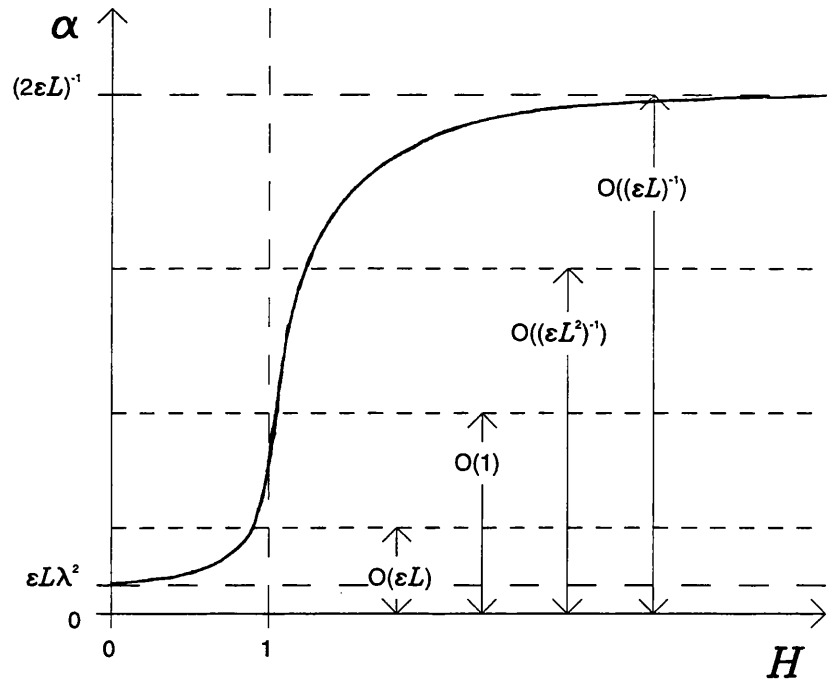

Figure 2.7: The variation of α as a function of the separation distance H.

2.6 Additional comments and conclusion

In concluding this chapter we present graphically the variation of the wavenumber α as a function of the scaled separation distance H. Figure 2.7 identifies the regimes considered by indicating on the graph the size of α to leading order and maps the behaviour for $\alpha \ll 1$ as calculated numerically in §2.5.

We can see from the graph that as $H \to \infty$ the wavenumber approaches the value obtained when the presence of the wall is ignored, i.e. $(2\epsilon L)^{-1}$. Moving our point of interest back upstream towards separation the effects of the wall become important. Here $\alpha = (\epsilon L)^{-1}\alpha_0$ to leading order, where in terms of the separation distance H

$$\alpha_0 = 1 - \frac{\alpha_0}{\tanh \alpha_0 H}. \tag{2.69}$$

Moving progressively further upstream as $H \to 0$ it is (2.69) which yields the critical value $H = H_c(= 1)$ at which α vanishes to leading order, indicating the need for a more thorough investigation of the behaviour of α at H-values close to this critical value.

To leading order the expansion for α is now $O((\epsilon L^2)^{-1})$ and we add to the critical H-value a small perturbation parameter $\hat{h}$ of $O(L^{-1})$. The analysis in this regime shows that α continues to approach zero as $H \to H_c$ and, when $\hat{h} = A_G\lambda^{-1}$, again α vanishes to leading order, motivating the form of the expansion for H in the third and final regime.

Here $\alpha = O(1)$ and we move upstream of the point at which H attains its critical value H_c, α remaining positive. As $\alpha \to 0$ numerical analysis affirms the assumptions made in the matched-asymptotic approach and the neutral curve is completed as we move towards the triple-deck region of the flow.

At this point our particular investigation ends and we pick it up again in Chapter 4 in which we consider the possibility of Rayleigh instabilities in triple-deck flows.

Chapter 3

Long-wave analysis of a two-dimensional separating interactive boundary layer

3.1 Introduction

Continuing on from the work of Chapter 2 in which the possibility of neutral-wave solutions just beyond the point of separation of a two-dimensional interactive boundary layer is investigated, this chapter considers the linear stability of the same flow to long-wave inviscid perturbations.

The eigenvalue problem defined by the Rayleigh equation

$$(\bar{u} - c)(\phi'' - \alpha^2\phi) = \bar{u}''\phi, \tag{3.1}$$

along with the boundary conditions that ϕ must vanish at the wall and as $y \to \infty$, is not easy to solve explicitly when $\bar{u}(y)$ is a smoothly varying function. However, if $\bar{u}(y)$ is piecewise-linear the solutions of the Rayleigh equation are simple exponential or hyperbolic functions which must satisfy certain matching conditions at

discontinuities in $\bar{u}(y)$ or $\bar{u}'(y)$. The use of piecewise-linear profiles thus provides us with a simple method of modeling some features of smoothly varying profiles.

Therefore, by way of an introduction to long-wave analysis, we begin this chapter by first solving (3.1) using a piecewise-linear approximation to the undisturbed velocity profile $\bar{u}$, considering the solution in the long-wave limit as $\alpha \to 0$.

Detailed asymptotic solutions of (3.1) in the limit $\alpha \to 0$ are then presented. Here the basic velocity profile $\bar{u}$ remains unspecified, although we assume it to be a smoothly varying function which satisfies appropriate conditions at the edge of the boundary layer and at the wall.

In §3.2 below we solve (3.1) with $\bar{u}$ taken to be a piecewise-linear profile and consider the limit as $\alpha \to 0$. Long-wave perturbations to the separating boundary layer are considered for the full Rayleigh equation in §3.3. In each of these two cases we approach the problem for a semi-infinite flow, i.e. we take into account the presence of the wall, lying at $y = -h$, and its effect on the flow and its stability.

3.2 Piecewise-linear velocity profile

We aim to solve the eigenvalue problem of (3.1), along with the appropriate boundary conditions, for a basic velocity $\bar{u}$ of the form described in (2.3) and (2.4) of Chapter 2. By approximating $\bar{u}$ using a piecewise-linear profile which possesses some of its main features we can solve what originally appears a difficult problem in little more than a page of working.

If we normalize the transverse coordinate so that the boundary layer region is denoted by $0 \leq y \leq 1$, the features we wish to retain on approximating $\bar{u}$ are:

(i) within the boundary layer $\bar{u}$ behaves linearly to leading order,

(ii) as $y \to 1^-$, $\bar{u}$ approaches the mainstream flow,

(iii) between the separated boundary layer and the wall $\bar{u} = 0$.

This can probably best be achieved using a piecewise-linear profile of the form

$$\bar{u} = \begin{cases} 1 & \text{if} \quad y > 1, \\ y & \text{if} \quad 0 < y < 1, \\ 0 & \text{if} \quad -h < y < 0. \end{cases} \tag{3.2}$$

At a point of discontinuity in $\bar{u}$ and $\bar{u}'$, $y = y_0$ say, two matching conditions must hold, namely

$$\Delta[(\bar{u} - c)\phi' - \bar{u}'\phi] = 0, \tag{3.3}$$

$$\Delta[\frac{\phi}{(\bar{u} - c)}] = 0, \tag{3.4}$$

where $\Delta f = f(y_0^+) - f(y_0^-)$ denotes the 'jump' in $f(y)$ at y_0. For a detailed description of the derivation of conditions (3.3) and (3.4) see Drazin and Reid (1981).

When $\bar{u}'' \equiv 0$ the Rayleigh equation reduces to

$$(\bar{u} - c)(\phi'' - \alpha^2\phi) = 0$$

and, ignoring the continuous part of the spectrum, this is equivalent to

$$\phi'' - \alpha^2\phi = 0.$$

The solution takes the form

$$\phi(y) = \begin{cases} A(\cosh \alpha y - \sinh \alpha y) & \text{if} \quad y > 1, \\ B \cosh \alpha y + C \sinh \alpha y & \text{if} \quad 0 < y < 1, \\ D \sinh \alpha(y + h) & \text{if} \quad -h < y < 0, \end{cases} \tag{3.5}$$

and the boundary conditions are automatically satisfied. On applying the matching conditions (3.3) and (3.4) we obtain the eigenvalue relation

$$\alpha^2c^2(1+X)(1+Y) - \alpha^2c(1+X)(1+Y) + \alpha cX(1-Y) + \alpha Y(1+X) - XY = 0, \tag{3.6}$$

where $X = \tanh \alpha$ and $Y = \tanh \alpha h$.

Before we consider the long-wave limit $\alpha \to 0$ we will use (3.6) to establish a more complete stability picture for the boundary layer flow under investigation. In Chapter 2 we obtained the neutral curve as a function of the separation-height parameter h, all that remains is to determine whether instability is likely to occur at large or small wavenumbers.

In order to achieve this, for a fixed value of the separation-height parameter h we solve (3.6) numerically using 'the formula' for calculating the roots of a quadratic equation, the positive root taken where necessary. For each value of h we plot c_r, c_i and $f(\alpha, h)$ against the wavenumber α; $c = c_r + ic_i$ representing the wave speed and $f \equiv B^2 - 4AC$. Results are presented in Figures 3.3–3.14 for $h = 1, 0.5, 0.25, 0.125$, found at the close of this chapter.

It can be seen from these graphs that $c_i \neq 0$ for small wavenumbers α, which in physical terms implies that the flow is unstable to long-wave perturbations. For large α, $c_i = 0$, implying stability to short waves. As $h \to \infty$, in accordance with (2.2) the value of the wavenumber α_s at which neutral stability occurs increases (see Figure 2.7), thus showing increasing instability with increased distance downstream from the point of separation.

We may deduce from these results that above the neutral curve, obtained in Chapter 2 as a function of the separating-height parameter h, the flow is stable to linear disturbances, and below it the flow is unstable. The stability picture is thus complete.

To serve as an analytical check we let $\alpha \to \infty$ in (3.6). It follows then that to leading order the eigenvalue relation between α and c reduces to

$$2\alpha^2 c^2 - 2\alpha^2 c + \alpha = 0. \tag{3.7}$$

Assuming firstly that there exists a root c_1 of $O(1)$, we may further approximate

(3.7) by the equation

$$\alpha^2 c(c-1) = 0$$

which has the non-trivial solution $c_1 = 1$. If we now assume that there exists a root c_2 such that $c_2 \ll 1$, (3.7) becomes

$$-2\alpha^2 c + \alpha = 0,$$

with solution $c_2 = (2\alpha)^{-1}$. These solutions for c at large wavenumbers are in good agreement with the results obtained numerically. To enable a comparison to made more easily, Figure 3.1 presents a plot of c_r against α for $h = 1$, showing the behaviour of both roots as $\alpha \to \infty$.

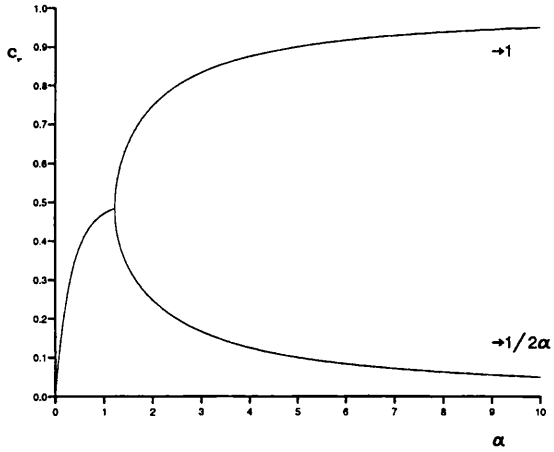

Figure 3.1: Plot of c_r against α with $h = 1$ showing the behaviour of both roots as $\alpha \to \infty$.

If we now let $\alpha \to 0$ in such a way that $H = \alpha h = O(1)$, (3.6) becomes

$$c^2(1+t) - 2ct + t = 0$$

to leading order which, on taking the positive root, has solution

$$c = \frac{t + i\sqrt{t}}{(1+t)}, \tag{3.8}$$

where $t = \tanh H$.

Thus, in modeling the basic velocity profile $\bar{u}$ using a piecewise-linear profile, we have been able to determine the nature of the stability to linear disturbances of the two-dimensional flow described in Chapter 2. Also, in considering the limit $\alpha \to 0$ in (3.6) above, we have at least gained a feeling for the solution of the Rayleigh equation for long-wave disturbances.

3.3 Generalized analysis of long-wave solutions

In this section, as in the above, long-wave inviscid perturbations to the separating interactive boundary layer are investigated, but here the full eigenvalue problem posed by (3.1) is considered. The basic flow velocity $\bar{u}(y)$ will remain unspecified although we assume that it is a smoothly varying function satisfying appropriate conditions at the edge of the boundary layer and at the wall. If $y = O(1)$ inside the boundary layer then the boundary conditions satisfied by $\bar{u}$ are;

$$\bar{u} \to 1 \quad \text{as} \quad y \to \infty, \tag{3.9}$$

$$\bar{u} = 0 \quad \text{at} \quad y = -h. \tag{3.10}$$

Asymptotic solutions in the limit $\alpha \to 0$ are presented, the structure of the flow as shown in Figure 3.2.

Boundary layer

Inside the boundary layer $y = O(1)$, $-\infty < y < \infty$, the basic velocity profile satisfies the conditions (3.9) and (3.10) above, and the appropriate expansions for ϕ and c are

$$\phi = \phi_0 + \alpha\phi_1 + \alpha^2\phi_2 + \ldots, \tag{3.11}$$

$$c = c_0 + \alpha c_1 + \alpha^2 c_2 + \ldots. \tag{3.12}$$

When (3.11) and (3.12) are substituted into the Rayleigh equation (3.1) and powers of α are equated, the following equations are obtained for the three leading

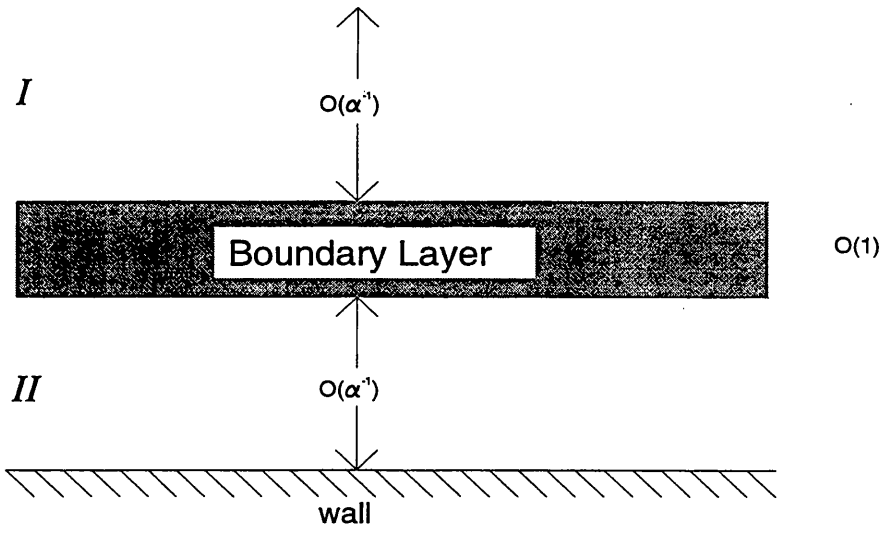

Figure 3.2: The various regions in which long waves develop.

components of ϕ;

$$(\bar{u} - c_0)\phi_0'' - \bar{u}''\phi_0 = 0, \tag{3.13}$$

$$(\bar{u} - c_0)\phi_1'' - \bar{u}''\phi_1 = c_1\phi_0'', \tag{3.14}$$

$$(\bar{u} - c_0)\phi_2'' - \bar{u}''\phi_2 = c_2\phi_0'' + c_1\phi_1'' + (\bar{u} - c_0)\phi_0. \tag{3.15}$$

A solution of (3.13) is the simple displacement solution $\phi_0 = A_0(\bar{u} - c_0)$ where A_0 is a constant. The solutions of (3.14) and (3.15) then take the form

$$\phi_1 = -\frac{c_1 A_0}{c_0}\bar{u} + d_1(\bar{u} - c_0)\int_{-\infty}^{y}(\bar{u} - c_0)^{-2}dy_1, \tag{3.16}$$

$$\begin{aligned}\phi_2 = {} & -A_0(c_2 - \frac{c_1^2}{c_0})\bar{u} + A_0(\bar{u} - c_0)\int_{-\infty}^{y}(\bar{u} - c_0)^{-2}\int_{-\infty}^{y_1}(\bar{u} - c_0)^2 dy_2\, dy_1 \\ & -c_1 d_1\int_{-\infty}^{y}(\bar{u} - c_0)^{-2}dy_1 + 2c_1 d_1(\bar{u} - c_0)\int_{-\infty}^{y}(\bar{u} - c_0)^{-3}dy_1 \\ & +d_2(\bar{u} - c_0)\int_{-\infty}^{y}(\bar{u} - c_0)^{-2}dy_1.\end{aligned} \tag{3.17}$$

Noting condition (3.9), it follows that as $y \to \infty$

$$\phi_0 \sim A_0(1 - c_0), \tag{3.18}$$

$$\phi_1 \sim \frac{d_1}{(1 - c_0)} y + \ldots, \tag{3.19}$$

$$\phi_2 \sim \frac{1}{2} A_0(1 - c_0) y^2 + \ldots. \tag{3.20}$$

We now proceed into region I.

Region I

In the upper region I $y = \alpha^{-1} Y$ for $0 \leq Y < \infty$ and $\bar{u} \sim 1$. Here too the wave velocity c is given by (3.12) and ϕ has the expansion

$$\phi = \Phi_0 + \alpha \Phi_1 + \alpha^2 \Phi_2 + \ldots. \tag{3.21}$$

Substitution of expansions (3.12) and (3.21) into the Rayleigh equation yields equations of the form

$$\Phi_j'' - \Phi_j = 0$$

for $j = 0, 1, 2, \ldots$ and therefore, in order to satisfy the condition that $\phi \to 0$ as $Y \to \infty$,

$$\Phi_j = k_j e^{-Y}.$$

Matching with the solution in the boundary layer we deduced that

$$k_0 = A_0(1 - c_0) = -\frac{d_1}{(1 - c_0)},$$

and hence

$$d_1 = -A_0(1 - c_0)^2. \tag{3.22}$$

Region II

In the lower region II $y = \alpha^{-1}Y$ for $-H \leq Y \leq 0$ ($h = \alpha^{-1}H$), $\bar{u} \sim 0$, and we write

$$\phi = \bar{\Phi}_0 + \alpha\bar{\Phi}_1 + \alpha^2\bar{\Phi}_2 + \ldots. \tag{3.23}$$

Again substitution into the Rayleigh equation leads to equations of the form $\bar{\Phi}_j'' - \bar{\Phi}_j = 0$ for $j = 0, 1, 2, \ldots$, but in region II the condition that $\phi = 0$ at the wall must be satisfied.

If the presence of the wall is neglected, i.e. $H \to \infty$, and the extent of the flow assumed infinite in both the positive and negative y-directions, this boundary condition is replaced by the condition $\phi(-\infty) = 0$, implying

$$\bar{\Phi}_j = \bar{k}_j e^Y$$

for $j = 0, 1, 2, \ldots$.

We note here that as $y \to -\infty$ inside the boundary layer

$$\begin{aligned}
\phi_0 &\sim -c_0 A_0, \\
\phi_1 &\sim -\frac{d_1}{c_0} y, \\
\phi_2 &\sim -\frac{1}{2} c_0 A_0 y^2,
\end{aligned}$$

and matching with the solution obtained in region II it follows that

$$\begin{aligned}
\bar{k}_0 &= -c_0 A_0 = -\frac{d_1}{c_0}, \\
d_1 &= c_0^2 A_0.
\end{aligned} \tag{3.24}$$

Therefore, combining (3.24) with (3.22) we deduce that

$$c_0 = \frac{1}{2}(1 + i). \tag{3.25}$$

This result is in full agreement with Drazin and Howard's (1962) treatment of long-wave linear instability in parallel shear flows which concludes that as $\alpha \to 0^+$, on taking the root with $c_i > 0$,

$$c \to \frac{1}{2}\{\bar{u}(\infty) + \bar{u}(-\infty)\} + i\frac{1}{2}\{\bar{u}(\infty) - \bar{u}(-\infty)\}. \tag{3.26}$$

If however the effects of the wall at $y = -h$ are taken into consideration, the appropriate boundary condition to be satisfied for $j = 0, 1, 2, \ldots$ is $\bar{\Phi}_j(-H) = 0$, $h = \alpha^{-1}H$. Matching similar to that above yields the result

$$c_0 = \frac{t + i\sqrt{t}}{(1+t)}, \tag{3.27}$$

where $t = \tanh H$. This result is in full agreement with (3.8) obtained in the previous section in the limit as α tends to zero.

In conclusion, for the separating boundary layer considered in this and the previous chapter we have demonstrated that by modeling the basic velocity profile using the piecewise-linear profile described in (3.2) we are able to establish some of the major characteristics and behaviours of the flow itself, achieved employing relatively simple mathematics. Such a method of solution provides us with a useful tool for checking more rigorous calculations, which can only strengthen the results obtained.

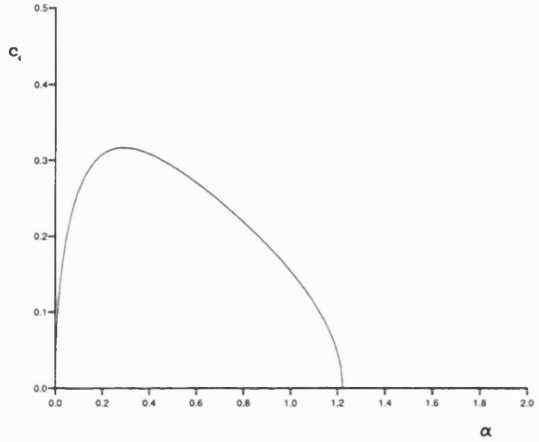

Figure 3.3: Plot of c_i against α with $h = 1$.

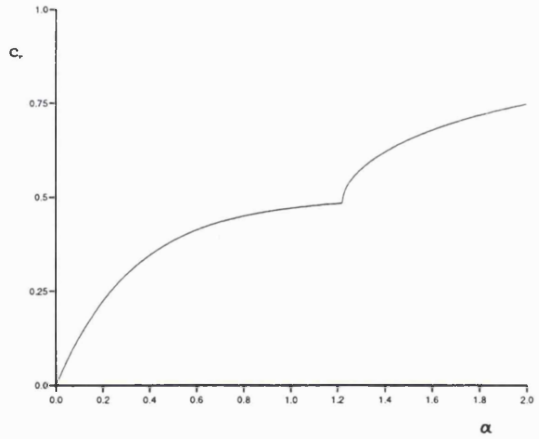

Figure 3.4: Plot of c_r against α with $h = 1$.

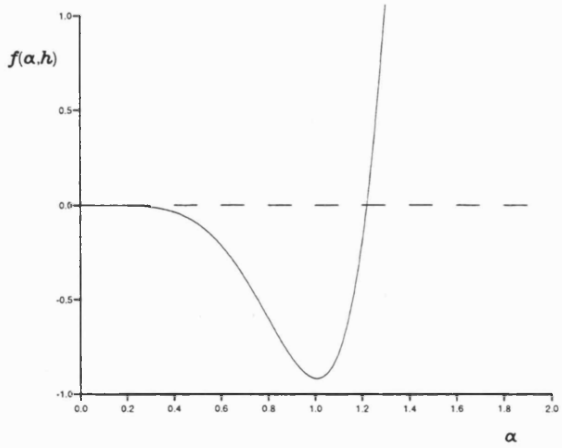

Figure 3.5: Plot of $f(\alpha, h)$ against α with $h = 1$.

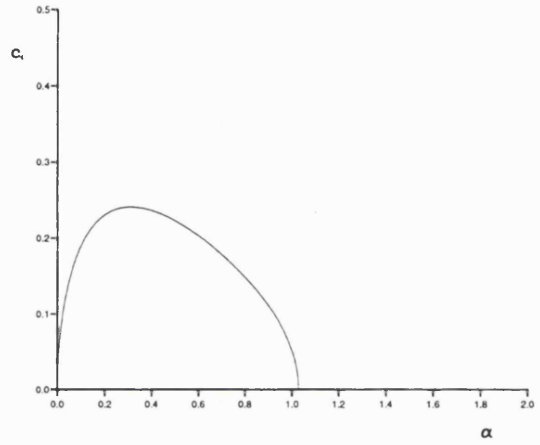

Figure 3.6: Plot of c_i against α with $h = 0.5$.

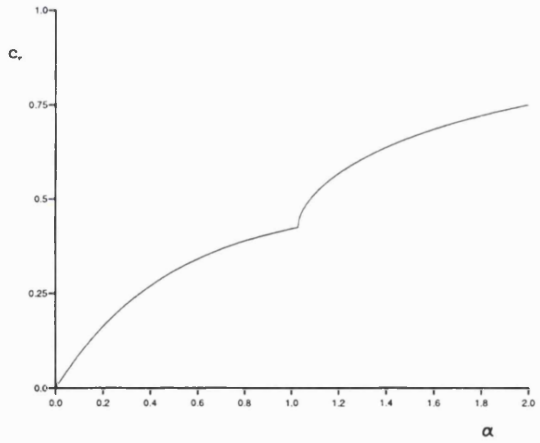

Figure 3.7: Plot of c_r against α with $h = 0.5$.

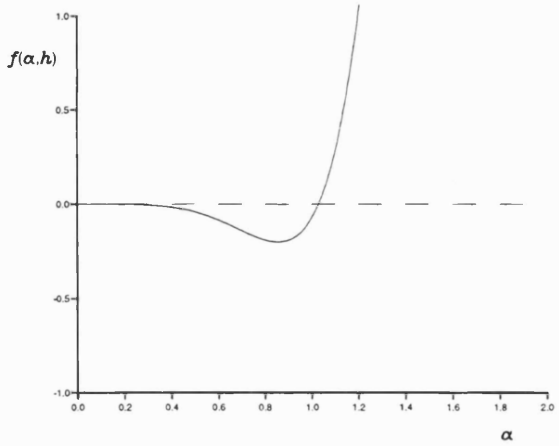

Figure 3.8: Plot of $f(\alpha, h)$ against α with $h = 0.5$.

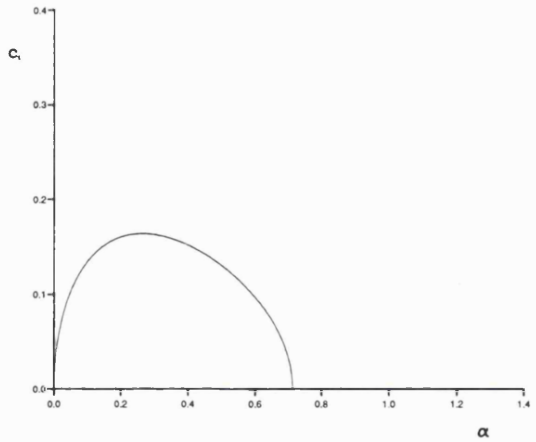

Figure 3.9: Plot of c_i against α with $h = 0.25$.

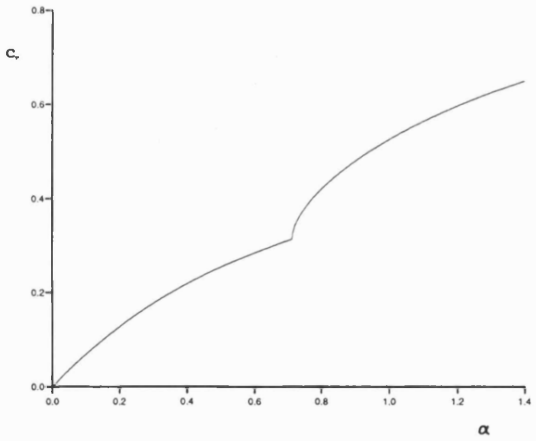

Figure 3.10: Plot of c_r against α with $h = 0.25$.

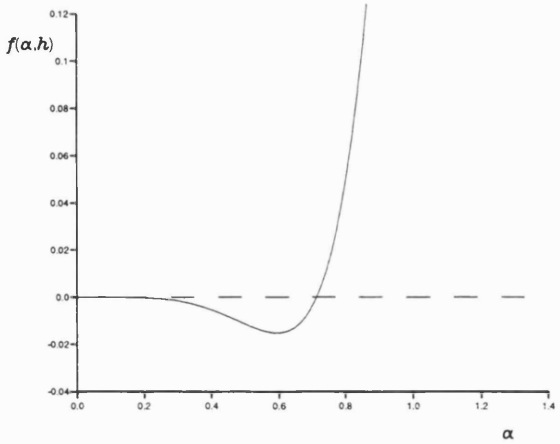

Figure 3.11: Plot of $f(\alpha, h)$ against α with $h = 0.25$.

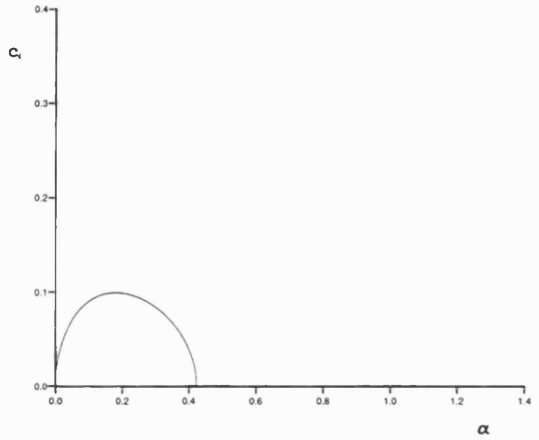

Figure 3.12: Plot of c_i against α with $h = 0.125$.

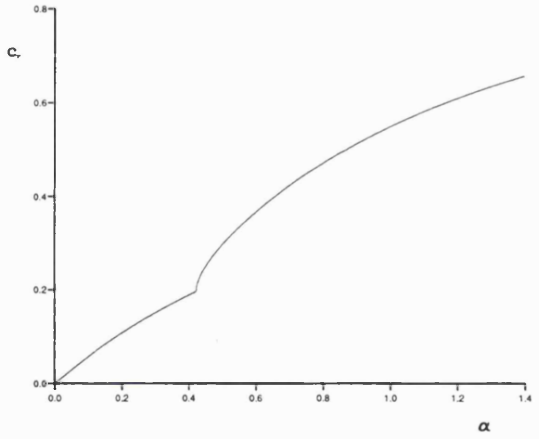

Figure 3.13: Plot of c_r against α with $h = 0.125$.

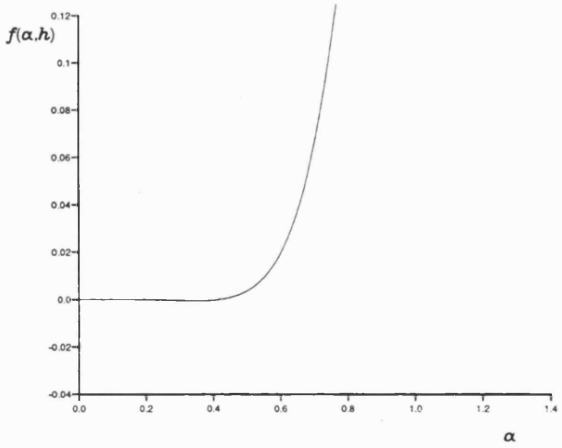

Figure 3.14: Plot of $f(\alpha, h)$ against α with $h = 0.125$.

Chapter 4

Linear instability of triple-deck flows

4.1 Introduction

This somewhat brief chapter concerning Rayleigh instability within triple-deck flows serves as a link between the linear studies of downstream breakaway separating boundary layers (Chapters 2–3) and the nonlinear studies concerning more local separating-type interactive flows which follow in Chapters 5–7.

The effects of small surface-mounted obstacles, or other local distortions, on the boundary layer flow over a solid surface have been of great experimental interest for many years. Among the more notable of these effects, and relating to the work of this thesis, are the phenomena of separation, of small or large scale, and instability, often leading to transition to turbulence. This latter aspect is commonly employed in aerodynamics to deliberately produce a turbulent boundary layer downstream by means of transition due to a small trip wire placed on or near the surface, see Van Dyke (1982). As mentioned in Chapter 1, experimental studies of flow transition over surface-mounted obstacles are given in Acarlar and Smith (1987) and references therein, while computational studies include Mason and Morton (1987) and others.

Our concerns in this chapter are with the essentially inviscid, i.e Rayleigh, instabilities which occur within separating two-dimensional boundary layer flows as a result of inflectional velocity profiles produced locally, for example in the case of nonparallel flow past a short, smooth obstacle mounted on a flat surface.

In what follows we demonstrate, by means of a model problem presented in Smith and Bodonyi's (1985) paper concerning shortscale instability in boundary flows past surface-mounted obstacles of relative height h, that in some specific contexts the existence, locally, of a point of inflection is not a sufficient condition for Rayleigh instability to occur.

In §4.2 the two-dimensional governing equations are set down and in §4.3 we describe in detail the model solution of Smith and Bodonyi (1985). In considering the situation of a two-dimensional separating boundary layer flow of triple-deck form, and with reference to the above-mentioned model solution, we show that as the boundary layer undergoes increased separation, corresponding to the inflection point moving upwards in the positive y-direction towards the main deck of the flow, a cut-off point, x_1 say, occurs at which the flow ceases to be unstable, prior to the point, x_2 say, at which the inflection point leaves the lower deck. It is interesting to observe that this departure of the inflection point x_2 from the lower deck is consistent with the flow further downstream studied in Chapters 2 and 3, as well as with the downstream asymptote of the lower deck flow solution and the Papageorgiou and Smith (1989) near-wake profile. It should also be noted that the cut-off point x_1 may actually be far upstream in some separating flows.

Finally, in §4.4 we consider three-dimensional triple-deck flows and, in particular, we show that very oblique waves allow the criterion for inflectional instability to be satisfied even at small h-values. This is in comparison with the two-dimensional case of Smith and Bodonyi (1985) in which the authors show that an order-one value of h is needed for inflectional instability, or its onset, to occur even though inflection points are present for any smaller value of h, corresponding to smaller hump heights.

4.2 Two-dimensional governing equations

If the lengthscale and height of the obstacle, centred at $x = x_0 > 0$, are $O(Re^{-3/8})$ and $O(Re^{-5/8})$ respectively then the local steady motion is controlled by the lower deck equations which in scaled form are

$$\frac{\partial u}{\partial X} + \frac{\partial v}{\partial Y} = 0, \tag{4.1}$$

$$u\frac{\partial u}{\partial X} + v\frac{\partial u}{\partial Y} = -p'(X) + \frac{\partial^2 u}{\partial Y^2}, \tag{4.2}$$

with $F(X)$ the given scaled shape of the obstacle and

$$u = v = 0 \quad \text{on} \quad Y = 0, \tag{4.3}$$

$$u \sim Y + A(X) + F(X) \quad \text{as} \quad Y \to \infty, \tag{4.4}$$

$$(u, v, p', A') \to (Y, 0, 0, 0) \quad \text{as} \quad |X| \to -\infty. \tag{4.5}$$

The pressure p is related to the displacement increment $-A(X)$ by the Cauchy-Hilbert integral

$$p(X) = \frac{1}{\pi} \int\!\!\!\!\!\!- _{-\infty}^{\infty} \frac{dA}{d\xi}(\xi) \frac{d\xi}{(x - \xi)}.$$

If the Prandtl shift $Y \to Y - F(X)$ is applied, the shortscale disturbances are then governed by Rayleigh's equation for the disturbance streamfunction ϕ,

$$(u - c)\left\{\frac{\partial^2 \phi}{\partial Y^2} - \alpha^2 \phi\right\} = \frac{\partial^2 u}{\partial Y^2}\phi,$$

subject to the boundary conditions $\phi = 0$ at $Y = 0$ and as $Y \to \infty$.

4.3 Two-dimensional triple-deck flows

The model inflectional velocity profile considered by Smith and Bodonyi (1985), typical of flow past a surface-mounted obstacle, provides us with valuable physical

insight into the problem of Rayleigh instability in triple-deck flows. Before applying its findings to the case of a separating boundary layer flow, we first outline the model itself for $F(X) = O(h)$ where h is of $O(1)$ or less.

If the Rayleigh equation is rewritten in the form

$$\frac{\partial^2 \phi}{\partial Y^2} = \left[\alpha^2 + g(Y)\right] \phi, \tag{4.6}$$

where

$$g(Y) = \frac{1}{(u-c)} \frac{\partial^2 u}{\partial Y^2}, \tag{4.7}$$

and α is assumed real and non-negative, $g(Y)$ is generally of $O(h)$ and tends to zero exponentially as $Y \to \infty$. Since $u = c$ at the single inflection point it follows also that $g(Y)$ is smooth for all $Y > 0$ in the neutral case α, c real. A representative example for $g(Y)$ is therefore

$$g(Y) = -he^{-2Y}. \tag{4.8}$$

Thus, the local velocity profile implied by (4.7) and (4.8) is

$$u = c - \frac{\pi}{2} Y_0(z) + bJ_0(z) \tag{4.9}$$

where J_0 and Y_0 are the standard Bessel functions of zero order and

$$z = h^{1/2} e^{-Y}, \tag{4.10}$$

$$c = (J_0(h^{1/2}) - 1)^{-1} \left\{ \left[A + F + \frac{1}{2} \log(\frac{h}{4}) + \gamma \right] J_0(h^{1/2}) - \frac{\pi}{2} Y_0(h^{1/2}) \right\}, \tag{4.11}$$

$$b = (J_0(h^{1/2}))^{-1} \left\{ \frac{\pi}{2} Y_0(h^{1/2}) - c \right\}. \tag{4.12}$$

The coefficients of J_0, Y_0 are such that as $Y \to \infty$ (4.4) holds. In terms of z this implies that $u \sim -\log z + O(1)$ as $z \to 0$, the $O(1)$ term corresponding to the displacement effect $A + F$. The no-slip condition is satisfied at $Y = 0$ and the velocity profile has an inflection point at $u = c$, as is required.

With (4.8) holding, and the Rayleigh equation written in the form (4.6), by making the substitution (4.10) it may be deduced that the streamfunction ϕ satisfies the Bessel equation

$$z^2\frac{\partial^2\phi}{\partial z^2}+z\frac{\partial\phi}{\partial z}+(z^2-\alpha^2)\phi=0, \tag{4.13}$$

subject to the conditions $\phi=0$ at $z=0$ and $z=h^{1/2}$. On applying a normalization it follows that $\phi=J_\alpha(z)$ in order to satisfy the condition at $z=0$. The condition at $z=h^{1/2}$ then requires that $J_\alpha(h^{1/2})=0$ and therefore

$$h=z_\alpha^{(m)^2}$$

determines values of α implicitly in terms of h. For $m=1,2,\ldots$ the $z_\alpha^{(m)}$ are the positive zeros of the Bessel function $J_\alpha(z)$.

However, since α is real the smallest root possible is the first root $z_0^{(1)}$ of $J_0(z)$. Therefore

$$h\geq h_c=z_0^{(1)^2}[\approx 5.7831] \tag{4.14}$$

must hold if a neutral solution is to exist.

If we assume that Rayleigh instability can only occur for a range of positive values of α, thus requiring at least one neutral solution to exist, then we may deduce from (4.14) that there is a cut-off value $h=h_c$ below which the profile (4.9) is inviscidly stable. Therefore, this demonstrates that in the present context the existence of an inflection point in the local velocity profile is a necessary but not sufficient condition for Rayleigh instability to occur.

Following on from the above we now show that in the case of a separating two-dimensional boundary layer flow of triple-deck form and with local velocity profile as in (4.9), the existence of an inflection point is again not a sufficient condition for the occurrence of Rayleigh instability.

We suppose firstly that the critical layer ($u = c$) lies at $z = \hat{z}$ say, implying from (4.9) that

$$\frac{\pi}{2}Y_0(\hat{z}) = bJ_0(\hat{z}).$$

Since b is given by (4.12) it follows then that $\hat{z}$ is determined by

$$J_0(\hat{z})Y_0(h^{1/2}) - Y_0(\hat{z})J_0(h^{1/2}) = \frac{2c}{\pi}J_0(\hat{z}) \tag{4.15}$$

in the range $0 \leq \hat{z} \leq h^{1/2}$ (i.e. $0 \leq Y < \infty$).

We now consider a particular profile of the form (4.9) which possesses a large value of the wave speed c. This corresponds to the downstream region of the flow where the critical layer, or inflection point, is about to leave the lower deck of the triple-deck structure. Assuming $h = O(1)$, for the lefthand side of (4.15) to balance with the righthand side, $\hat{z} \ll 1$ must hold. Therefore, since $J_0(\hat{z}) \sim 1 - \hat{z}^2/4$ and $Y_0(\hat{z}) \sim 2\pi^{-1}\log\hat{z} + O(1)$ as $\hat{z} \to 0$, (4.15) can be written in the form

$$Y_0(h^{1/2}) - \left\{\frac{2}{\pi}\log\hat{z} + \ldots\right\}J_0(h^{1/2}) = \frac{2c}{\pi}, \tag{4.16}$$

implying that

$$-\log\hat{z} \sim \frac{c}{J_0(h^{1/2})} + \ldots. \tag{4.17}$$

Re-writing this in terms of Y, it follows from (4.10) that

$$\hat{Y} \sim \frac{c}{J_0(h^{1/2})} + \ldots \tag{4.18}$$

where $\hat{z} = h^{1/2}e^{-\hat{Y}}$, $\hat{Y} \gg 1$ denoting the critical layer. However at large Y, $u(= c) \sim Y + \ldots$ and therefore, given $h = O(1)$, we have a contradiction with (4.18).

The suggestion then from the above is that $c \gg 1$ only if h is small. But, from (4.13) and (4.14), h being small implies no instability, or at least no neutral solution.

In conclusion we may deduce that if x_2 is the station at which the inflection point leaves the lower deck of the flow, there exists a cut-off point x_1, prior to x_2, downstream of which the profile is inviscidly stable. This again demonstrates that the existence of an inflection point in the local velocity profile is a necessary but not sufficient condition for Rayleigh instability to occur.

We mention briefly that attempts were made to find a region of inviscid instability ahead of some cut-off point x_1. The results were found to be inconclusive and it may be that x_1 is indeed far upstream. But, on the other hand, there are probably some breakaway separating flows such as in supersonic or hypersonic boundary layers, channel and pipe flows, wall-jet flows, etc. which do admit such inviscid instability over a finite scaled portion of the separation process prior to the departure of the inflectional point, as above.

4.4 Three-dimensional triple-deck flows

An interesting point should be mentioned here concerning three-dimensional inflectional instabilities in near-wall shear flows. The point actually arises from Smith and Bodonyi's (1985) study of two-dimensional waves in which the inviscid instability of a profile $u = y + O(h)$ is examined for y typically of order one. This is

for flow past a surface-mounted hump in the lower deck with relative hump height h, for example. Most significantly, Smith and Bodonyi (1985) show by means of an exact solution of the Rayleigh equation (see §4.3) that an order-one value of h is needed for inflectional instability, or its onset, to occur, i.e.

$$u - y = O(1), \tag{4.19}$$

even though inflection points are present for any smaller value of h, corresponding to smaller hump heights.

Let us consider three-dimensional waves instead for which the equivalent Rayleigh equation is

$$(\bar{\bar{u}} - c)(\Phi'' - \gamma^2\Phi) = \bar{\bar{u}}''\Phi, \tag{4.20}$$

where $\gamma^2 \equiv \alpha^2 + \beta^2$ and

$$\bar{\bar{u}} \propto (\alpha\bar{u} + \beta\bar{w}) \tag{4.21}$$

for disturbances proportional to $\exp[i\alpha X + i\beta Z - i\alpha cT]$ of a basic flow with profiles $\bar{u}$ and $\bar{w}$. We indicate below that inflectional instability is likely for any value of h, no matter how small, unlike in the two-dimensional case discussed earlier. Thus, when h is small, the profiles have the form $\bar{u} = y + O(h)$ and $\bar{w} = h\bar{w}_1$ say, where $\bar{w}_1$ is of order unity and has a wall-jet shape in y including at least one inflection point: see solutions in Smith *et al* (1977).

So, for most (O(1)) values of the wavenumbers α, β, the effective profile $\bar{\bar{u}}$ in (4.21) is dominated by the $\bar{u}$-term, i.e. by $y + O(h)$, and hence, in view of the requirement (4.19), there is stability.

In contrast, for very oblique waves such that $\beta \gg \alpha$, with $\alpha \sim h\beta$, $\bar{\bar{u}} \propto \beta[(\alpha/\beta)\bar{u} + \bar{w}]$ gives

$$\bar{\bar{u}} \propto h\beta\left[\left(\frac{\alpha}{h\beta}\right)y + \bar{w}_1\right], \tag{4.22}$$

and so the effective profile $\bar{\bar{u}}$ can be strongly inflectional as the two terms in the square brackets of (4.22) are now comparable, both being $O(1)$. Also, γ^2 is dominated by β^2 here, leaving (4.20) in the relatively full form

$$\left\{\left[\left(\frac{\alpha}{h\beta}\right)y + \bar{w}_1\right] - \bar{c}\right\}(\Phi'' - \beta^2\Phi) = \bar{w}_1''\Phi \tag{4.23}$$

provided β remains typically $O(1)$, with α then having to be of order h, while $y = O(1)$; $\bar{c}$ would be the effective inflectional speed for the neutral inviscid case.

In essence, those very oblique waves allow the criterion (4.19) for inflectional instability to be satisfied even at small h-values. For flow past three-dimensional humps for instance, as in Smith *et al* (1977), a wide variety of wall-jet profiles $\bar{w}_1$ is produced, and likewise in other three-dimensional sublayer motions, and it seems likely from (4.19)–(4.23) that a range of those profiles will provoke inflectional instability. It is of much interest that almost any three-dimensional hump on a surface can provoke inviscidly unstable flow past it, even for a very shallow hump (or dent, wing-body junction, injection hole, and so on).

Chapter 5

Nonlinear vortex/wave interaction in an interactive boundary layer

5.1 Introduction

The recently developed theory of vortex/wave interaction is seen as a potential breakthrough in the search for an increased rational understanding of the early stages of certain transitions to turbulence in boundary layers, or pipe and channel flows. It concerns the nonlinear interplay between the mean vortex part and the wave part of the flow, the former comprising longitudinal or streamwise vortices of a relatively long lengthscale in comparison with that of the latter. For example, when nonlinear interactions between longitudinal vortex flow and inviscid inflectional waves are considered for the incompressible boundary layer, see Hall and Smith (§4, 1991), the induced Rayleigh waves are of typical wavelength $O(Re^{-1/2})$ compared with the $O(1)$ lengthscale of the vortex motion.

Vortex/wave interaction may be categorized as weakly or strongly nonlinear. If the effect of the vortex motion is a small amplitude three-dimensional perturbation to

the original incident mean flow, the interaction is termed weakly nonlinear, whereas if the mean flow consists entirely of vortex motion, the interaction is termed strongly nonlinear. Both weakly and strongly nonlinear interactions may be further classified, depending on the nature of the wave motion to leading order. Two types of nonlinear wave contribution have been considered to date, namely Tollmien-Schlichting waves (viscous) and inflectional Rayleigh waves (inviscid), see Smith *et al* (1993), Brown *et al* (1993), and Hall and Smith (1991). Related theory by Stewart and Smith (1992) and Smith and Bowles (1992) shows good agreement with the transition experiments of Klebanoff and Tidstrom (1959) and Nishioka *et al* (1979). Other related works and comments are provided in Chapter 1.

Partly by way of an introduction to or basis for the work which follows in subsequent chapters, this chapter is given mostly over to a detailed description of the work of Smith *et al* (1993), hereinafter referred to as SBB, in which the starting process of strongly nonlinear vortex/Rayleigh-wave interaction in a laminar boundary layer is considered on a shorter lengthscale than that of previous studies; see in particular Brown *et al* (1993), and Hall and Smith (1991). However, significant temporal effects are also included. On the new shorter lengthscale the abrupt starting of the interaction is smoothed out, compared with that of the latter two references, and the bifurcation equation satisfied by the wave-pressure amplitude downstream is replaced by an integro-differential equation which, depending on the relative signs of the coefficients, possesses a solution that matches downstream. In addition, other important solution paths (transition paths) are also found.

Before setting out the problem mathematically, we call upon SBB to provide us with a brief description of what is envisaged at the start of the vortex/wave interaction:

A two-dimensional boundary layer, either classical or possibly of triple-deck or related form, has, when it attains a particular station, a streamwise velocity profile with a point of inflection (e.g. under an adverse pressure gradient). This station represents a neutral point for the corresponding two-dimensional Rayleigh equation which possesses a non-trivial eigen-

solution. The *three-dimensional* nonlinear interaction now begins, and the vortex flow develops downstream in such a way as to keep the Rayleigh wave neutral, according to the description in Brown *et al.* (1993). A critical level is initiated and persists, the developing three-dimensionality gradually eroding the inflection-point condition.

In what follows we shall restrict ourselves to a boundary layer with the interactive triple-deck structure. The reason for this particular choice is that we are concerned eventually with interactive/possibly separating basic flows and their transition, with other basic separating flows following as limiting forms of the triple-deck case.

The basic interactive motion referred to here could be steady flow past a surface-mounted hump or dent, steady flow past a convex or concave corner, steady breakaway separating flow, a nonlinear Tollmien-Schlichting unsteady motion, or so on. The precise scales involved for the triple-deck basic case prove significant in subsequent chapters.

In §5.2 the variables are defined and the Navier-Stokes equations set out in a convenient form. Subsequent sections give the solution of the Navier-Stokes equations for the various regions of the flow. In §5.3 we consider the solution within the inviscid core flow, and in §5.4 that in the viscous buffer layers which are situated above and below the critical layer. The solution in the critical layer itself is not described in detail and the reader is referred to SBB or Brown (1993) for a more indepth discussion. The matching of the solution between the various horizontal layers is completed in §5.5 and the above-mentioned integro-differential equation obtained.

For the sake of later chapters, and following on directly from the results obtained in this chapter, we complete §5.5 by considering the influence of a slow time derivative ∂_{t_1} on the wave-amplitude equation. This time derivative is absent in the original SBB approach where only spatial developments are under investigation.

Further comments and concluding remarks are made in §5.6.

5.2 The outline of the problem

The full incompressible three-dimensional Navier-Stokes equations form the basis of the problem. If L is a representative length and U a representative speed, we may write the starred dimensional Cartesian coordinates (x^*, y^*, z^*), velocity components (u^*, v^*, w^*), pressure/density ratio p^*/ρ^* and time t^* as

$$\begin{aligned}(x^*, y^*, z^*) &= L(x, y, z),\\ (u^*, v^*, w^*) &= U(u, v, w),\\ p^*/\rho^* &= U^2 p,\\ t^* &= Ut/L.\end{aligned}$$

In terms of these nondimensional quantities the Navier-Stokes equations are

$$\begin{aligned}\frac{\partial u}{\partial t} + u\frac{\partial u}{\partial x} + v\frac{\partial u}{\partial y} + w\frac{\partial u}{\partial z} &= -\frac{\partial p}{\partial x} + \frac{1}{Re}\left\{\frac{\partial^2 u}{\partial x^2} + \frac{\partial^2 u}{\partial y^2} + \frac{\partial^2 u}{\partial z^2}\right\},\\ \frac{\partial v}{\partial t} + u\frac{\partial v}{\partial x} + v\frac{\partial v}{\partial y} + w\frac{\partial v}{\partial z} &= -\frac{\partial p}{\partial y} + \frac{1}{Re}\left\{\frac{\partial^2 v}{\partial x^2} + \frac{\partial^2 v}{\partial y^2} + \frac{\partial^2 v}{\partial z^2}\right\},\\ \frac{\partial w}{\partial t} + u\frac{\partial w}{\partial x} + v\frac{\partial w}{\partial y} + w\frac{\partial w}{\partial z} &= -\frac{\partial p}{\partial z} + \frac{1}{Re}\left\{\frac{\partial^2 w}{\partial x^2} + \frac{\partial^2 w}{\partial y^2} + \frac{\partial^2 w}{\partial z^2}\right\},\\ \frac{\partial u}{\partial x} + \frac{\partial v}{\partial y} + \frac{\partial w}{\partial z} &= 0,\end{aligned} \tag{5.1}$$

where Re is the Reynolds number defined as

$$Re = \frac{UL}{\nu}$$

(assumed to be large throughout), and ν is the kinematic viscosity of the fluid.

Confined to the lower deck of the triple-deck structure where y has $O(Re^{-5/8})$ for a flow developing on a streamwise lengthscale $O(Re^{-3/8})$, there is a transverse dependence which gives a three-dimensionality to the flow on a scale $O(Re^{-5/8})$.

We write

$$x = \epsilon^3 \bar{x}, \quad y = \epsilon^5 \bar{y}, \quad z = \epsilon^5 \bar{z}, \tag{5.2}$$

where, for convenience, $\epsilon = Re^{-1/8}$.

The vortex/wave interaction solution is the sum of two contributions, namely the *wave component* of the solution and the *vortex (or mean flow) component.* The wave part of the solution has an exponential factor of the form

$$E = \exp[i(\alpha_0 X - \Omega T)], \tag{5.3}$$

where $T = \epsilon^4 t$ and the fast scale X is defined by

$$\alpha_0 X = \epsilon^{-2} \int \alpha(\bar{x}) d\bar{x}. \tag{5.4}$$

Within the lower deck of the triple-deck structure the inviscid Rayleigh-type disturbance typically has a $Re^{-5/8}$-cube scaling which justifies the definition of X in (5.4) above.

Here the *prescribed* frequency Ω is real, as is the wavenumber $\alpha(\bar{x})$ which is to be determined. The vortex part of the solution is E-independent and must satisfy conventional boundary conditions as $\bar{y} \to \infty$ and at the wall. It is linked to the wave by a jump condition on the transverse shear stress across the (unknown) critical surface $\bar{y} = f(\bar{x}, \bar{z})$ at which the streamwise velocity component has the value $\Omega/\alpha(\bar{x})$.

We now introduce the new shorter streamwise lengthscale over which the vortex/wave interaction is considered. This will enable us to examine more closely the starting process of the interaction within the lower deck. In terms of the streamwise variable $\bar{x}$ the new scaling is

$$\bar{x} = \epsilon x_1, \tag{5.5}$$

where $x_1 = O(1)$. We proceed by considering the flow within the core region and the buffer layers, in each case describing the structure and scales used. The final

result, obtained by matching the solutions in the various regions of the flow, is an integro-differential equation for the amplitude of the wave pressure.

5.3 The core region

In the core regions $x_1 = O(1)$, $\bar{y} = O(1)$, $\bar{z} = O(1)$ and in (5.1) we write

$$\begin{aligned} u &= \epsilon U_0(\bar{y}) + \epsilon^2 U_1(x_1, \bar{y}) + \ldots + \epsilon^{10/3} E\bar{u}_0 + \epsilon^{13/3} E\bar{u}_1 + \ldots, \\ v &= \epsilon^3 V_1(\bar{y}) + \epsilon^4 V_2(x_1, \bar{y}, \bar{z}) + \ldots + \epsilon^{10/3} E\bar{v}_0 + \epsilon^{13/3} E\bar{v}_1 + \ldots, \\ w &= \epsilon^4 W_1(x_1, \bar{y}, \bar{z}) + \ldots + \epsilon^{10/3} E\bar{w}_0 + \epsilon^{13/3} E\bar{w}_1 + \ldots, \\ p &= \epsilon^2 p_{00} + \epsilon^3 x_1 p_0 + \ldots + \epsilon^{13/3} E\bar{p}_0 + \epsilon^{16/3} E\bar{p}_1 + \ldots, \end{aligned} \tag{5.6}$$

where we have only specified the terms which it will be necessary to consider. In (5.6) p_{00} and p_0 are constants and $\bar{u}_0$ etc. are functions of x_1, $\bar{y}$, $\bar{z}$; the complex conjugates $\bar{u}_0^* E^{-1}$ etc. also occur in (5.6) but for simplicity have not been displayed.

Here the unperturbed flow, comprising $u = \epsilon U_0(y)$, $v = \epsilon^3 V_1(y)$ and $p = \epsilon^2 p_{00}$, is in fact a basic interactive triple-deck steady flow solution satisfying the lower deck equations

$$\frac{\partial U_0}{\partial \bar{x}} + \frac{\partial V_1}{\partial \bar{y}} = 0,$$
$$U_0 \frac{\partial U_0}{\partial \bar{x}} + V_1 \frac{\partial U_0}{\partial \bar{y}} = -\frac{dp_{00}}{d\bar{x}} + \frac{\partial^2 U_0}{\partial \bar{y}^2},$$

with

$$U_0 \sim \bar{y} + A \quad \text{as} \quad \bar{y} \to \infty,$$

the slow scale $\bar{x}$-dependence of U_0, V_1 and p_{00} not given explicitly in (5.6) above. The unknown displacement increment $-A$ is linked to the pressure p_{00} by the Cauchy-Hilbert integral

$$p_{00}(\bar{x}) = \frac{1}{\pi} \int_{-\infty}^{\infty} \frac{dA}{d\xi}(\xi) \frac{d\xi}{(\bar{x} - \xi)},$$

and we note that for shorter-scale flows A is effectively zero.

5.3.1 The vortex solution

The solutions for V_1 and U_1 are

$$V_1 = U_0(\bar{y})\left\{\int_{\bar{a}_0}^{\bar{y}} \frac{p_0 - U_0''}{U_0^2} dy + \frac{V_0}{c_0}\right\}, \tag{5.7}$$

$$-\frac{U_1}{x_1} = \frac{p_0 - U_0''}{U_0} + U_0'\left\{\int_{\bar{a}_0}^{\bar{y}} \frac{p_0 - U_0''}{U_0^2} dy + \frac{V_0}{c_0}\right\}. \tag{5.8}$$

The constant V_0 is the value of the normal velocity v at the initiation of the critical level, which has been taken here to be at $y = \bar{a}_0$, and the constant c_0 is such that $U_0(\bar{a}_0) = c_0$ and is the leading term in the expansion

$$\Omega/\alpha(x_1) = c_0 + \epsilon c_2 x_1 + \ldots.$$

Therefore, since Ω is a prescribed constant, it follows that the wavenumber $\alpha(x_1)$ is given by

$$\alpha(x_1) = \alpha_0 + \epsilon\alpha_2 x_1 + \ldots,$$

where $\alpha_0 c_2 + \alpha_2 c_0 = 0$.

5.3.2 The wave solution

The leading order pressure term $\bar{p}_0$ satisfies the Rayleigh equation

$$\frac{\partial^2 \bar{p}_0}{\partial \bar{y}^2} + \frac{\partial^2 \bar{p}_0}{\partial \bar{z}^2} - \frac{2U_0'}{(U_0 - c_0)}\frac{\partial \bar{p}_0}{\partial \bar{y}} - \alpha_0^2 \bar{p}_0 = 0 \tag{5.9}$$

such that $\bar{p}_0 \to 0$ as $\bar{y} \to \infty$ and $\partial \bar{p}_0/\partial \bar{y} = 0$ on $\bar{y} = 0$. We write

$$\bar{p}_0(x_1, \bar{y}, \bar{z}) = P_0(\bar{y})\left\{r_1(x_1)e^{i\beta_0 \bar{z}} + r_2(x_1)e^{-i\beta_0 \bar{z}}\right\} \tag{5.10}$$

for a pair of waves obliquely inclined to the mainstream direction and aim, in what follows, to find an equation relating the wave-amplitude functions $r_1(x_1)$ and $r_2(x_1)$.

We will note here that as $\bar{y} \to \bar{a}_0$ the inflectional velocity profile $U_0(\bar{y})$ is such that

$$U_0(\bar{y}) = c_0 + b_1(\bar{y} - \bar{a}_0) + \sum_{n=3}^{\infty} \frac{b_n(\bar{y} - \bar{a}_0)^n}{n!}. \tag{5.11}$$

From (5.11) it follows that as $\bar{y} \to \bar{a}_0$

$$\frac{U_1}{x_1} = \sum_{n=0}^{\infty} \frac{d_n(\bar{y} - \bar{a}_0)^n}{n!}, \qquad P_0 = 1 + \sum_{n=2}^{\infty} \frac{q_n(\bar{y} - \bar{a}_0)^n}{n!}, \tag{5.12}$$

where

$$\begin{cases} d_0 = -(p_0 + V_0 b_1)/c_0, \quad d_1 = b_3/c_0, \\ d_2 = (b_4 - V_0 b_3 - b_1 b_3/c_0)/c_0, \end{cases} \tag{5.13}$$

and

$$\begin{cases} q_2 = -(\alpha_0^2 + \beta_0^2) = -\gamma_0^2, \ \text{say}, \\ q_4 = q_2(4b_3/b_1 + 3\gamma_0^2). \end{cases} \tag{5.14}$$

The value of the constant q_3 cannot be fixed by such local expansions and instead must be obtained by integrating (5.9).

The equation satisfied by $\bar{p}_1$ is a forced Rayleigh equation of the form

$$\begin{aligned} 2\frac{\partial}{\partial x_1}\left\{\alpha_0^2\bar{p}_0 - \frac{c_0 U_0'}{(U_0 - c_0)^2}\frac{\partial \bar{p}_0}{\partial \bar{y}}\right\} \\ + 2i\alpha_0 x_1 \left\{\alpha_0\alpha_2\bar{p}_0 + \frac{1}{(U_0 - c_0)}\left\{\bar{U}_1' - \frac{(\bar{U}_1 - c_2)}{(U_0 - c_0)}U_0'\right\}\frac{\partial \bar{p}_0}{\partial \bar{y}}\right\} \\ = i\alpha_0\left\{\frac{\partial^2 \bar{p}_1}{\partial \bar{y}^2} + \frac{\partial^2 \bar{p}_1}{\partial \bar{z}^2} - \alpha_0^2\bar{p}_1 - \frac{2U_0'}{(U_0 - c_0)}\frac{\partial \bar{p}_1}{\partial \bar{y}}\right\}, \end{aligned} \tag{5.15}$$

where we have set $U_1(x_1, \bar{y}) = x_1\bar{U}_1(\bar{y})$, U_1 given in (5.8).

If we write

$$\bar{p}_1(x_1,\bar{y},\bar{z}) = P_0(\bar{y})\left\{Q_1(x_1,\bar{y})e^{i\beta_0\bar{z}} + Q_2(x_1,\bar{y})e^{-i\beta_0\bar{z}}\right\} \tag{5.16}$$

then the solution of (5.15) which satisfies the condition $\bar{p}_1(\infty) = 0$ is given by, for $\bar{y} > \bar{a}_0$,

$$\frac{\partial Q_i}{\partial \bar{y}}\frac{P_0^2}{(U_0-c_0)^2} = \int_\infty^{\bar{y}} \frac{P_0}{(U_0-c_0)^3}\left\{x_1 r_i(x_1)R_a + ic_0 r_i'(x_1)R_b\right\}dy \tag{5.17}$$

and, for $\bar{y} < \bar{a}_0$,

$$\begin{aligned}\frac{\partial Q_i}{\partial \bar{y}}\frac{P_0^2}{(U_0-c_0)^2} &= \int_0^{\bar{y}} \frac{P_0}{(U_0-c_0)^3}\left\{x_1 r_i(x_1)R_a + ic_0 r_i'(x_1)R_b\right\}dy \\ &+ \frac{P_0(0)}{c_0^2}Q_w^- r_i(x_1)\end{aligned} \tag{5.18}$$

for $i = 1,2$, where the functions $R_a(\bar{y})$ and $R_b(\bar{y})$ are defined as

$$R_a = 2\left\{\alpha_0\alpha_2(U_0-c_0)P_0 + \left(\bar{U}_1' - \frac{(\bar{U}_1-c_2)}{(U_0-c_0)}U_0'\right)P_0'\right\} \tag{5.19}$$

and

$$R_b = \frac{2}{\alpha_0}\left\{\frac{U_0'P_0'}{(U_0-c_0)} - \frac{\alpha_0^2}{c_0}(U_0-c_0)P_0\right\}. \tag{5.20}$$

The value of the constant Q_w^- in (5.18) is determined by the wall layer which, for the purpose of the following chapter, bears no great significance. We therefore refer the reader to Appendix A of SBB where the result

$$Q_w^- = -\gamma_0^2 P_0(0)(-i\alpha_0 c_0)^{-1/2} \tag{5.21}$$

is obtained.

The integrands in (5.17) and (5.18) have triple poles at $\bar{y} = \bar{a}_0$ and it can be shown that near $\bar{y} = \bar{a}_0$

$$R_a \frac{P_0}{(U_0 - c_0)^3} = \frac{a_{-3}}{(\bar{y} - \bar{a}_0)^3} + \frac{a_{-2}}{(\bar{y} - \bar{a}_0)^2} + \frac{a_{-1}}{(\bar{y} - \bar{a}_0)} + O(1), \tag{5.22}$$

$$R_b \frac{P_0}{(U_0 - c_0)^3} = \frac{b_{-3}}{(\bar{y} - \bar{a}_0)^3} + \frac{b_{-2}}{(\bar{y} - \bar{a}_0)^2} + \frac{b_{-1}}{(\bar{y} - \bar{a}_0)} + O(1), \tag{5.23}$$

where

$$\begin{cases} a_{-3} &= 2q_2(c_2 - d_0)/b_1^3, \\ a_{-2} &= \{q_3(c_2 - d_0) - 2\alpha_0^2 b_1 c_2/c_0\}/b_1^3, \\ a_{-1} &= \{d_2 q_2 + (d_0 - c_2)(b_3 q_2/3b_1 - q_4/3 - q_2)\}/b_1^3, \\ b_{-3} &= 2q_2/\alpha_0 b_1^3, \\ b_{-2} &= q_3/\alpha_0 b_1^3 - 2\alpha_0/b_1^2 c_0, \\ b_{-1} &= b_3 q_2/\alpha_0 b_1^4. \end{cases} \tag{5.24}$$

In fact, in matching the solution in the buffer layers with that of the core we find that a_{-1} vanishes, as will be shown in § 5.4. Combining (5.17), (5.18), (5.22) and (5.23), as $\bar{y} \to \bar{a}_0^{\pm}$ $\bar{p}_1$ takes the form

$$\begin{aligned} \bar{p}_1(x_1, \bar{y}, \bar{z}) &- \bar{p}_1(x_1, \bar{a}_0, \bar{z}) \\ &\approx b_1^2(\bar{y} - \bar{a}_0)\left\{x_1 r_1(x_1)\left[-\frac{a_{-3}}{2} - \frac{a_{-2}}{2}(\bar{y} - \bar{a}_0) + \frac{1}{3}G_a^{\pm}(\bar{y} - \bar{a}_0)^2\right]\right. \\ &+ ic_0 r_1'(x_1)\left[-\frac{b_{-3}}{2} - \frac{b_{-2}}{2}(\bar{y} - \bar{a}_0) + \frac{b_{-1}}{3}(\bar{y} - \bar{a}_0)^2 \log|\bar{y} - \bar{a}_0|\right. \\ &\left.\left. + \frac{1}{3}G_b^{\pm}(\bar{y} - \bar{a}_0)^2\right] + \frac{P_0(0)}{3c_0^2}Q_w^{\pm} r_1(x_1)(\bar{y} - \bar{a}_0)^2\right\} e^{i\beta_0 \bar{z}} \\ &+ b_1^2(\bar{y} - \bar{a}_0)\left\{x_1 r_2(x_1)\left[-\frac{a_{-3}}{2} - \frac{a_{-2}}{2}(\bar{y} - \bar{a}_0) + \frac{1}{3}G_a^{\pm}(\bar{y} - \bar{a}_0)^2\right]\right. \\ &+ ic_0 r_2'(x_1)\left[-\frac{b_{-3}}{2} - \frac{b_{-2}}{2}(\bar{y} - \bar{a}_0) + \frac{b_{-1}}{3}(\bar{y} - \bar{a}_0)^2 \log|\bar{y} - \bar{a}_0|\right. \\ &\left.\left. + \frac{1}{3}G_b^{\pm}(\bar{y} - \bar{a}_0)^2\right] + \frac{P_0(0)}{3c_0^2}Q_w^{\pm} r_2(x_1)(\bar{y} - \bar{a}_0)^2\right\} e^{-i\beta_0 \bar{z}}, \end{aligned} \tag{5.25}$$

where Q^+ is zero, Q^- is given by (5.21), and $G_a^{\pm}$ and $G_b^{\pm}$ are constants whose differences we will need later. The values of these differences are

$$\begin{aligned} G_a^+ - G_a^- &= -\int_0^\infty \left\{ \frac{R_a P_0}{(U_0 - c_0)^3} - \frac{a_{-3}}{(\bar{y} - \bar{a}_0)^3} - \frac{a_{-2}}{(\bar{y} - \bar{a}_0)^2} \right\} d\bar{y} \\ &\quad - \frac{a_{-3}}{2\bar{a}_0^2} + \frac{a_{-2}}{\bar{a}_0} \end{aligned} \tag{5.26}$$

and

$$\begin{aligned} G_b^+ - G_b^- &= -\int_0^\infty \left\{ \frac{R_b P_0}{(U_0 - c_0)^3} - \frac{b_{-3}}{(\bar{y} - \bar{a}_0)^3} - \frac{b_{-2}}{(\bar{y} - \bar{a}_0)^2} - \frac{2b_{-1}\bar{a}_0}{(\bar{y}^2 - \bar{a}_0^2)} \right\} d\bar{y} \\ &\quad - \frac{b_{-3}}{2\bar{a}_0^2} + \frac{b_{-2}}{\bar{a}_0}, \end{aligned} \tag{5.27}$$

where R_a and R_b are defined in (5.19) and (5.20) respectively.

5.4 The buffer layers

The buffer layers are sandwiched between the core region and the critical layer and it is here that the mean (vortex) flow feels viscous effects at leading order, implying that, for $x_1 = O(1)$, the appropriate $\bar{y}$-scaling takes the form

$$\bar{y} - f(x_1, \bar{z}) = \epsilon^{1/2} \mathrm{Y}, \tag{5.28}$$

where $f(x_1, \bar{z}) = \bar{a}_0 + \epsilon \bar{a}_2 x_1 + \ldots$. We write

$$\begin{aligned} u &= \epsilon c_0 + \epsilon^{3/2} b_1 \mathrm{Y} + \epsilon^2 c_2 x_1 + \epsilon^{5/2} b_3 \left(\frac{1}{6}\mathrm{Y}^3 + \frac{x_1 \mathrm{Y}}{c_0} \right) + \epsilon^3 u_4 + \ldots \\ &\qquad + E\epsilon^{17/6} \left[\tilde{u}_0 + \epsilon^{1/2}\tilde{u}_1 + \epsilon \tilde{u}_2 + \epsilon^{3/2}\tilde{u}_3 + \ldots \right] + \ldots, \\ v &= \epsilon^3 V_0 + \epsilon^{7/2}(\bar{a}_2 b_1 - c_2)\mathrm{Y} + \epsilon^4 v_2 + \ldots + E\epsilon^{10/3} \left[\tilde{v}_0 + \epsilon^{1/2}\tilde{v}_1 + \epsilon \tilde{v}_2 + \ldots \right] + \ldots, \\ w &= \epsilon^{7/2} w_0 + \ldots + E\epsilon^{17/6} \left[\tilde{w}_0 + \epsilon^{1/2}\tilde{w}_1 + \epsilon \tilde{w}_2 + \ldots \right] + \ldots, \\ p &= \epsilon^2 p_{00} + \epsilon^3 p_0 x_1 + \ldots + \epsilon^{13/3} E \left[\tilde{p}_0 + \epsilon^{1/2}\tilde{p}_1 + \epsilon \tilde{p}_2 + \epsilon^{3/2}\tilde{p}_3 + \epsilon^2 \tilde{p}_4 + \epsilon^{5/2}\tilde{p}_5 + \ldots \right] + \ldots, \end{aligned} \tag{5.29}$$

where, again for simplicity, terms in E^{-1}, E^2, etc. have not been displayed. The powers of ϵ in (5.29) and some of the E-independent terms have been anticipated from the solution in the core region, in particular, if we consider the normal velocity component v, a match between the two regions implies

$$c_0 c_2 = -b_1(V_0 - \bar{a}_2 c_0) - p_0. \tag{5.30}$$

5.4.1 The vortex solution

The equation for w_0 is obtained from the $\bar{z}$-momentum equation as the diffusion equation

$$c_0 \frac{\partial w_0}{\partial x_1} = \frac{\partial^2 w_0}{\partial \mathrm{Y}^2} \tag{5.31}$$

with the conditions $w_0 \to 0$ as $|\mathrm{Y}| \to \infty$ and as $x_1 \to -\infty$. As in SBB we will assume that w_0 is continuous across $\mathrm{Y} = 0$ but that the critical layer forces a jump, $J_0(x_1, \bar{z})$ say, in $\partial w_0/\partial \mathrm{Y}$ across $\mathrm{Y} = 0$. To justify this assumption we refer the reader to Appendix B of SBB where the solution in the critical layer is discussed in detail. If we define the Fourier transform of w_0 with respect to x_1 to be

$$\mathcal{F}(w_0) = \int_{-\infty}^{\infty} w_0(x_1, \mathrm{Y}, \bar{z}) e^{-i\omega x_1} dx_1$$

with parameter ω, then (5.31) implies

$$\mathcal{F}(w_0) = -\frac{\mathcal{F}(J_0)}{2(ic_0\omega_1)^{1/2}} \exp[-(ic_0\omega_1)^{1/2}|\mathrm{Y}|] \tag{5.32}$$

where $i^{1/2} = e^{i\pi/4}$, $\omega_1 = \omega - i\tau$, τ being a small positive parameter, and $\omega_1^{1/2}$ is real and positive when ω is large, real and positive. Therefore,

$$w_0 = -\frac{1}{2(\pi c_0)^{1/2}} \int_{-\infty}^{x_1} \frac{J_0(s, \bar{z})}{(x_1 - s)^{1/2}} \exp[-c_0 \mathrm{Y}^2/4(x_1 - s)] ds. \tag{5.33}$$

The continuity equation gives us

$$\frac{\partial v_2}{\partial \mathrm{Y}} = -\frac{\partial w_0}{\partial \bar{z}} - \frac{b_3 \mathrm{Y}}{c_0},$$

from which it follows that

$$v_2 = -\frac{1}{2}\frac{b_3}{c_0}\mathrm{Y}^2 - \frac{\partial}{\partial \bar{z}}\int_0^{\mathrm{Y}} w_0 dy - A_4(x_1, \bar{z}), \tag{5.34}$$

where $A_4(x_1, \bar{z})$ is an arbitrary function which gives the value of v_2 at the critical level.

Finally, from the $\bar{x}$-momentum equation we obtain a forced diffusion equation for u_4, namely

$$\begin{aligned} c_0\frac{\partial u_4}{\partial x_1} - \frac{\partial^2 u_4}{\partial \mathrm{Y}^2} &= -\frac{1}{2}b_3\mathrm{Y}^2\left(\frac{b_1}{c_0} + V_0 - \bar{a}_2 c_0\right) + b_1\frac{\partial}{\partial \bar{z}}\int_0^{\mathrm{Y}} w_0 dy \\ &\quad + \bar{A}_4(x_1, \bar{z}), \end{aligned} \tag{5.35}$$

where $\bar{A}_4(x_1, \bar{z})$ is a combination of $A_4(x_1, \bar{z})$ and linear terms in x_1. If we write

$$u_4 = \bar{\bar{u}}_4 + b_3\frac{\mathrm{Y}^4}{24}\left(\frac{b_1}{c_0} + V_0 - \bar{a}_2 c_0\right) + \frac{1}{c_0}\int \bar{A}_4 dx_1 \tag{5.36}$$

then it follows that

$$c_0\frac{\partial \bar{\bar{u}}_4}{\partial x_1} - \frac{\partial^2 \bar{\bar{u}}_4}{\partial \mathrm{Y}^2} = b_1\frac{\partial}{\partial \bar{z}}\int_0^{\mathrm{Y}} w_0 dy. \tag{5.37}$$

We require that the term $O(\mathrm{Y}^4)$ in (5.36) matches with the term $O(y^4)$ of $U_0(y)$ in the core, therefore implying that

$$b_4 = b_3\left(\frac{b_1}{c_0} + V_0 - \bar{a}_2 c_0\right).$$

This, together with (5.13), leads to the vanishing of a_{-1} in (5.24).

5.4.2 The wave solution

Our aim in this section is to obtain an expression for $\tilde{p}_5$ in (5.29) and in particular the terms in $\tilde{p}_5$ of $O(|\mathrm{Y}|^3)$ which must match, as $|\mathrm{Y}| \to \infty$, with those $O(\bar{y} - \bar{a}_0)^3$ in (5.25) as $\bar{y} \to \bar{a}_0^{\pm}$.

The early E-dependent terms in (5.29) are easily obtained by direct matching with the solution in the core. We deduce that

$$\tilde{p}_0 = \bar{p}_0(x_1, \bar{a}_0, \bar{z}), \quad \tilde{p}_1 = 0. \tag{5.38}$$

It then follows that

$$\begin{aligned} \tilde{w}_0 = \frac{i}{\alpha_0 b_1 \mathrm{Y}} \frac{\partial \tilde{p}_0}{\partial \bar{z}}, \quad \tilde{v}_0 &= \frac{i}{\alpha_0 b_1} \left(\frac{\partial^2 \tilde{p}_0}{\partial \bar{z}^2} - \alpha_0^2 \tilde{p}_0 \right), \\ \tilde{u}_0 = \frac{i}{\alpha_0} \frac{\partial \tilde{w}_0}{\partial \bar{z}}, \quad \tilde{p}_2 &= -\frac{1}{2} i \alpha_0 b_1 \tilde{v}_0 \mathrm{Y}^2 + \bar{p}_1(x_1, \bar{a}_0, \bar{z}), \end{aligned} \tag{5.39}$$

and

$$\begin{aligned} \tilde{w}_1 = \frac{i}{\alpha_0 b_1 \mathrm{Y}} \left(c_0 \frac{\partial \tilde{w}_0}{\partial x_1} - \frac{\partial^2 \tilde{w}_0}{\partial \mathrm{Y}^2} \right), \quad \tilde{v}_1 &= \frac{1}{2} \frac{q_3}{q_2} \tilde{v}_0 \mathrm{Y}, \\ \tilde{u}_1 = \frac{i}{\alpha_0} \left(\frac{\partial \tilde{w}_1}{\partial \bar{z}} + \frac{1}{2} \frac{q_3}{q_2} \tilde{v}_0 \right), & \\ \tilde{p}_3 = -\frac{1}{6} i \alpha_0 b_1 \tilde{v}_0 \frac{q_3}{q_2} \mathrm{Y}^3 - c_0 \mathrm{Y} \frac{\partial \tilde{v}_0}{\partial x_1} + \hat{p}_3(x_1, \bar{z}), & \end{aligned} \tag{5.40}$$

where the arbitrary function $\hat{p}_3(x_1, \bar{z})$ is of no consequence. The expressions for $\tilde{w}_2$, $\tilde{v}_2$, $\tilde{u}_2$ and $\tilde{p}_4$ are more complicated and only needed as steps in obtaining the required information, namely $\tilde{p}_5$. For this reason we will omit their details here and refer the reader to Brown (1993) for a more lengthy discussion, moving straight to the equation for $\tilde{p}_5$ which is

$$\frac{\partial^2 \tilde{p}_5}{\partial \mathrm{Y}^2} - \frac{2}{\mathrm{Y}} \frac{\partial \tilde{p}_5}{\partial \mathrm{Y}} = \frac{c_0 b_3}{b_1} \mathrm{Y} \frac{\partial \tilde{v}_0}{\partial x_1} - 2 i \alpha_0 \left[\tilde{v}_0 \left(\frac{\partial \bar{\tilde{u}}_4}{\partial \mathrm{Y}} - \frac{1}{\mathrm{Y}} \bar{\tilde{u}}_4 \right) + \tilde{w}_0 \frac{\partial \bar{\tilde{u}}_4}{\partial \bar{z}} \right]. \tag{5.41}$$

On the righthand side of (5.41) only the terms with factors $\bar{\tilde{u}}_4$ or $O(\mathrm{Y})$ have been included since, as mentioned above, it is the terms of this nature which are required for the match of the solution with that in the core region.

On integrating (5.41) we get

$$\begin{aligned}\frac{1}{\mathrm{Y}^2}\frac{\partial \tilde{p}_5}{\partial \mathrm{Y}} &- \frac{ib_3c_0}{\alpha_0 b_1^2}\log|\mathrm{Y}|\frac{\partial}{\partial x_1}\left(\frac{\partial^2\tilde{p}_0}{\partial \bar{z}^2} - \alpha_0^2\tilde{p}_0\right) \\ &= \frac{1}{b_1}\left(\frac{\partial^2\tilde{p}_0}{\partial \bar{z}^2} - \alpha_0^2\tilde{p}_0\right)\left[\frac{1}{\mathrm{Y}^2}\left(\bar{\bar{u}}_4 - \mathrm{Y}\frac{\partial \bar{\bar{u}}_4}{\partial \mathrm{Y}}\right) + \int_0^{\mathrm{Y}}\frac{1}{\mathrm{Y}}\frac{\partial^2\bar{\bar{u}}_4}{\partial \mathrm{Y}^2}d\mathrm{Y}\right] \\ &- \frac{1}{b_1}\left(\frac{\partial \tilde{p}_0}{\partial \bar{z}}\frac{\partial}{\partial \bar{z}}\right)\left[\frac{1}{\mathrm{Y}^2}\left(\bar{\bar{u}}_4 + \mathrm{Y}\frac{\partial \bar{\bar{u}}_4}{\partial \mathrm{Y}}\right) - \int_0^{\mathrm{Y}}\frac{1}{\mathrm{Y}}\frac{\partial^2\bar{\bar{u}}_4}{\partial \mathrm{Y}^2}d\mathrm{Y}\right] \\ &+ D^{\pm}(x_1,\bar{z}),\end{aligned} \tag{5.42}$$

according as $\mathrm{Y} < 0$ or $\mathrm{Y} > 0$. It can be shown that $\bar{\bar{u}}_4$ is an odd function of Y, and that

$$\int_0^{\infty}\frac{1}{\mathrm{Y}}\frac{\partial^2\bar{\bar{u}}_4}{\partial \mathrm{Y}^2}d\mathrm{Y} = \frac{b_1}{4c_0}\frac{\partial}{\partial \bar{z}}T_0(x_1,\bar{z}) \tag{5.43}$$

where

$$T_0(x_1,\bar{z}) = \int_{-\infty}^{x_1} J_0(s,\bar{z})ds. \tag{5.44}$$

The term in $\tilde{p}_5$ of order $|\mathrm{Y}|^3$ is needed both as $|\mathrm{Y}| \to \infty$ (to match with the core region) and as $|\mathrm{Y}| \to 0$ (to match with the critical layer). We see from (5.42), (5.43) and (5.44) that the constant term on the righthand side of (5.42) required to give the match is, for $|\mathrm{Y}| \ll 1$,

$$D^{\pm}(x_1,\bar{z}) \tag{5.45}$$

and, for $|\mathrm{Y}| \gg 1$,

$$D^{\pm}(x_1,\bar{z}) \pm \frac{1}{4c_0}\left\{\left(\frac{\partial^2\tilde{p}_0}{\partial \bar{z}^2} - \alpha_0^2\tilde{p}_0\right)\frac{\partial T_0}{\partial \bar{z}} + \frac{\partial \tilde{p}_0}{\partial \bar{z}}\frac{\partial^2 T_0}{\partial \bar{z}^2}\right\} \tag{5.46}$$

according as $\mathrm{Y} < 0$ or $\mathrm{Y} > 0$. The match with the critical layer determines the difference $D^+ - D^-$, namely

$$D^+ - D^- = (i\pi)\frac{ib_3c_0}{\alpha_0 b_1^2}\frac{\partial}{\partial x_1}\left(\frac{\partial^2\tilde{p}_0}{\partial \bar{z}^2} - \alpha_0^2\tilde{p}_0\right). \tag{5.47}$$

In the following section we match the terms of order $|\mathrm{Y}|^3$ in $\tilde{p}_5$ to the corresponding terms of the solution in the core.

5.5 The matching and the final equation

On matching the difference in the terms in $|\mathrm{Y}|^3$ for the buffer layers and the core region we obtain

$$\begin{aligned} D^+ - D^- + \frac{1}{2c_0}\left\{\left(\frac{\partial^2\tilde{p}_0}{\partial\bar{z}^2} - \alpha_0^2\tilde{p}_0\right)\frac{\partial T_0}{\partial\bar{z}} + \frac{\partial\tilde{p}_0}{\partial\bar{z}}\frac{\partial^2 T_0}{\partial\bar{z}^2}\right\} \\ = b_1^2\left\{x_1 r_1(x_1)\left(G_a^+ - G_a^-\right) + ic_0 r_1'(x_1)\left(G_b^+ - G_b^-\right) - \frac{P_0(0)}{c_0^2}Q_w^- r_1(x_1)\right\}\hat{E} \\ + b_1^2\left\{x_1 r_2(x_1)\left(G_a^+ - G_a^-\right) + ic_0 r_2'(x_1)\left(G_b^+ - G_b^-\right) - \frac{P_0(0)}{c_0^2}Q_w^- r_2(x_1)\right\}\hat{E}^{-1}, \end{aligned} \tag{5.48}$$

where $\hat{E} = e^{i\beta_0\bar{z}}$.

The jump $J_0(x_1,\bar{z})$ in $\partial w_0/\partial\bar{z}$ across $\mathrm{Y}=0$ forced by the presence of a critical layer is derived in Appendix B of SBB. Here we simply quote the result

$$J_0(x_1,\bar{z}) = \frac{2\pi(2/3)^{2/3}(-2/3)!}{(\alpha_0 b_1)^{5/3}}\frac{\partial}{\partial\bar{z}}\left(\left|\frac{\partial\tilde{p}_0}{\partial\bar{z}}\right|^2\right). \tag{5.49}$$

On setting $\tilde{p}_0 = r_1(x_1)e^{i\beta_0\bar{z}} + r_2(x_1)e^{-i\beta_0\bar{z}}$ and equating terms in $e^{i\beta_0\bar{z}}$ and $e^{-i\beta_0\bar{z}}$ respectively in (5.48), we obtain two integro-differential equations linking $r_1(x_1)$ and $r_2(x_1)$, namely

$$\begin{aligned} \frac{\pi b_3\gamma_0^2 c_0}{\alpha_0 b_1^2}r_1'(x_1) + \frac{4\pi(2/3)^{2/3}(-2/3)!}{c_0(\alpha_0 b_1)^{5/3}}\beta_0^4(2\beta_0^2 - \gamma_0^2)r_2(x_1)\int_{-\infty}^{x_1} r_1(s)r_2^*(s)ds \\ = b_1^2\left\{x_1 r_1(x_1)(G_a^+ - G_a^-) + ic_0 r_1'(x_1)(G_b^+ - G_b^-) - \frac{Q_w^-}{c_0^2}r_1(x_1)\right\}, \end{aligned} \tag{5.50}$$

and

$$\frac{\pi b_3\gamma_0^2 c_0}{\alpha_0 b_1^2}r_2'(x_1) + \frac{4\pi(2/3)^{2/3}(-2/3)!}{c_0(\alpha_0 b_1)^{5/3}}\beta_0^4(2\beta_0^2-\gamma_0^2)r_1(x_1)\int_{-\infty}^{x_1} r_1^*(s)r_2(s)ds$$
$$= b_1^2\left\{x_1 r_2(x_1)(G_a^+ - G_a^-) + ic_0 r_2'(x_1)(G_b^+ - G_b^-) - \frac{Q_w^-}{c_0^2}r_2(x_1)\right\}. \tag{5.51}$$

Here the constant Q_w^- is given by (5.21), noting that $P_0(0) = 1$, $(G_a^+ - G_a^-)$ and $(G_b^+ - G_b^-)$ are given by (5.26) and (5.27) respectively, and r_1^* denotes the complex conjugate of r_1.

If however $r_1 \equiv r_2$, $\tilde{p}_0$ can be written in the form

$$\tilde{p}_0 = r(x_1)\cos\beta_0\bar{z}. \tag{5.52}$$

It then follows that on equating terms in $\cos\beta_0\bar{z}$ in (5.48) we obtain the equation satisfied by $r(x_1)$, namely

$$\frac{\pi b_3\gamma_0^2 c_0}{\alpha_0 b_1^2}r'(x_1) + \frac{\pi(2/3)^{2/3}(-2/3)!}{c_0(\alpha_0 b_1)^{5/3}}\beta_0^4(2\beta_0^2-\gamma_0^2)r(x_1)\int_{-\infty}^{x_1}|r^2(s)|ds$$
$$= b_1^2\left\{x_1 r(x_1)(G_a^+ - G_a^-) + ic_0 r'(x_1)(G_b^+ - G_b^-) - \frac{Q_w^-}{c_0^2}r(x_1)\right\} \tag{5.53}$$

where $r \equiv 2r_1$, accounting for the factor 4 which appears in (5.50) and (5.51) but not in (5.53).

It is equation (5.53) which forms the basis of the work carried out in Chapter 6, in which the behaviour of the solution is investigated for small α_0, and subsequent work.

Before concluding this chapter, and in preparation for the next, we consider here the additional influence of a slow time derivative ∂_{t_1} accompanying the slow spatial

derivative ∂_{x_1}.This is found to entail replacing the operator $c_0\partial_{x_1}$ with the operator $\partial_{t_1}+c_0\partial_{x_1}$ on the lefthand side of (5.53), along with a corresponding replacement of the operator $(G_b^+-G_b^-)c_0\partial_{x_1}$ with $(G_c^+-G_c^-)\partial_{t_1}+(G_b^+-G_b^-)c_0\partial_{x_1}$ on the righthand side, thus yielding the equation

$$\begin{aligned}\mathrm{K}_1\left(\frac{\partial r}{\partial t_1}+c_0\frac{\partial r}{\partial x_1}\right)+\mathrm{K}_2\,r(x_1,t_1)\int_{-\infty}^{x_1}|r^2(s,t_1)|ds\\ =b_1^2\left\{x_1(G_a^+-G_a^-)\,r(x_1,t_1)+i(G_b^+-G_b^-)c_0\frac{\partial r}{\partial x_1}+i(G_c^+-G_c^-)\frac{\partial r}{\partial t_1}\right\}\\ -b_1^2\frac{Q_w^-}{c_0^2}r(x_1,t_1),\end{aligned}\tag{5.54}$$

in place of (5.53), for the time-dependent wave-amplitude function $r(x_1,t_1)$. Here

$$\begin{aligned}\mathrm{K}_1&=\frac{\pi b_3\gamma_0^2}{\alpha_0 b_1^2},\\ \mathrm{K}_2&=\frac{\pi(2/3)^{2/3}(-2/3)!}{c_0(\alpha_0 b_1)^{5/3}}\beta_0^4(2\beta_0^2-\gamma_0^2),\end{aligned}$$

and, analogously with (5.20) and (5.27),

$$\begin{aligned}(G_c^+-G_c^-)&=-\int_0^\infty\frac{R_cP_0}{(U_0-c_0)^3}d\bar{y},\\ R_c&=\frac{2}{\alpha_0}\frac{U_0'P_0'}{(U_0-c_0)}.\end{aligned}\tag{5.55}$$

We leave this result for the moment, referring back to it in §6.7 of the proceeding chapter.

5.6 Additional comments

In summary, the present chapter has examined the starting process of strongly nonlinear vortex/Rayleigh-wave interaction in an interactive boundary layer on a streamwise lengthscale shorter than that considered by previous works (see Brown

et al (1993) and Hall and Smith (1991)), the main outcome being the integro-differential equation (5.53) for the amplitude of the wave pressure. In particular, this chapter has concentrated on the flow structure and scales appropriate to an otherwise laminar steady triple-deck motion. Extra temporal dependence has also been included however, as in (5.54), and a similar extension holds for the case of two unequal waves in (5.50), (5.51).

In the next chapter we move on to consider the same nonlinear vortex/wave interaction or transition process as above, this time reducing the wavenumber α in order that such a transition process occurs closer to the point at which the inflectional instability first appears.

Chapter 6

Analysis of the new vortex/wave interaction for small wavenumbers

6.1 Introduction

The integro-differential equation (5.53), derived in the previous chapter and obtained in SBB (1993), is the starting point for the investigation carried out in this chapter. Our original aim in conducting this particular part of the study was ultimately to link up the work of SBB, more specifically the triple-deck basic flow as described in Chapter 5, with pure three-dimensional unsteady triple-deck flow and its shortscale waves and nonlinear finite-time break-up. Along the way some more interesting new features were/are found to emerge, based essentially on the extension of (5.53) to (5.54), and these are described in the following.

Our investigation is based on the assumption that

$$\alpha = \alpha_0 + \epsilon\alpha_2 x_1 + \ldots,$$

$$\beta = \beta_0 + \ldots,$$

which represent the two wavenumbers in the direction of and transverse to the mainstream flow respectively, are comparable at leading order throughout ($\alpha_0 \sim \beta_0$). We consider the results of Chapter 5 for small α, β, effectively taking $\alpha_0 \ll 1$ and $\beta_0 \ll 1$ in the integro-differential wave-pressure amplitude equation (5.53). In other words, if we put $\gamma_0^2 = \alpha_0^2 + \beta_0^2$ essentially we are considering the case of γ_0 small.

The reason we choose to take this approach is that we are interested in what transition processes can occur as inflectional instability first appears. That first appearance, or onset, happens for small Rayleigh wavenumbers or relatively long waves (Smith and Bodonyi (1985), Tutty and Cowley (1986)), and is also connected with the nonlinear finite-time break-up phenomenon of Smith (1988) in two dimensions. Physically we might expect nonlinear three-dimensional transition processes such as vortex/wave interactions to be more relevant if they arise early (close to such a first inflectional-instability point) rather than later (as at a fully fledged inflectional-instability point), the latter being the situation addressed in SBB and in the previous chapter. Our focus is now on the former onset stage.

In the pursuit of clarity we need to simplify our notation by writing α, β and γ hereinafter when referring to the terms α_0, β_0 and γ_0 respectively of Chapter 5 since we are concerned only with the behaviour of the wavenumbers to leading order.

First, with the same structure and scales as those of Chapter 5, we begin by discussing the wave and vortex solutions within the core region of the flow for small wavenumbers. By dividing the core into two further regions (or tiers) and matching accordingly we are able to understand the response of the coefficients in (5.53) at small α, γ. In doing so we highlight some important features, indeed restrictions, of SBB and related work which are eliminated when we then proceed to consider the flow on a new lengthscale; this elimination therefore further generalizes the application of vortex/Rayleigh-wave interactions in interactive boundary layer flows. Moreover, the investigation yields particular situations in which the coefficients in the wave-pressure amplitude equation can be derived more explicitly than in SBB.

In §6.2 the wave solution in the core is obtained for small wavenumbers, employing the same structure and scales as in Chapter 5. Here it is shown that before the wave-pressure amplitude equation is derived at second order, at leading order the scaled input frequency Ω of the Rayleigh wave is fixed in terms of the inflectional velocity profile and the known inflectional speeds, thus implying that (5.53) can only hold for certain input frequencies.

The corresponding core vortex-solution is outlined in §6.3, yielding the behaviour of the vortex velocity components, denoted U_v, V_v, W_v, in terms of α, ℓ and Δ; ℓ the x_1-scale, Δ the p_v-scale, p_v the leading order pressure-vortex term. In §6.4 we analyse the integro-differential equation (5.53) for small α, β, γ, and obtain the behaviour of x_1 and p_v, and hence U_v, V_v, W_v, in terms of α alone, as required.

Second, a new regime, distinct from that of Chapter 5, is then set up in which $\alpha \sim \epsilon^{2/3}$. §6.5 describes the reasoning behind this choice of α and outlines the scales involved. The wave-pressure amplitude equation is then obtained for this new regime, consisting of the integro-differential equation of Chapter 5 combined with the equation obtained for γ in (6.16) of §6.2; both now seen acting together at leading order. Other regimes arising at even smaller values of α are also identified in §6.6.

Finally, in §6.7 we briefly interpret the work of §6.5 in terms of a new spatio-temporal form which seems appropriate to an initial-value problem, generalizing from the fixed frequency setting used hitherto in this work and other works on vortex/wave interactions.

6.2 The core wave-solution for small wavenumbers

With the same structure and scales as those of Chapter 5, the leading order wave part of the pressure solution in the core region satisfies the equation

$$\frac{\partial^2 p}{\partial \bar{y}^2} - \frac{2U'}{(U-c)}\frac{\partial p}{\partial \bar{y}} - \gamma^2 p = 0 \tag{6.1}$$

with boundary conditions $p(\infty) = 0$ and $\partial p/\partial \bar{y}(0) = 0$. Again, for the sake of a more simple notation we have replaced U_0, c_0 and $\bar{p}_0$ of Chapter 5 with U, c and p.

For $\gamma \ll 1$ we further subdivide the core region into a two-tier structure as described in §6.2.1 and §6.2.2 and obtain the solution of (6.1) in each of the tiers, matching accordingly. Expanding in terms of the now small parameter α we write

$$\gamma = \alpha\hat{\gamma}_0 + \alpha^2\hat{\gamma}_1 + \alpha^3\hat{\gamma}_2 + \ldots, \tag{6.2}$$

$$c = \hat{c}_0 + \alpha\hat{c}_1 + \alpha^2\hat{c}_2 + \ldots, \tag{6.3}$$

where $\hat{\gamma}_0$ etc. are constants and $\hat{c}_0$ etc. are known inflectional speeds.

6.2.1 The outer-tier solution

Here $\bar{y} = \alpha^{-1}\tilde{y}$ where $\tilde{y} = O(1)$, $U \sim (\tilde{y} + A)$ where A is a constant, and in terms of α

$$p = \hat{p}_0(x_1, \tilde{y}, \bar{z}) + \alpha\hat{p}_1(x_1, \tilde{y}, \bar{z}) + \alpha^2\hat{p}_2(x_1, \tilde{y}, \bar{z}) + \ldots. \tag{6.4}$$

On substituting (6.2)–(6.4) into (6.1), along with the scaling for $\bar{y}$ and the approximation to U, we obtain at first order an equation for $\hat{p}_0$, namely

$$\frac{\partial^2 \hat{p}_0}{\partial \tilde{y}^2} - \frac{2}{\tilde{y}}\frac{\partial \hat{p}_0}{\partial \tilde{y}} - \hat{\gamma}_0^2\hat{p}_0 = 0. \tag{6.5}$$

The solution to (6.5) satisfying the boundary conditions $\hat{p}_0(\infty) = 0$ and $\partial\hat{p}_0/\partial\tilde{y}(0) = 0$ is

$$\hat{p}_0 = \hat{P}_0(x_1, \bar{z})(1 + \hat{\gamma}_0\tilde{y})e^{-\hat{\gamma}_0\tilde{y}}. \tag{6.6}$$

As $\tilde{y} \to 0$ the form of $\hat{p}_0$ which we must match with the solution in the inner tier as $\bar{y} \to \infty$ is

$$\hat{p}_0 \approx \hat{P}_0(x_1, \bar{z})\left(1 - \frac{1}{2}\hat{\gamma}_0^2\tilde{y}^2 + \frac{1}{3}\hat{\gamma}_0^3\tilde{y}^3 \ldots\right). \tag{6.7}$$

We now consider the wave solution in the inner tier of the core.

6.2.2 The inner-tier solution

In this tier $\bar{y}$ remains $O(1)$ and U and p take the forms

$$U = \hat{U}_0(\bar{y}) + \alpha\hat{U}_1(\bar{y}) + \alpha^2\hat{U}_2(\bar{y}) + \ldots, \tag{6.8}$$

$$p = \hat{P}_0(x_1, \bar{z}) + \alpha^2\hat{P}_2(x_1, \bar{y}, \bar{z}) + \alpha^3\hat{P}_3(x_1, \bar{y}, \bar{z}) + \ldots, \tag{6.9}$$

the leading order term $\hat{P}_0(x_1, \bar{z})$ of p having been anticipated from the solution in the outer tier. On substituting (6.2), (6.3), (6.8) and (6.9) into (6.1) we obtain at first and second order

$$\frac{\partial^2\hat{P}_2}{\partial\bar{y}^2} - \frac{2\hat{U}_0'}{(\hat{U}_0 - \hat{c}_0)}\frac{\partial\hat{P}_2}{\partial\bar{y}} - \hat{\gamma}_0^2\hat{P}_0 = 0, \tag{6.10}$$

$$\frac{\partial^2\hat{P}_3}{\partial\bar{y}^2} - \frac{2\hat{U}_0'}{(\hat{U}_0 - \hat{c}_0)}\frac{\partial\hat{P}_3}{\partial\bar{y}} + \frac{2\hat{U}_0'(\hat{U}_1 - \hat{c}_1)}{(\hat{U}_0 - \hat{c}_0)^2}\frac{\partial\hat{P}_2}{\partial\bar{y}} - \frac{2\hat{U}_1'}{(\hat{U}_0 - \hat{c}_0)}\frac{\partial\hat{P}_2}{\partial\bar{y}} - 2\hat{\gamma}_0\hat{\gamma}_1\hat{P}_0 = 0. \tag{6.11}$$

From (6.10)

$$\frac{\partial\hat{P}_2}{\partial\bar{y}} = \hat{\gamma}_0\hat{P}_0(\hat{U}_0 - \hat{c}_0)^2\int_\infty^{\bar{y}}\frac{1}{(\hat{U}_0 - \hat{c}_0)^2}dy, \tag{6.12}$$

and on applying the wall-condition it follows that

$$\int_0^\infty \frac{1}{(\hat{U}_0 - \hat{c}_0)^2} d\bar{y} = 0, \tag{6.13}$$

linking with the papers mentioned in the introduction to this chapter and with Chapter 4. It is emphasized by Smith (1988) in the nonlinear context in particular.

If we put $\mathrm{I}(\bar{y}) = \int_\infty^{\bar{y}} (\hat{U}_0 - \hat{c}_0)^{-2} d\bar{y}$ then from (6.11)

$$\frac{\partial \hat{P}_3}{\partial \bar{y}} = (\hat{U}_0 - \hat{c}_0)^2 \left\{ A_3(x_1, \bar{z}) + 2\hat{\gamma}_0 \hat{\gamma}_1 \hat{P}_0 \mathrm{I} + 2\hat{\gamma}_0^2 \hat{P}_0 \int_\infty^{\bar{y}} f(\bar{y}) \mathrm{I}(\bar{y}) dy \right\} \tag{6.14}$$

where

$$f(\bar{y}) = \frac{d}{d\bar{y}} \left\{ \frac{(\hat{U}_1 - \hat{c}_1)}{(\hat{U}_0 - \hat{c}_0)} \right\}. \tag{6.15}$$

A match with (6.7) implies that $A_3 = \hat{\gamma}_0^3 \hat{P}_0$ and on applying the wall-condition $\partial p / \partial \bar{y}(0) = 0$ we have

$$\hat{\gamma}_0 = 2 \int_0^\infty f(\bar{y}) \mathrm{I}(\bar{y}) d\bar{y}, \tag{6.16}$$

fixing $\hat{\gamma}_0$. In general $\hat{\gamma}_0$ could be complex, for example if c were not equal to an inflectional speed. Here however we are concerned with the neutral case in which $\hat{\gamma}_0$ is real.

6.3 The core vortex-solution for small wavenumbers

The E-independent vortex components of the solution in the core region of the flow are of the form

$$u = \epsilon U(\bar{y}) + \epsilon^2 x_1 \bar{U}(\bar{y}) + \epsilon^3 U_v(x_1, \bar{y}, \bar{z}) + \ldots, \tag{6.17}$$

$$v = \epsilon^3 V(\bar{y}) + \epsilon^4 V_v(x_1, \bar{y}, \bar{z}) + \ldots, \tag{6.18}$$

$$w = \epsilon^4 W_v(x_1, \bar{y}, \bar{z}) + \ldots, \tag{6.19}$$

$$p = \ldots + \epsilon^6 p_v(x_1, \bar{y}, \bar{z}) + \ldots, \tag{6.20}$$

where the terms with suffix v represent the vortex effects within the flow.

Substituting these expansions into the Navier-Stokes equations we obtain the set of equations governing the vortex motion to leading order, namely

$$\begin{aligned} \frac{\partial U_v}{\partial x_1} + \frac{\partial V_v}{\partial \bar{y}} + \frac{\partial W_v}{\partial \bar{z}} = 0, \qquad & U\frac{\partial V_v}{\partial x_1} = -\frac{\partial p_v}{\partial \bar{y}}, \\ U\frac{\partial U_v}{\partial x_1} + V_v U' = 0, \qquad & U\frac{\partial W_v}{\partial x_1} = -\frac{\partial p_v}{\partial \bar{z}}, \end{aligned} \tag{6.21}$$

which, after some algebraic manipulation, yield a Rayleigh-like equation for p_v of the form

$$\frac{\partial^2 p_v}{\partial \bar{y}^2} + \frac{\partial^2 p_v}{\partial \bar{z}^2} - \frac{2U'}{U}\frac{\partial p_v}{\partial \bar{y}} = 0. \tag{6.22}$$

We will solve (6.22) in each of the two tiers and match accordingly.

6.3.1 The outer-tier solution

With $\bar{y} = \alpha^{-1}\tilde{y}$ and $U \sim (\tilde{y} + A)$ we assume that p_v takes the form

$$p_v(x_1, \tilde{y}, \bar{z}) = \left(\bar{p}_0(x_1, \tilde{y}) + \alpha\, \bar{p}_1(x_1, \tilde{y}) + \alpha^2 \bar{p}_2(x_1, \tilde{y}) + \ldots\right) e^{i\beta\bar{z}}, \tag{6.23}$$

where $\beta = \alpha\,\hat{\beta}$. Substituting (6.23) into (6.22), along with the expressions for $\bar{y}$ and U, we obtain the equation

$$\frac{\partial^2 \bar{p}_0}{\partial \tilde{y}^2} - \frac{2}{\tilde{y}}\frac{\partial \bar{p}_0}{\partial \tilde{y}} + \hat{\beta}^2 \bar{p}_0 = 0 \tag{6.24}$$

for $\bar{p}_0$ which, in order to satisfy the boundary conditions $\bar{p}_0(\infty) = 0$ and $\partial\bar{p}_0/\partial\tilde{y}(0) = 0$, has solution

$$\bar{p}_0 = \pi_0(x_1)\left(1 + \hat{\beta}\tilde{y}\right) e^{-\hat{\beta}\tilde{y}}. \tag{6.25}$$

We note that the arbitrary function $\pi_0(x_1)$ is of no consequence in what follows.

6.3.2 The inner-tier solution

In the inner tier, where $\bar{y} = O(1)$, the leading vortex-pressure term has expansion

$$p_v = \left(\pi_0(x_1) + \alpha^2 \bar{P}_2(x_1, \bar{y}) + \alpha^3 \bar{P}_3(x_1, \bar{y}) + \ldots\right) e^{i\beta\bar{z}}, \tag{6.26}$$

U given by (6.8). It follows then that $\bar{P}_2$ satisfies the equation

$$\frac{\partial^2 \bar{P}_2}{\partial \bar{y}^2} - \frac{2\hat{U}_0'}{\hat{U}_0}\frac{\partial \bar{P}_2}{\partial \bar{y}} - \hat{\beta}^2 \pi_0 = 0. \tag{6.27}$$

If we let $\bar{P}_2^+$ denote the solution of (6.27) above the critical and $\bar{P}_2^-$ denote its solution below the critical we have

$$\frac{\partial \bar{P}_2^{\pm}}{\partial \bar{y}} = \hat{U}_0^2 \left\{ B_3^{\pm}(x_1) + \hat{\beta}^2 \pi_0 \int_{\infty}^{\bar{y}} \frac{1}{\hat{U}_0^2} dy \right\}. \tag{6.28}$$

Matching with the outer solution (6.25) we may deduce that $B_3^+ = \hat{\beta}^3 \pi_0$. We simply note here that by matching the jump $(\bar{P}_2^+ - \bar{P}_2^-)'$ with its equivalent in the buffer layer B_3^- may be fixed.

From the vortex solution within the core region we obtain expressions

$$U_v \sim \alpha^2 \Delta \ell^2, \quad V_v \sim \alpha^2 \Delta \ell, \quad W_v \sim \alpha \Delta \ell, \tag{6.29}$$

for the behaviour of the vortex velocities in terms of α, ℓ and Δ, ℓ the x_1-scale and Δ the p_v-scale. All that remains is to establish the magnitudes of the scales ℓ and Δ in terms of α. For that we turn to the integro-differential equation (5.53) of Chapter 5.

6.4 Analysis of the integro-differential equation for small wavenumbers

The integro-differential equation (5.53) can be written in the form

$$Cr'(x_1) + Ar(x_1)\int_{-\infty}^{x_1} |r^2(s)|ds - (Bx_1 + iD)r(x_1) = 0 \tag{6.30}$$

where A, B are real constants and C is a complex constant. With a change in the origin of x_1 the constant D may be taken to be real. Therefore in what follows we will assume this to be true.

If we write $r(x_1) = \rho(x_1)\exp[i\theta(x_1)]$, where both $\rho(x_1)$ and $\theta(x_1)$ are real functions of x_1, then putting $C = \lambda + i\mu$ it follows that

$$\frac{\lambda^2+\mu^2}{\lambda}\rho' + A\rho\int_{-\infty}^{x_1}\rho^2 ds - Bx_1\rho = 0, \tag{6.31}$$

and

$$\theta' = \frac{1}{\lambda}(D - \mu\rho'/\rho), \tag{6.32}$$

a second change in the origin of x_1 having eliminated a term $D\rho$ in (6.31). Considering the expressions for $(G_a^+ - G_a^-)$ and $(G_b^+ - G_b^-)$ given in (5.26) and (5.27) respectively, from (5.53) we may deduce that

$$\begin{aligned} &\lambda \sim \alpha, \qquad A \sim \alpha^{13/3} \\ &\mu \sim \alpha, \qquad B \sim \alpha^2 \end{aligned} \tag{6.33}$$

at small α. From a balance of terms in (6.31) it then follows that

$$x_1 \sim \alpha^{-1/2}, \quad \rho \sim \alpha^{-7/6}, \tag{6.34}$$

in other words $\ell = O(\alpha^{-1/2})$. On considering the solution in the buffer layers it may be deduced that $\Delta = O(\alpha^{-2})$ which, together with (6.29), yields the expressions

$$U_v \sim \alpha^{-1}, \quad V_v \sim \alpha^{-1/2}, \quad W_v \sim \alpha^{-3/2} \tag{6.35}$$

for the vortex velocities in terms of the small wavenumber α.

We now proceed by considering the full solution of the Navier-Stokes equations for particular values of small α, the resulting physical effects which come in to play provoking significant change.

6.5 The new regime with wavenumbers of order $\epsilon^{2/3}$

This new regime comes about if we compare the relative error $O(\alpha)$ in U (see (6.8)) with the relative error $O(\epsilon x_1)$ due to nonparallelism of the basic flow (see (6.17)). We note here that only the core region alters under this new regime, the buffer layers and the critical layer remaining unchanged. Therefore in what follows we restrict our analysis to the core region of the flow. The lengthscales involved are

$$x = \epsilon^{11/3} x_0, \quad y = \epsilon^5 \bar{y}, \quad z = \epsilon^{13/3} z_0$$

and we write

$$\begin{aligned}
u &= \epsilon U_0(\bar{y}) + \epsilon^{5/3} U_1(x_0, \bar{y}) + \epsilon^{7/3} U_v(x_0, \bar{y}, z_0) + \ldots + \epsilon^{23/9} E \left\{ \hat{u}_0 + \epsilon^{2/3} \hat{u}_1 + \ldots \right\} + \ldots, \\
v &= \epsilon^{11/3} V_v(x_0, \bar{y}, z_0) + \ldots + \epsilon^{29/9} E \left\{ \hat{v}_0 + \epsilon^{2/3} \hat{v}_1 + \ldots \right\} \ldots, \\
w &= \epsilon^3 W_v(x_0, \bar{y}, z_0) + \ldots + \epsilon^{23/9} E \left\{ \hat{w}_0 + \epsilon^{2/3} \hat{w}_1 + \ldots \right\} + \ldots, \\
p &= \ldots + \epsilon^{32/9} E \left\{ \hat{p}_0(x_0, z_0) + \epsilon^{2/3} \hat{p}_1 \ldots \right\} + \ldots .
\end{aligned} \tag{6.36}$$

Here $U_1(x_0, \bar{y}) = \hat{U}_1(\bar{y}) + x_0 \bar{U}_1(\bar{y})$ and, unless otherwise stated, $\hat{u}_0$ etc. are functions of x_0, $\bar{y}$ and z_0. Again $E = \exp[i\alpha_0(X - c_0 T)]$ with $t = \epsilon^{10/3} T$, $x = \epsilon^{13/3} X$, and

$$\alpha = \alpha_0 + \epsilon^{2/3} \alpha_1 + \epsilon^{4/3} \alpha_2 + \ldots,$$

$$\beta = \beta_0 + \epsilon^{2/3}\beta_1 + \epsilon^{4/3}\beta_2 + \ldots,$$
$$c = c_0 + \epsilon^{2/3}c_1 + \epsilon^{4/3}c_2 + \ldots, \tag{6.37}$$

while as a reminder $\epsilon = Re^{-1/8}$. Substituting (6.37) into the Navier-Stokes equations, the leading order equations governing the wave motion are

$$\begin{aligned} i\alpha_0(U_0 - c_0)\hat{u}_0 + U_0'\hat{v}_0 &= -i\alpha_0\hat{p}_0, \\ i\alpha_0(U_0 - c_0)\hat{v}_0 &= -\frac{\partial \hat{p}_2}{\partial \bar{y}}, \\ i\alpha_0(U_0 - c_0)\hat{w}_0 &= -\frac{\partial \hat{p}_0}{\partial z_0}, \\ i\alpha_0\hat{u}_0 + \frac{\partial \hat{v}_0}{\partial \bar{y}} + \frac{\partial \hat{w}_0}{\partial z_0} &= 0. \end{aligned} \tag{6.38}$$

If we write

$$\hat{p}_0(x_0, z_0) = r_1(x_0)\hat{E} + r_2(x_0)\hat{E}^{-1}, \tag{6.39}$$

where $\hat{E} = e^{i\beta_0 z_0}$, from (6.38) we may deduce that

$$\begin{aligned} \hat{w}_0 &= \frac{\beta_0}{\alpha_0(U_0 - c_0)}\left\{-r_1\hat{E} + r_2\hat{E}^{-1}\right\}, \\ \hat{v}_0 &= \frac{i\gamma_0^2}{\alpha_0}(U_0 - c_0)\mathrm{I}\left\{r_1\hat{E} + r_2\hat{E}^{-1}\right\}, \\ \hat{u}_0 &= \left[\frac{-\gamma_0^2}{\alpha_0^2}\left\{U_0'\mathrm{I} + \frac{1}{(U_0 - c_0)}\right\} + \frac{\beta_0^2}{\alpha_0^2(U_0 - c_0)}\right]\left\{r_1\hat{E} + r_2\hat{E}^{-1}\right\}, \\ \hat{p}_2 &= \gamma_0^2\int_\infty^{\bar{y}}(U_0 - c_0)^2\mathrm{I}dy\left\{r_1\hat{E} + r_2\hat{E}^{-1}\right\}. \end{aligned} \tag{6.40}$$

Here $\gamma_0^2 = \alpha_0^2 + \beta_0^2$ and $\mathrm{I}(\bar{y}) = \int_\infty^{\bar{y}}(U_0 - c_0)^{-2}dy$. Therefore, as $\bar{y} \to \infty$

$$\hat{p}_2 \sim -\frac{\gamma_0^2}{2}\bar{y}^2\left\{r_1\hat{E} + r_2\hat{E}^{-1}\right\}, \tag{6.41}$$

matching with the outer region of §6.2 as $\tilde{y} \to 0$. Proceeding to the second order equations we have

$$
\begin{aligned}
(U_0-c_0)\left\{\frac{U_0}{(U_0-c_0)}\frac{\partial \hat{u}_0}{\partial x_0}+i\alpha_0\hat{u}_1+i\alpha_1\hat{u}_0\right\} &+ i\alpha_0(U_1-c_1)\hat{u}_0+U_0'\hat{v}_1 \\
&+ U_1'\hat{v}_0=-i\alpha_0\hat{p}_1-\frac{\partial \hat{p}_0}{\partial x_0}, \\
(U_0-c_0)\left\{\frac{U_0}{(U_0-c_0)}\frac{\partial \hat{v}_0}{\partial x_0}+i\alpha_0\hat{v}_1+i\alpha_1\hat{v}_0\right\} &+ i\alpha_0(U_1-c_1)\hat{v}_0=-\frac{\partial \hat{p}_3}{\partial \bar{y}}, \\
(U_0-c_0)\left\{\frac{U_0}{(U_0-c_0)}\frac{\partial \hat{w}_0}{\partial x_0}+i\alpha_0\hat{w}_1+i\alpha_1\hat{w}_0\right\} &+ i\alpha_0(U_1-c_1)\hat{w}_0=-\frac{\partial \hat{p}_1}{\partial z_0}, \\
i\alpha_0\hat{u}_1+i\alpha_1\hat{u}_0+\frac{\partial \hat{u}_0}{\partial x_0} &+ \frac{\partial \hat{v}_1}{\partial \bar{y}}+\frac{\partial \hat{w}_1}{\partial z_0}=0.
\end{aligned}
\tag{6.42}
$$

If for convenience we put $\bar{u}=(U_0-c_0)$ and suppose that

$$
\hat{p}_1=R_1(x_0)\hat{E}+R_2(x_0)\hat{E}^{-1}, \tag{6.43}
$$

writing $\hat{u}_0=\hat{u}_{01}(x_0,\bar{y})\hat{E}+\hat{u}_{02}(x_0,\bar{y})\hat{E}^{-1}$ etc. it follows that

$$
\hat{w}_{11}=-\frac{\beta_0 R_1}{\alpha_0\bar{u}}-\frac{i\beta_0}{\alpha_0^2\bar{u}}\left\{\frac{U_0}{\bar{u}}r_1'+i\alpha_1 r_1\right\}+\frac{(U_1-c_1)}{\alpha_0\bar{u}^2}\beta_0 r_1 \tag{6.44}
$$

where, apart from a change in the signs, $\hat{w}_{12}$ has the same form. For this reason we will only give details of the solution for the $\hat{E}$-components, assuring the reader that the final result in terms of the $\hat{E}^{-1}$-components of the solution is obtained in the same way as the working below.

Continuing,

$$
\begin{aligned}
-\bar{u}^2\frac{\partial}{\partial \bar{y}}\left\{\frac{\hat{v}_{11}}{\bar{u}}\right\} &= -i\alpha_0(U_1-c_1)\hat{u}_{01}-U_1'\hat{v}_{01}-i\alpha_0 R_1-r_1'-c_0\frac{\partial \hat{u}_{01}}{\partial x_0} \\
&+ i\beta_0\bar{u}\left\{-\frac{\beta_0 R_1}{\alpha_0\bar{u}}+s_1\right\}
\end{aligned}
\tag{6.45}
$$

where

$$
s_1=-\frac{i\beta_0}{\alpha_0^2\bar{u}}\left\{\frac{U_0}{\bar{u}}r_1'+i\alpha_1 r_1\right\}+\frac{(U_1-c_1)}{\alpha_0\bar{u}^2}\beta_0 r_1.
$$

We further simplify this equation by singling out the dependence of $\hat{v}_{11}$ on the function $R_1(x_0)$ so that

$$-\bar{u}^2\frac{\partial}{\partial\bar{y}}\left\{\frac{\hat{v}_{11}}{\bar{u}}\right\}=-\frac{i\gamma_0^2}{\alpha_0}R_1-s_2 \tag{6.46}$$

where

$$s_2=i\alpha_0(U_1-c_1)\hat{u}_{01}+U_1'\hat{v}_{01}+r_1'+c_0\frac{\partial\hat{u}_{01}}{\partial x_0}-i\beta_0\bar{u}s_1.$$

We note here that (6.13) still holds as the leading order result. On integrating (6.46) it follows that

$$\hat{v}_{11}=\bar{u}\left\{-i\alpha_0A_1^{\pm}+\frac{i\gamma_0^2}{\alpha_0}R_1\int_{\infty}^{\bar{y}}\frac{1}{\bar{u}^2}dy+\int_{\infty}^{\bar{y}}\frac{s_2}{\bar{u}^2}dy\right\} \tag{6.47}$$

where $A_1^{\pm}$ are unknown functions of x_0. From (6.42) we obtain an equation for $\partial\hat{p}_{31}/\partial\bar{y}$, namely

$$\begin{aligned}-\frac{\partial\hat{p}_{31}}{\partial\bar{y}} &= -\gamma_0^2(U_1-c_1)\mathrm{I}\bar{u}r_1+\bar{u}^2\left\{\left(i\alpha_1+\frac{U_0}{\bar{u}}\frac{\partial}{\partial x_0}\right)\frac{i\gamma_0^2}{\alpha_0}\mathrm{I}r_1\right\}\\ &\quad+i\alpha_0\bar{u}^2\left\{-i\alpha_0A_1^{\pm}+\frac{i\gamma_0^2}{\alpha_0}\mathrm{I}R_1+\int_{\infty}^{\bar{y}}\frac{s_2}{\bar{u}^2}dy\right\},\end{aligned} \tag{6.48}$$

which we must then match to the outer region of §6.2 as $\bar{y}\to\infty$. To achieve this we require that $\hat{p}_{31}\sim\gamma_0^3r_1\bar{y}^3/3$, i.e. $\partial\hat{p}_{31}/\partial\bar{y}\sim\gamma_0^3r_1\bar{y}^2$, and therefore we may deduce from this match that

$$i\alpha_0\bar{y}^2\left\{-i\alpha_0A_1^{+}\right\}\sim-\gamma_0^3r_1\bar{y}^2, \tag{6.49}$$

implying that

$$A_1^{+}=-\frac{\gamma_0^3r_1}{\alpha_0^2}. \tag{6.50}$$

We now define

$$J_0 \equiv \left[\frac{i\hat{v}_{11}}{\alpha_0\bar{u}}\right]_-^+ = (A_1^+ - A_1^-) \tag{6.51}$$

as the jump in $i(\alpha_0\bar{u})^{-1}\hat{v}_{11}$ across the buffer layer. Applying the wall-condition to $\hat{v}_{11}$ fixes A_1^- such that

$$A_1^- = \frac{i}{\alpha_0}\int_0^\infty \frac{s_2}{\bar{u}^2}d\bar{y} - q_\omega^- r_1\,, \tag{6.52}$$

so from (6.50) and (6.52) it follows that

$$i\left\{\frac{\gamma_0^3}{\alpha_0}r_1 + \alpha_0 J_0\right\} = \int_0^\infty \frac{s_2}{\bar{u}^2}d\bar{y} - q_w^- r_1, \tag{6.53}$$

the constant $q_w^- = Q_w^-/(i\alpha_0 c_0^2)$ determined by the wall layer, Q_w^- given by (5.21). We can write s_2 in the form $s_2 = ir_1[L] + r_1'[M]$ where

$$\begin{aligned} L &= -\gamma_0^2\frac{(U_1 - c_1)}{\alpha_0}\left\{\frac{1}{\bar{u}} + U_0'\mathrm{I}\right\} + \frac{\gamma_0^2}{\alpha_0}\bar{u}U_1'\mathrm{I} - \frac{\beta_0^2\alpha_1}{\alpha_0^2}, \\ M &= 1 - \frac{\beta_0^2}{\alpha_0^2} - \frac{c_0\gamma_0^2}{\alpha_0^2}\left\{\bar{u}'\mathrm{I} + \frac{1}{\bar{u}}\right\}, \end{aligned} \tag{6.54}$$

which, after some algebraic manipulation, implies that

$$\begin{aligned} i\left\{\frac{\gamma_0^3}{\alpha_0}r_1 + \alpha_0 J_0\right\} &= \frac{2i\gamma_0^2}{\alpha_0}r_1\int_0^\infty \mathrm{I}(\bar{y})\frac{\partial}{\partial\bar{y}}\left[\frac{(U_1 - c_1)}{\bar{u}}\right]d\bar{y} \\ &\quad - \frac{2c_0\gamma_0^2}{\alpha_0^2}r_1'\int_0^\infty \frac{1}{\bar{u}^3}d\bar{y} - q_w^- r_1. \end{aligned} \tag{6.55}$$

We expect the solution in the buffer layers and the critical layer to remain unchanged on this shorter streamwise lengthscale. Therefore, for the purposes of matching, we assume the results obtained in Chapter 5 in these regions, in particular (5.47).

Thus, it follows from (6.55) that

$$\frac{i\gamma_0^3}{\alpha_0}r_1 + \frac{1}{i\alpha_0 b_1^2}\left\{\frac{\pi b_3\gamma_0^2 c_0}{\alpha_0 b_1^2}r_1' + \frac{4\pi(2/3)^{2/3}(-2/3)!}{c_0(\alpha_0 b_1)^{5/3}}\beta_0^4(2\beta_0^2-\gamma_0^2)r_2\int_{-\infty}^{x_0} r_1 r_2^* ds\right\}$$
$$= \frac{2i\gamma_0^2}{\alpha_0}\left\{\int_0^\infty \mathrm{I}(\bar{y})\frac{\partial}{\partial\bar{y}}\left[\frac{(\bar{U}_1-\bar{c}_1)}{\bar{u}}\right]d\bar{y}\; x_0 + \int_0^\infty \mathrm{I}(\bar{y})\frac{\partial}{\partial\bar{y}}\left[\frac{(\hat{U}_1-\hat{c}_1)}{\bar{u}}\right]d\bar{y}\right\} r_1$$
$$- \frac{2c_0\gamma_0^2}{\alpha_0^2}r_1'\int_0^\infty \frac{1}{\bar{u}^3}d\bar{y} - q_w^- r_1, \tag{6.56}$$

where $c_1 = \bar{c}_1 x_0 + \hat{c}_1$ and $q_w^- = Q_w^-/(i\alpha_0 c_0^2)$; Q_w^- given by (5.21).

As was mentioned earlier, a similar result is obtained for the E^{-1}-component of the solution and is in fact that of (6.56) with r_1 replaced throughout by r_2, and vice versa. It is also noted here that from the definition of $(G_a^+ - G_a^-)$ in (5.26) and the expression for $\hat{p}_2$ in (6.38), we have to leading order

$$(G_a^+ - G_a^-) \sim -\int_0^\infty \frac{2}{\bar{u}^3}\frac{\partial}{\partial\bar{y}}\left[\frac{(\bar{U}_1-\bar{c}_1)}{\bar{u}}\right]\bar{u}^3\gamma_0^2\mathrm{I}(\bar{y})d\bar{y}$$
$$= -2\gamma_0^2\int_0^\infty \mathrm{I}(\bar{y})\frac{\partial}{\partial\bar{y}}\left[\frac{(\bar{U}_1-\bar{c}_1)}{\bar{u}}\right]d\bar{y} \tag{6.57}$$

which, when multiplied by the $\bar{x}$-coordinate, corresponds to the first coefficient of r_1 within the brackets on the righthand side of (6.56). Similarly from the definition of $(G_b^+ - G_b^-)$ in (5.27) we have at leading order

$$(G_b^+ - G_b^-) \sim -\int_0^\infty \frac{2}{\alpha_0\bar{u}^3}\frac{\bar{u}'}{\bar{u}}\bar{u}^2\gamma_0^2 d\bar{y}$$
$$= -\frac{2\gamma_0^2}{\alpha_0}\int_0^\infty \frac{1}{\bar{u}^3}d\bar{y}, \tag{6.58}$$

corresponding to the coefficient of r_1' on the righthand side of (6.56). In conclusion, the coefficients in the wave-pressure amplitude equation have been obtained more explicitly than those of SBB.

In fact, we may deduce from (5.27) and (6.13) that (6.58) is exactly $(G_b^+ - G_b^-)$. Moreover, from the definition (5.55) of $(G_c^+ - G_c^-)$ we may conclude that for small wavenumbers $(G_b^+ - G_b^-) \equiv (G_c^+ - G_c^-)$ which will be of importance in §6.7.

6.6 Additional comments and conclusion

The main outcome so far of the present investigation into vortex/wave interactions for wavenumbers of order $\epsilon^{2/3}$ (i.e. $\alpha \sim Re^{-1/12}$) is the integro-differential equation (6.56) for the wave-pressure amplitude and its differences as compared with (5.53), obtained in Chapter 5 for $\alpha \sim 1$. Here, in addition, all the coefficients in the amplitude equation can be evaluated quite explicitly, unlike in (5.53).

From the preliminary investigation of this chapter, in which we considered the core solution of SBB for small wavenumbers α, we conclude that $\gamma^2 = \alpha^2 + \beta^2$ is fixed to leading order by (6.16) before the integro-differential equation (5.50) can come into play at second order. Fixing γ in turn fixes the input frequency $\Omega = \alpha c$ (since β and c are known), thus restricting the range of frequencies to which the vortex/wave interaction theory of SBB may be applied.

Under the scalings of the new regime in which $\alpha \sim \epsilon^{2/3}$, the wave-pressure amplitude equation obtained comprises the integro-differential equation (5.50) and (6.16), now seen acting together at leading order. Therefore this new wave-pressure amplitude equation holds for arbitrary input frequencies Ω, further generalizing the application of vortex/Rayleigh-wave interactions in interactive boundary layer flows.

In Chapter 7 we present some solutions of (6.56) with the addition of forcing, corresponding to a nonlinear receptivity problem. The results, obtained numerically, show typical responses downstream (giving four transition paths in principle) and comparisons are made with the solutions obtained by SBB in the non-forcing case.

We conclude this subsection by noting that, along with the $\epsilon^{2/3}$-regime discussed in

§6.5, two other possible regimes, $\alpha \sim \epsilon$ and $\alpha \sim \epsilon^2$, are of physical importance and have been brought to light in this work.

The second regime $\alpha \sim \epsilon$ is implied by the outer tier of §6.2 and §6.3 whose y-coordinate becomes $O(\epsilon^4)$ when $\alpha \to O(\epsilon)$. As a result the full Blasius profile, U_B say, exerts influence and we are required to solve

$$\frac{\partial^2 \hat{p}_0}{\partial \tilde{y}^2} - \frac{2U_B'}{U_B}\frac{\partial \hat{p}_0}{\partial \tilde{y}} - \hat{\gamma}_0^2 \hat{p}_0 = 0$$

such that

$$\hat{p}_0 \sim \hat{P}_0(x_1, \bar{z})\left\{1 - \tfrac{1}{2}\hat{\gamma}_0^2 \tilde{y}^2\right\} + \nu(x_1, \bar{z})\tilde{y}^3 + \ldots \quad \text{as} \quad \tilde{y} \to 0^+$$

and $\hat{p}_0(\infty) = 0$ for various $\hat{\gamma}_0$-values, thus obtaining ν. Here $y = \epsilon^4 \tilde{y}$, $\hat{\gamma}_0$ is unknown and $A_3 = \nu^3 \hat{P}_0$ in (6.14), thus fixing $\hat{\gamma}_0$ on applying the wall-condition.

The third regime $\alpha \sim \epsilon^2$ comes about on balancing the leading vortex terms $\epsilon^3 U_v$, etc. with the leading wave terms $\epsilon^{10/3} E \bar{u}_0$, etc. in the core region. At such small α we would arrive at the fully nonlinear and nonparallel three-dimensional triple-deck structure.

6.7 The initial-value formulation

Before moving on to numerical solutions of (6.56) in Chapter 7, we complete this chapter by interpreting the work of §6.5 in terms of a new spatio-temporal form which seems appropriate to an initial-value problem. In doing so we generalize (formally) from the fixed frequency setting used up until now in this work and other work on vortex/wave interactions.

In mathematical terms we achieve this new interpretation by replacing the multiplier $i\alpha_0$ with the operator $\partial/\partial X$ in the appropriate equations, X being the fast scale in the mainstream direction. The replacement is equivalent to a Fourier-transform

approach for covering more general X variations. Thus at leading order, replacing (6.38), we have

$$\begin{aligned}
(U_0 - c_0)\frac{\partial \hat{u}_0}{\partial X} + U_0'\hat{v}_0 &= -\frac{\partial \hat{p}_0}{\partial X}, \\
(U_0 - c_0)\frac{\partial \hat{v}_0}{\partial X} &= -\frac{\partial \hat{p}_2}{\partial \bar{y}}, \\
(U_0 - c_0)\frac{\partial \hat{w}_0}{\partial X} &= -\frac{\partial \hat{p}_0}{\partial z_0}, \\
\frac{\partial \hat{u}_0}{\partial X} + \frac{\partial \hat{v}_0}{\partial \bar{y}} + \frac{\partial \hat{w}_0}{\partial z_0} &= 0,
\end{aligned} \tag{6.59}$$

from which we obtain

$$\begin{aligned}
\hat{w}_{01} &= -\frac{i\beta_0}{(U_0 - c_0)}\int_{-\infty}^{X} r_1 \, dX_1, \\
\hat{v}_{01} &= (U_0 - c_0)\left\{ \mathrm{I}\frac{\partial r_1}{\partial X} - \beta_0^2 \mathrm{I}\int_{-\infty}^{X} r_1 \, dX_1 \right\}, \\
\frac{\partial \hat{u}_{01}}{\partial X} &= -U_0'\left\{ \mathrm{I}\frac{\partial r_1}{\partial X} - \beta_0^2 \mathrm{I}\int_{-\infty}^{X} r_1 \, dX_1 \right\} - \frac{1}{(U_0 - c_0)}\frac{\partial r_1}{\partial X}, \\
\frac{\partial \hat{p}_{21}}{\partial \bar{y}} &= -(U_0 - c_0)\frac{\partial \hat{v}_{01}}{\partial X},
\end{aligned} \tag{6.60}$$

for the $\hat{E}$-components of the solution, $\hat{p}_0 = r_1(x_0, X)\hat{E} + r_2(x_0, X)\hat{E}^{-1}$. At second order the governing equations become

$$\begin{aligned}
(U_0 - c_0)\left\{ \frac{U_0}{(U_0 - c_0)}\frac{\partial \hat{u}_0}{\partial x_0} + \frac{\partial \hat{u}_1}{\partial X} \right\} + (U_1 - c_1)\frac{\partial \hat{u}_0}{\partial X} + U_0'\hat{v}_1 & \\
+ U_1'\hat{v}_0 = -\frac{\partial \hat{p}_1}{\partial X} - \frac{\partial \hat{p}_0}{\partial x_0}, & \\
(U_0 - c_0)\left\{ \frac{U_0}{(U_0 - c_0)}\frac{\partial \hat{v}_0}{\partial x_0} + \frac{\partial \hat{v}_1}{\partial X} \right\} + (U_1 - c_1)\frac{\partial \hat{v}_0}{\partial X} = -\frac{\partial \hat{p}_3}{\partial \bar{y}}, & \\
(U_0 - c_0)\left\{ \frac{U_0}{(U_0 - c_0)}\frac{\partial \hat{w}_0}{\partial x_0} + \frac{\partial \hat{w}_1}{\partial X} \right\} + (U_1 - c_1)\frac{\partial \hat{w}_0}{\partial X} = -\frac{\partial \hat{p}_1}{\partial z_0}, & \\
\frac{\partial \hat{u}_1}{\partial X} + \frac{\partial \hat{u}_0}{\partial x_0} + \frac{\partial \hat{v}_1}{\partial \bar{y}} + \frac{\partial \hat{w}_1}{\partial z_0} = 0 &
\end{aligned} \tag{6.61}$$

and hence

$$(U_0 - c_0)\frac{\partial \hat{w}_{11}}{\partial X} = -i\beta_0 R_1 + \frac{i\beta_0 U_0}{(U_0 - c_0)}\int_{-\infty}^{X} \frac{\partial r_1}{\partial x_0}\, dX_1 + i\beta_0 \frac{(U_1 - c_1)}{(U_0 - c_0)} r_1.$$

As in §6.5 we write $\hat{v}_{11}$ in the form

$$-(U_0 - c_0)^2 \frac{\partial}{\partial \bar{y}}\left\{\frac{\hat{v}_{11}}{(U_0 - c_0)}\right\} = \beta_0^2 \int_{-\infty}^{X} R_1\, dX_1 - \frac{\partial R_1}{\partial X} - s$$

where

$$\begin{aligned} -s = & -\beta_0^2 \frac{(U_1 - c_1)}{(U_0 - c_0)}\int_{-\infty}^{X} r_1\, dX_1 - \beta_0^2 \frac{U_0}{(U_0 - c_0)}\int_{-\infty}^{X}\int_{-\infty}^{X_2} \frac{\partial r_1}{\partial x_0}\, dX_1 dX_2 \\ & + \frac{(U_1 - c_1)}{(U_0 - c_0)}\frac{\partial r_1}{\partial X} + U_0'(U_1 - c_1)\left\{\mathrm{I}\frac{\partial r_1}{\partial X} - \beta_0^2 \mathrm{I}\int_{-\infty}^{X} r_1\, dX_1\right\} \\ & - U_1'(U_0 - c_0)\left\{\mathrm{I}\frac{\partial r_1}{\partial X} - \beta_0^2 \mathrm{I}\int_{-\infty}^{X} r_1\, dX_1\right\} - c_0 \frac{\partial \hat{u}_{01}}{\partial x_0} - \frac{\partial r_1}{\partial x_0} \end{aligned}$$

and $\hat{p}_1 = R_1(x_0, X)\hat{E} + R_2(x_0, X)\hat{E}^{-1}$. Therefore

$$\hat{v}_{11} = (U_0 - c_0)\left\{-\frac{\partial A_1^{\pm}}{\partial X} - \beta_0^2 \mathrm{I}\int_{-\infty}^{X} R_1\, dX_1 + \mathrm{I}\frac{\partial R_1}{\partial X} + \int_{\infty}^{\bar{y}} \frac{s}{(U_0 - c_0)^2} dy\right\} \tag{6.62}$$

and thus

$$\begin{aligned} -\frac{\partial \hat{p}_{31}}{\partial \bar{y}} = & (U_0 - c_0)^2\left\{-\frac{\partial^2 A_1^{\pm}}{\partial X^2} - \beta_0^2 \mathrm{I} R_1 + \frac{\partial^2 R_1}{\partial X^2} + \int_{\infty}^{\bar{y}} \frac{1}{(u_0 - c_0)^2}\frac{\partial s}{\partial X} dy\right\} \\ & + U_0(U_0 - c_0)\left\{\mathrm{I}\frac{\partial^2 r_1}{\partial x_0 \partial X} - \beta_0^2 \mathrm{I}\int_{-\infty}^{X} \frac{\partial r_1}{\partial x_0}\, dX_1\right\} \\ & + (U_1 - c_1)(U_0 - c_0)\left\{\mathrm{I}\frac{\partial^2 r_1}{\partial X^2} - \beta_0^2 \mathrm{I} r_1\right\}. \end{aligned} \tag{6.63}$$

If we use the result, conjectured and confirmed in Appendix A, that in matching with the outer solution the function $A_1^{+}(x_0, X)$ is such that

$$\frac{\partial^2 A_1^{+}}{\partial X^2} = -\frac{1}{2\pi}\int_{-\infty}^{\infty}\int_{-\infty}^{\infty} \frac{\nabla^4 r_1\, d\xi d\eta}{[(X - \xi)^2 + (z_0 - \eta)^2]^{1/2}}, \tag{6.64}$$

then, as in §6.5, it can be deduced that the wave-pressure amplitude equation is of the form

$$\begin{aligned}\frac{\partial^2 A_1^+}{\partial X^2} - \frac{1}{b_1^2}\left\{-\frac{i\pi b_3 c_0}{b_1^2}\left[\frac{\partial^2 r_1}{\partial x_0 \partial X} - \beta_0^2 \int_{-\infty}^{X} \frac{\partial r_1}{\partial x_0}\, dX_1\right] + N\right\} \\ = 2c_0 \mathrm{I}_1 \left\{\frac{\partial^2 r_1}{\partial x_0 \partial X} - \beta_0^2 \int_{-\infty}^{X} \frac{\partial r_1}{\partial x_0}\, dX_1\right\} - 2\mathrm{I}_2 \left\{\frac{\partial^2 r_1}{\partial X^2} - \beta_0^2 r_1\right\} \\ + \frac{1}{(\pi c_0^5)^{1/2}} \left\{\frac{\partial^2}{\partial X^2} - \beta_0^2\right\} \int_X^{\infty} \frac{r_1(s, x_0)}{(s-X)^{1/2}}\, ds \qquad (6.65)\end{aligned}$$

where

$$\mathrm{I}_1 = \int_0^{\infty} \frac{1}{(U_0 - c_0)^3} d\bar{y}, \quad \mathrm{I}_2 = \int_0^{\infty} \mathrm{I} \frac{\partial}{\partial \bar{y}} \left[\frac{(U_1 - c_1)}{(U_0 - c_0)}\right] d\bar{y}$$

.

N represents the nonlinear term derived from the jump condition across the buffer layer, its determination requiring a more detailed analysis than is carried out here.

By replacing $i\beta_0$ with the operator ∂_{z_0} in (6.65) we are able to further generalize the amplitude equation to include the full spectrum of waves. Thus, after differentiating with respect to the fast scale X we have

$$\begin{aligned}\frac{\partial^3 A_1^+}{\partial X^3} - \frac{1}{b_1^2}\left\{-\frac{i\pi b_3 c_0}{b_1^2} \frac{\partial}{\partial x_0}\left(\nabla^2 r\right) + \frac{\partial N}{\partial X}\right\} \\ = 2c_0 \mathrm{I}_1 \frac{\partial}{\partial x_0}\left(\nabla^2 r\right) - 2\mathrm{I}_2 \frac{\partial}{\partial X}\left(\nabla^2 r\right) \\ + \frac{\partial}{\partial X} \frac{\nabla^2}{(\pi c_0^5)^{1/2}} \int_X^{\infty} \frac{r}{(s-X)^{1/2}}\, ds, \qquad (6.66)\end{aligned}$$

where $\nabla^2 \equiv \partial_X^2 + \partial_{z_0}^2$.

Recalling (5.54) and the comments made at the close of §6.5 we now proceed to introduce the influence of the slow time derivative ∂_{t_0}. This is achieved here by replacing the operator $c_0 \partial_{x_0}$ by $\partial_{t_0} + c_0 \partial_{x_0}$ throughout (6.66), thus yielding the equation

$$b_1^2\frac{\partial^3 A_1^+}{\partial X^3} + \frac{i\pi b_3}{b_1^2}\left[\frac{\partial}{\partial t_0} + c_0\frac{\partial}{\partial x_0}\right]\left(\nabla^2 r\right) - \frac{\partial N}{\partial X}$$
$$= 2b_1^2\,\mathrm{I}_1\left[\frac{\partial}{\partial t_0} + c_0\frac{\partial}{\partial x_0}\right]\left(\nabla^2 r\right) - 2b_1^2\,\mathrm{I}_2\frac{\partial}{\partial X}\left(\nabla^2 r\right)$$
$$+ b_1^2\frac{\partial}{\partial X}\frac{\nabla^2}{(\pi c_0^5)^{1/2}}\int_X^\infty \frac{r}{(s-X)^{1/2}}\,ds. \qquad (6.67)$$

As was noted in Chapter 1, the above spatio-temporal interpretation has the makings of an initial-value problem for weakly nonlinear input in general at the onset of inflectional instability in boundary layer-like flows.

Work is in progress with Professor F T Smith in which three-dimensional initial-value problems are developed concerning the onset of transition over a surface roughness within interactive boundary layers and other related flows. The aim is to describe the free evolution of general disturbances rather than forced, fixed frequency or fixed wavelength evolutions.

Chapter 7

The Nonlinear receptivity problem

7.1 Introduction

On applying a shift in the origin of x_0 to incorporate the two new r_1-terms, the solution of the wave-pressure amplitude equation (6.56) is covered extensively by SBB for the case $r_1 \equiv r_2$; the case $r_1 \neq r_2$ yields a much wider range of solutions, as given in Brown and Smith (1995).

With the addition of a forcing term to the amplitude equation, corresponding to a nonlinear receptivity problem (see for example Hall and Smith (1982) and Smith (1987)), our aim in this chapter is to investigate numerically the effects of the forcing on the flow downstream of its point of introduction. In the case addressed below the forcing effectively dies away downstream. Comparisons are made with the solutions obtained by SBB in the non-forcing case.

In §7.2 the nonlinear receptivity problem is formulated and the method of approach described for a general forcing $F(x_0)$ before a specific form of F is considered in §7.3. The results are presented graphically and compared with those of SBB.

7.2 Formulation of the receptivity problem

In its simplest form the integro-differential equation for the wave-pressure amplitude is

$$Cr'(x_0) + Ar(x_0)\int_{-\infty}^{x_0} |r^2(s)|ds - (Bx_0 + iD)r(x_0) = 0, \tag{7.1}$$

where A, B, D are real constants, C is a complex constant, and $r(x_0)$ is the wave-amplitude function. Introducing the effects of forcing in the form of a complex function $F(x_0)$ added to the righthand side of (7.1) we obtain the balance

$$(\lambda + i\mu)(\rho' + i\theta'\rho)e^{i\theta} + A\rho e^{i\theta}\int_{-\infty}^{x_0} \rho^2 ds - Bx_0\rho e^{i\theta} = F(x_0), \tag{7.2}$$

where $r(x_0) = \rho(x_0)\exp[i\theta(x_0)]$, $C = \lambda + i\mu$ and a shift in the origin of x_0 has been applied in order to eliminate the constant D. If we write $F(x_0)$ in the form

$$F(x_0) = K(x_0)\exp[iL(x_0)]$$

then on substituting this into (7.2) we have

$$K\cos(L-\theta) = \lambda\rho' - \mu\rho\theta' + A\rho\int_{-\infty}^{x_0} \rho^2 ds - Bx_0\rho, \tag{7.3}$$

$$K\sin(L-\theta) = \mu\rho' + \lambda\rho\theta', \tag{7.4}$$

the system of equations governing the nonlinear receptivity problem to be solved for $\rho(x_0)$ and $\theta(x_0)$. In solving this system we are interested mostly in the relative signs of the coefficients λ, A and B, yielding four possible outcomes downstream (in principle).

To solve (7.3) and (7.4) numerically we employ the Runge-Kutta method of order two combined with the composite trapezoidal rule which is used to evaluate the integral in (7.3). We introduce the forcing at a point $x_0 = -a$ say, $\rho(x_0) = 0$ for $x_0 < -a$, and then march on in x_0 from this point.

7.3 $\mathbf{F(x_0) = \Gamma \exp[-x_0^2 + i\theta(x_0)]}$

The case addressed here is of the relatively simple form

$$F(x_0) = \Gamma \exp[-x_0^2 + i\theta(x_0)] \tag{7.5}$$

in which $L \equiv \theta$ in (7.3) and (7.4). Thus the two-equation system reduces to a single equation, namely

$$\frac{\lambda^2 + \mu^2}{\lambda}\rho' + A\rho \int_{-\infty}^{x_o} \rho^2 ds - Bx_o\rho = \Gamma e^{-x_0^2}, \tag{7.6}$$

independent of the function $\theta(x_0)$. The positive constant Γ represents the *strength* of the forcing applied and in the analysis which follows solutions are presented for varying values of this parameter.

Since we are concerned mostly in the relative signs of the coefficients in (7.6), we take

$$\left|\frac{\lambda^2 + \mu^2}{\lambda}\right| = |A| = |B| = 1$$

and consider all possible combinations of AB and λB positive or negative.

$\mathbf{AB > 0}$, $\mathbf{\lambda B > 0}$.

When $AB > 0$ and $\lambda B > 0$ the solutions obtained in SBB, for the case in which no forcing is added, are periodic in x_0. With the addition of forcing of the form given in (7.5) at $x_0 = -a$, the solutions of (7.6) for $\Gamma = 0.01, 0.2, 1, 6, 10$ are shown in Figures 7.1–7.5. The wave amplitude ρ is plotted against the short streamwise lengthscale x_0 and the same set of axes is used for each value of the strength Γ so that comparisons may be made between each set of results.

These figures show that the strength of the forcing applied varies the size of the peaks and troughs, and the distance between consecutive peaks, but overall the shape of the graph remains the same once the forcing itself has died out. Thus downstream

the solutions of (7.6) exhibit periodicity, as do the solutions of the wave-amplitude equation in the non-forcing case.

$AB < 0$, $\lambda B < 0$.

In the non-forcing case of SBB the wave-pressure disturbances die out as $x_0 \to \infty$ although the vortex flow persists downstream. Figures 7.7–7.9 show the solutions obtained for the receptivity problem when $\Gamma = 0.2, 1, 6, 10$ respectively.

Again it can be seen that once the forcing has died out there are no long term effects on the solution and the wave-pressure disturbances tend to zero as $x_0 \to 0$, as in the non-forcing case of SBB.

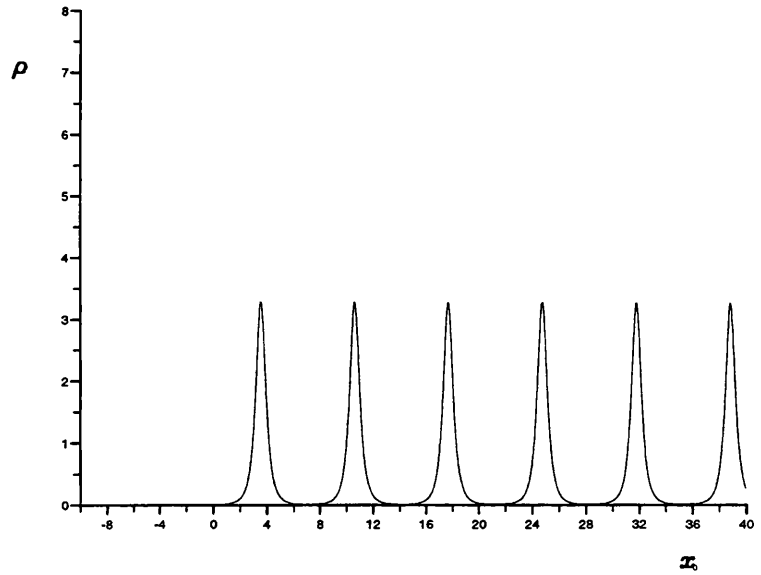

Figure 7.1: $AB > 0$, $\lambda B > 0$ and $\Gamma = 0.01$.

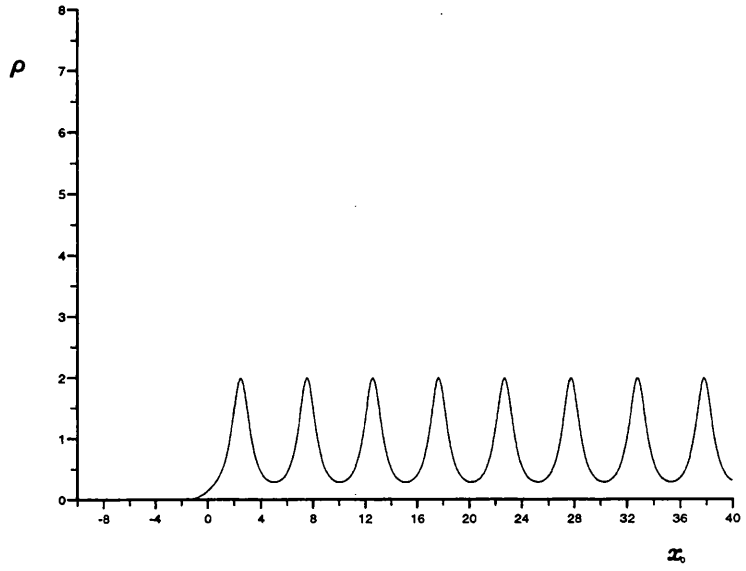

Figure 7.2: $AB > 0$, $\lambda B > 0$ and $\Gamma = 0.2$.

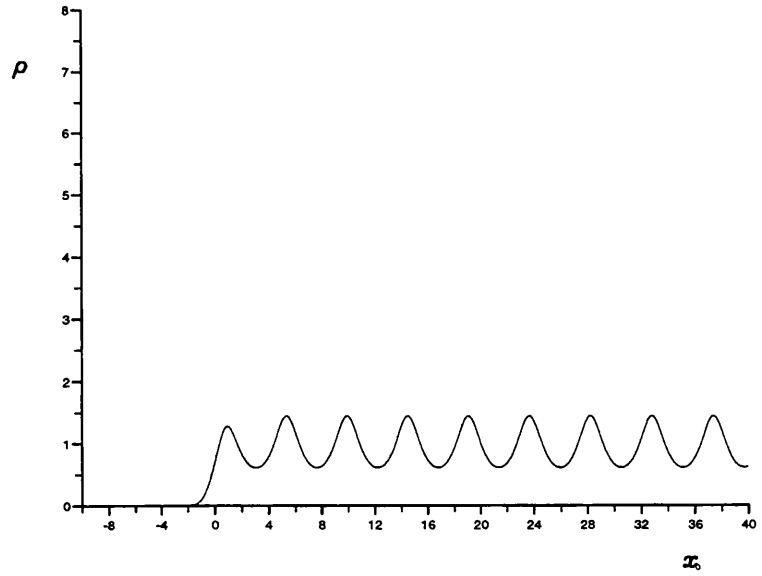

Figure 7.3: $AB > 0$, $\lambda B > 0$ and $\Gamma = 1$.

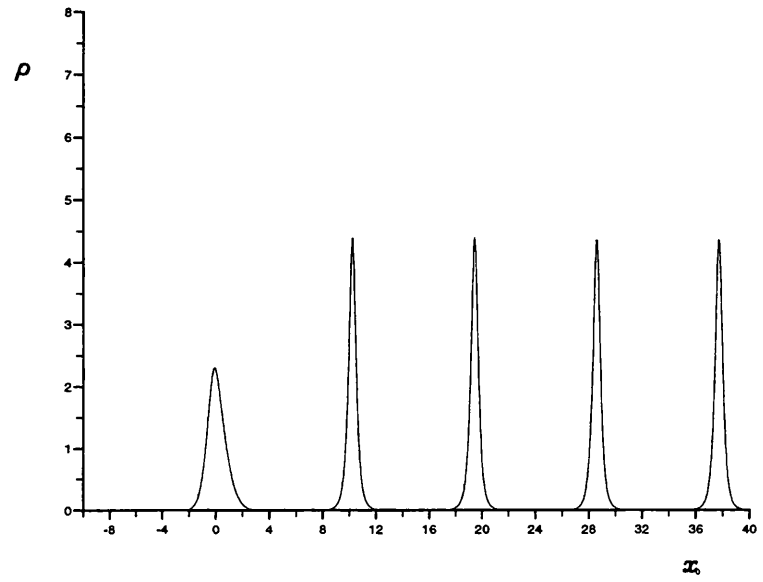

Figure 7.4: $AB > 0$, $\lambda B > 0$ and $\Gamma = 6$.

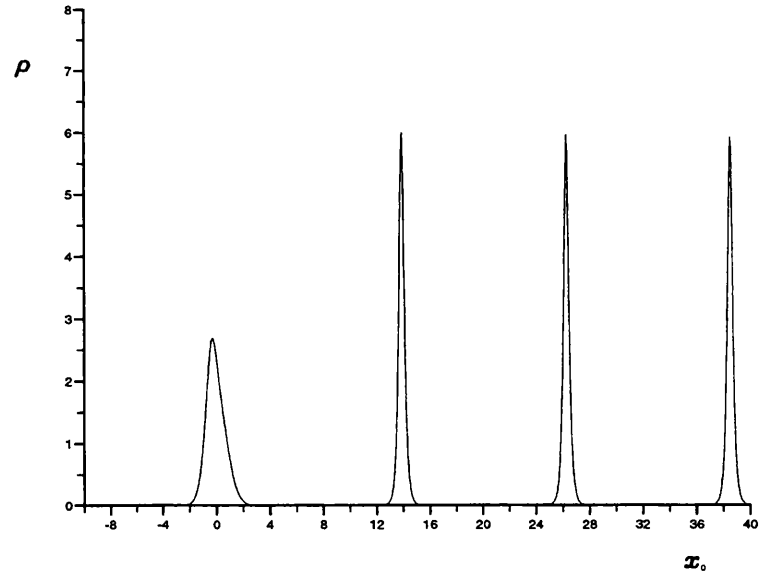

Figure 7.5: $AB > 0$, $\lambda B > 0$ and $\Gamma = 10$.

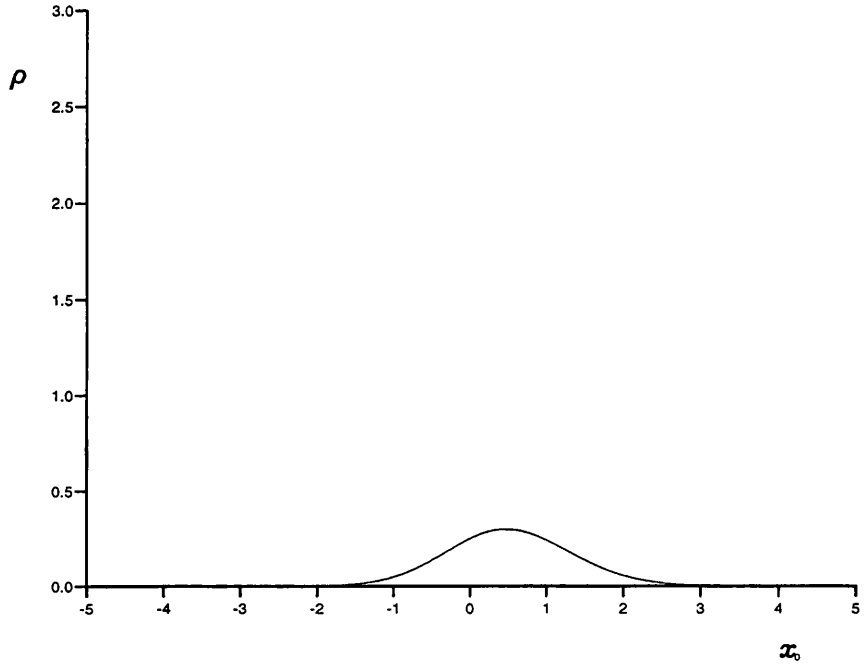

Figure 7.6: $AB < 0$, $\lambda B < 0$ and $\Gamma = 0.2$.

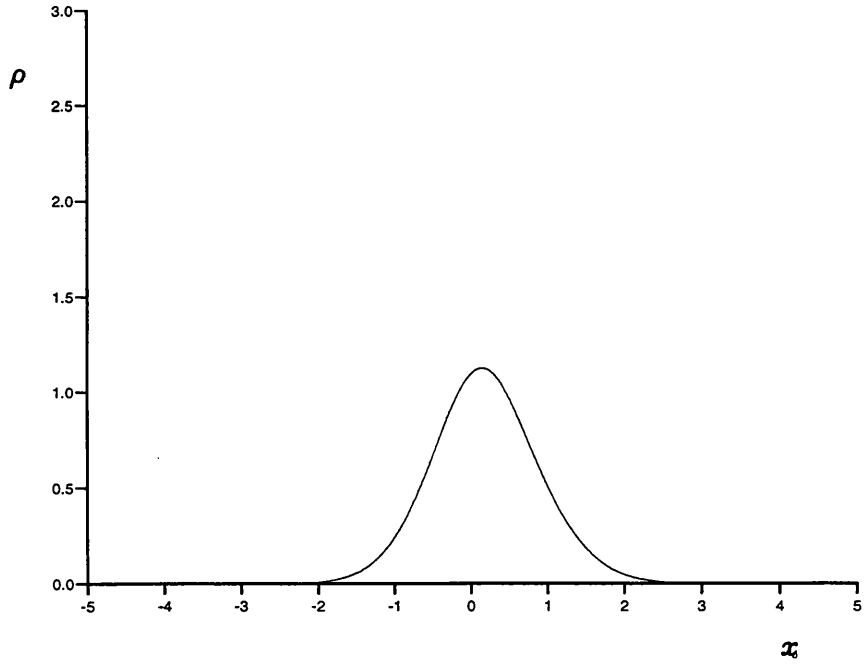

Figure 7.7: $AB < 0$, $\lambda B < 0$ and $\Gamma = 1$.

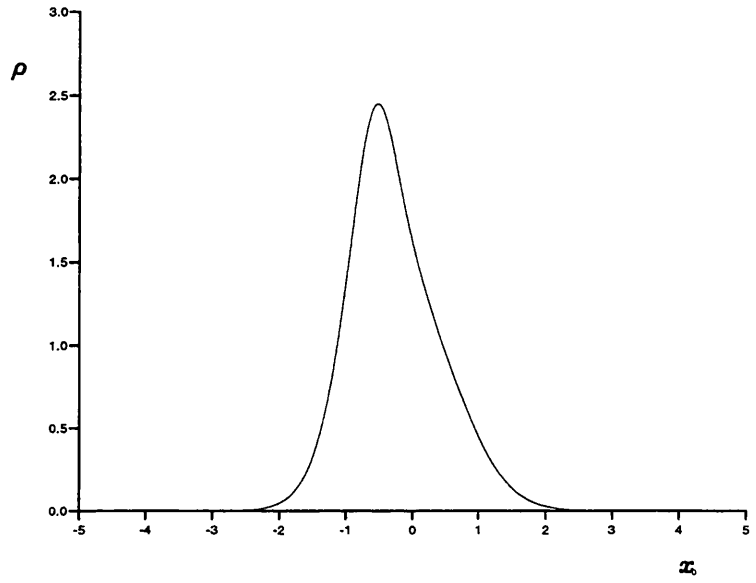

Figure 7.8: $AB < 0$, $\lambda B < 0$ and $\Gamma = 6$.

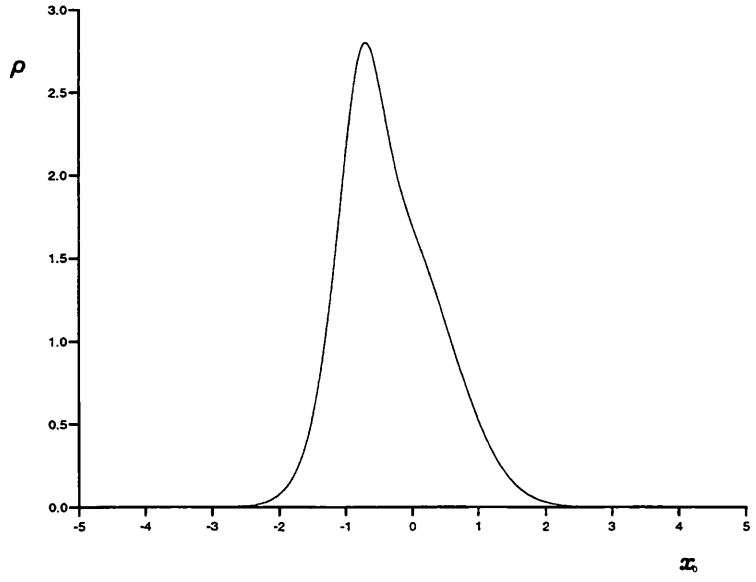

Figure 7.9: $AB < 0$, $\lambda B < 0$ and $\Gamma = 10$.

$AB < 0$, $\lambda B > 0$.

With the relative signs of the coefficients such that $AB < 0$ and $\lambda B > 0$ the non-forcing case produces solutions in which the wave-pressure disturbances shoot off to infinity as $x_0 \to \infty$. With forcing added of the form given in (7.5), Figures 7.10–7.12 show the results obtained for $\Gamma = 0.3, 1, 6$.

Once the forcing itself dies away no lasting effects are seen downstream and here too the wave-pressure disturbances shoot off to infinity. The strength of the forcing determines the distance downstream at which this shooting takes place, as Γ increases this distance decreases.

$AB > 0$, $\lambda B < 0$.

Finally, when $AB > 0$ and $\lambda B < 0$ the reverse situation to the above occurs. In the non-forcing case $\rho \to -\infty$ as $x_0 \to 0$. In physical terms the same thing takes place when forcing is added, again the strength of the force determining the distance downstream at which the shooting occurs; the larger Γ the shorter the distance.

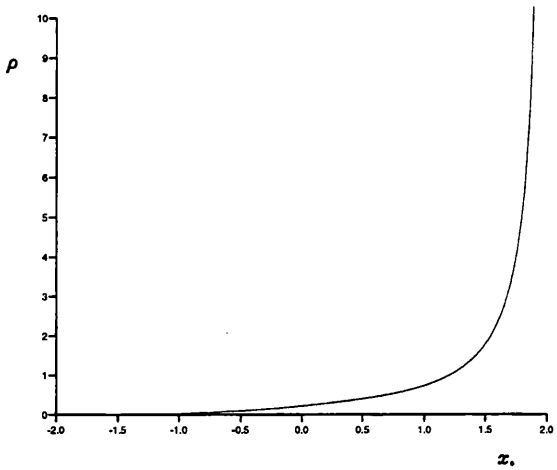

Figure 7.10: $AB < 0$, $\lambda B > 0$ and $\Gamma = 0.3$.

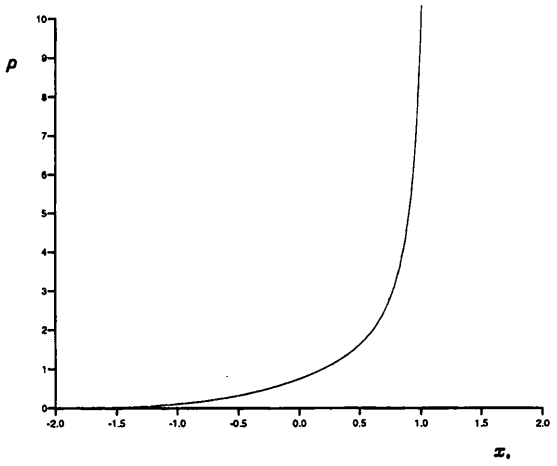

Figure 7.11: $AB < 0$, $\lambda B > 0$ and $\Gamma = 1$.

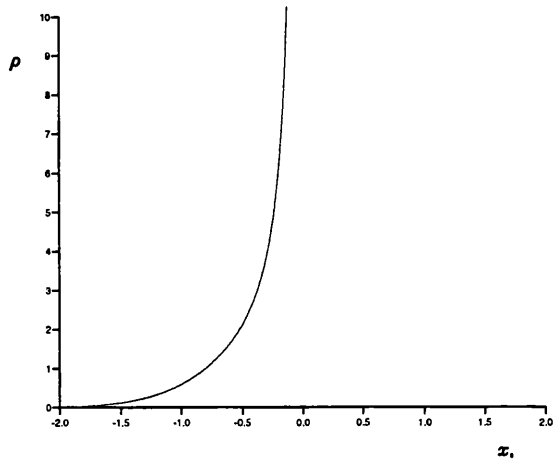

Figure 7.12: $AB < 0$, $\lambda B > 0$ and $\Gamma = 6$.

Strength Γ	Eqn. (7.6) a	Eqn. (7.9) b	% b:a
10	5.3901	3.0472	56.5
50	10.0103	8.9100	89.0
100	15.2532	14.1438	92.7
200	23.5684	22.4519	95.3
400	36.7130	35.6401	97.1
800	57.6994	56.5752	98.1
1000	66.7746	65.6497	98.3

Table 7.1: Comparison of values obtained for $\rho^2(0)$ calculated using (a) the full amplitude equation Eqn. (7.6), and (b) Eqn. (7.9), for various values of Γ.

To conclude this section, and indeed this chapter, we consider again the case in which periodic solutions result ($AB > 0$, $\lambda B > 0$). We note that by choosing Γ large the nonlinear integral-term in (7.6) dominates the lefthand side of the equation and we can approximate the amplitude equation by

$$\Gamma e^{-x_0^2} = \rho \int_{-\infty}^{x_0} \rho^2 \, ds, \tag{7.7}$$

A taking the value 1. If we then write $f(x_0) = \Gamma e^{-x_0^2}$, after some algebraic manipulation it can be shown that

$$\rho^2(x_0) = \left\{ 3 \int_{-\infty}^{x_0} f^2(s) ds \right\}^{-2/3} f^2(x_0) \tag{7.8}$$

and therefore

$$\rho^2(0) = \Gamma^2 \left\{ \frac{3}{2} \Gamma \sqrt{\frac{\pi}{2}} \right\}^{-2/3}. \tag{7.9}$$

Using the full amplitude equation (7.6) and (7.9) above we evaluate $\rho^2(0)$ for various values of $\Gamma \gg 1$ to verify that the appropriate asymptote has been chosen. The results obtained are compared in Table 7.1 above and show good agreement for $\Gamma > 100$.

Chapter 8

Summary

8.1 Conclusions

It is tempting to regard the linear and nonlinear studies of Chapters 2–3 and Chapters 5–7 respectively as two separate parts, the first concerning the downstream breakaway of separating boundary layers and the second concerning more local separation-type interactive flows. Chapter 4 however provides a link between the two, thus presenting this thesis more as one related study.

As stated in Chapter 1, the main novel contributions of this thesis are threefold. First, in Chapters 2–3, in which the behaviour of linear disturbances downstream of breakaway separation is investigated, the responses of neutral wavenumbers in the separating boundary layer are described as it detaches from the wall. A critical distance is found at which the linear properties change abruptly. Second, when considering nonlinear vortex/Rayleigh-wave interactions within an interactive triple-deck boundary layer flow, the inclusion of temporal effects at the onset of inflectional instability leads to the new initial-value problem there, described in Chapters 5–6. Finally, with the addition of forcing to the wave-pressure amplitude equation, nonlinear forced wave/vortex interaction solution properties are discussed in Chapter 7.

We note also that an analysis for small coefficients $b_n \ll 1$ could be performed, similar to that for $\alpha \ll 1$, which may produce a nonlinear link between the work of Chapters 2–3 for breakaway separating flows and that of Chapter 6.

As so often happens in the course of mathematical research, original aims become more directed as results obtained begin to highlight more interesting avenues of investigation. Such an occurrence led the work described in Chapter 6 towards the spatio-temporal interpretation of the integro-differential obtained therein, indicating the possibility of an initial-value problem for weakly nonlinear flows.

8.2 Acknowledgment

I would like to thank Professor F T Smith of University College London for his help and support throughout the course of my research studies. I wish to acknowledge EPSRC who supported this work.

Appendix A

Employing a similar approach to that of §6.2, our intention here is to obtain the wave solution in the outer tier of the core and match it with that obtained in the inner tier for the case of the initial-value problem set out in §6.7 under the new regime there.

In considering the initial-value formulation we must first replace the multipliers $i\alpha_0$, $i\beta_0$ and γ_0^2 with the operators ∂_X, ∂_{z_0} and $-(\partial_X^2 + \partial_{z_0}^2)$ respectively.

The governing equations for the wave-pressure solution p and the wave part of the normal velocity component v are

$$\frac{\partial^2 p}{\partial \tilde{y}^2} - \frac{2}{\tilde{y}}\frac{\partial p}{\partial \tilde{y}} + \frac{\partial^2 p}{\partial X^2} + \frac{\partial^2 p}{\partial z_0^2} = 0, \tag{A.1}$$

$$\frac{\partial^2 v}{\partial X^2} + \frac{\partial^2 v}{\partial \tilde{y}^2} + \frac{\partial^2 v}{\partial z_0^2} = 0. \tag{A.2}$$

If we suppose that

$$p \sim P_0 + \frac{1}{2}\left\{\frac{\partial^2 P_0}{\partial X^2} + \frac{\partial^2 P_0}{\partial z_0^2}\right\}\tilde{y}^2 + \frac{1}{3}K\tilde{y}^3 + \ldots,$$

$$v \sim \bar{V}_0 + \bar{V}_1\tilde{y} + \ldots$$

as $\tilde{y} \to 0^+$, then it follows that

$$\frac{\partial \bar{V}_0}{\partial X} = -\nabla^2 P_0, \qquad K = -\frac{\partial \bar{V}_1}{\partial X}, \tag{A.3}$$

where $\nabla^2 \equiv \partial_X^2 + \partial_{z_0}^2$.

The work of Smith *et al* (1977) shows that if

$$\nabla^2 d = 0, \tag{A.4}$$

$$(k^2 + l^2)^{1/2} D_0 = -D_1, \tag{A.5}$$

for some suitably bounded function $d(x, y)$ of the form $d(x, y) = D_0(x, z) + D_1(x, z)y$ at small y, then it follows that

$$D_0(x, z) = -\frac{1}{2\pi} \int_{-\infty}^{\infty} \int_{-\infty}^{\infty} \frac{D_1(\xi, \eta)\, d\xi d\eta}{[(x - \xi)^2 + (z - \eta)^2]^{1/2}}. \tag{A.6}$$

Fourier transforms ($X \rightarrow k$, $z_0 \rightarrow l$) are being assumed here. Re-writing (A.5) in the form

$$(k^2 + l^2) D_0 = -(k^2 + l^2)^{1/2} D_1,$$

i.e.

$$\nabla^2 D_0 = (k^2 + l^2)^{1/2} D_1,$$

we can invert the result (A.6) so that

$$D_1(x, z) = \frac{1}{2\pi} \int_{-\infty}^{\infty} \int_{-\infty}^{\infty} \frac{\nabla^2 D_0\, d\xi d\eta}{[(x - \xi)^2 + (z - \eta)^2]^{1/2}}. \tag{A.7}$$

By applying this result to the normal velocity component v we may deduce that

$$\bar{V}_1(X, z_0) = \frac{1}{2\pi} \int_{-\infty}^{\infty} \int_{-\infty}^{\infty} \frac{\nabla^2 \bar{V}_0\, d\xi d\eta}{[(X - \xi)^2 + (z_0 - \eta)^2]^{1/2}}.$$

On differentiating through with respect to X and substituting for $\bar{V}_0$ and $\bar{V}_1$ using (A.3), we obtain an equation for the function $K(X, z_0)$ in terms of P_0, namely

$$K(X, z_0) = \frac{1}{2\pi} \int_{-\infty}^{\infty} \int_{-\infty}^{\infty} \frac{\nabla^4 P_0\, d\xi d\eta}{[(X - \xi)^2 + (z_0 - \eta)^2]^{1/2}}. \tag{A.8}$$

Bibliography

[1] Acarlar M.S., Smith C.R. (1987) A study of hairpin vortices in a laminar boundary layer. Part 1: Hairpin vortices generated by a hemisphere protuberance. *J. Fluid Mech.* **175** 1–41.

[2] Acarlar M.S., Smith C.R. (1987) A study of hairpin vortices in a laminar boundary layer. Part 2: Hairpin vortices generated by fluid injection. *J. Fluid Mech.* **175** 43–83.

[3] Benney D.J., Chow C. (1989) A mean flow first harmonic theory for hydrodynamic instabilities. *Stud. Appl. Math.* **80** 37.

[4] Blasius H. (1908) The boundary layers in fluids with little friction. *Tech. Memor. Nat. Adv. Comm. Aero., Wash.* No. 1256.

[5] Brown P.G. (1993) *Ph. D. Thesis.* University College London.

[6] Brown P.G., Brown S.N., Smith F.T., Timoshin S.N. (1993) On the starting process of strongly nonlinear vortex/Rayleigh-wave interactions. *Mathematika* **40** 7–29.

[7] Brown S.N., Smith F.T. (1995) On vortex/wave interactions. Part I: Non-symmetrical input and cross-flow in boundary layers. *J. Fluid Mech.* - to appear.

[8] Brown S.N., Stewartson K. (1969) Laminar Separation. *Ann. Rev. Fluid Mech.* **1** 45–72.

[9] Drazin P.G., Howard L.N. (1962) The instability to long waves of unbounded parallel inviscid flow. *J. Fluid Mech.* **14** 257–283.

[10] Drazin P.G., Reid W.H. (1981) Hydrodynamic Stability. *Cambridge University Press.*

[11] Dovgal A.V., Kozlov V.V., Simonov O.A. (1986) Boundary-Layer Separation. *IUTAM Symposium* London (1986). 109–130.

[12] Goldstein M.E., Choi S.W. (1989) Nonlinear evolution of interacting oblique waves on two-dimensional shear layers. *J. Fluid Mech.* **207** 97-120. (corrigendum (1990) **216** 659–663)

[13] Goldstein S. (1930) Concerning some solutions of the boundary layer equations in hydrodynamics. *Proc. Camb. Phil. Soc.* **26** 1–30.

[14] Goldstein S. (1948) On laminar boundary layer flow near a point of separation. *Q. J. Mech. Appl. Math.* **1** 43–69.

[15] Hall P., Smith F.T. (1982) A suggested mechanism for nonlinear wall roughness effects on high Reynolds number flow stability. *Stud. Appl. Math.* **66** 241.

[16] Hall P., Smith F.T. (1988) The nonlinear interaction of Tollmien-Schlichting waves and Taylor-Görtler vortices in curved channel flows. *Proc. R. Soc. London A* **417** 252–282.

[17] Hall P., Smith F.T. (1989) Nonlinear Tollmien-Schlichting wave/vortex interaction in boundary layers. *Eur. J. Mech., B/Fluids* **8** 179–205.

[18] Hall P., Smith F.T. (1990) Theory on instability and transition. *ICASE Workshop on Instability and Transition Vol. II.* (ed. Husaini M. Y., Voigt R.G.) 5–39. Springer.

[19] Hall P., Smith F.T. (1991) On the strongly nonlinear vortex/wave interactions in boundary-layer transition. *J. Fluid Mech.* **227** 641–666.

[20] Khokhlov A.P. (1994) The theory of resonance interaction of Tollmien-Schlichting waves. *J. Appl. and Tech. Physics* **34** 508–515.

[21] Klebanoff P.S., Tidstrom K.D. (1959) The evolution of amplified waves leading to transition in a boundary layer with zero pressure gradient. *NASA Tech.* Note D - 195.

[22] Mason P.J., Morton B.R. (1987) Trailing vortices in the wakes of surface-mounted obstacles. *J. Fluid Mech.* **175** 247–293.

[23] Messiter A.F. (1970) Boundary layer flow near the trailing edge of a flat plate. *SIAM J. Appl. Math.* **18** 241–257.

[24] Neiland V. Ya. (1969) Towards a theory of separation of the laminar boundary layer in a supersonic stream. Transl. in *Fluid Dyn.* **4** 33–35.

[25] Nishioka M., Asai M., Iida S. (1979) An experimental investigation of the secondary instability. *Laminar-turbulent transition.* Springer.

[26] Papageorgiou D.T., Smith F.T. (1989) Linear instability of the wake behind a flat plate placed parallel to a uniform stream. *J. Fluid Mech.* **208** 67–89.

[27] Prandtl L. (1904) *Verhanglungen des III Internationalen Mathematika-Kongresses.* Heidelberg (1904). 484–491. Leipzig.

[28] Rayleigh Lord (1880) On the stability, or instability, of certain fluid motions. *Proc. Lond. Math. Soc.* **11** 57–70.
(see also: Scientific Papers (1899). *Cambridge University Press* **I** 474–487.)

[29] Reynolds O. (1883) An experimental investigation of the circumstances which determine whether the motion of water shall be direct or sinuous, and of the law of resistance in parallel channels. *Phil. Trans. R. Soc. Lond.* **174** 935–982.
(see also: Scientific Papers (1901). *Cambridge University Press* **II** 51-105.)

[30] Schubauer G.B., Skramstad H.K. (1947) Laminar boundary layer oscillations and transition on a flat plate. *J. Res. Nat. Bur. Stand.* **38** 251–292. (see also; *Rep. Nat. Adv. Comm. Aero., Wash.* No. 909.)

[31] Smith F.T. (1979a) On the nonparallel flow stability of the Blasius boundary layer. *Proc. Roy. Soc. London A* **366** 91–109.

[32] Smith F.T. (1979b) Nonlinear stability of boundary layers for disturbances of various sizes. *Proc. Roy. Soc. London A* **368** 573–589.

[33] Smith F.T. (1982) On the high Reynolds number theory of laminar flows. *IMA J. Appl. Math.* **28** 207–281.

[34] Smith F.T. (1986a) Steady and unsteady boundary-layer separation. *Ann. Rev. Fluid Mech.* **18** 197–220.

[35] Smith F.T. (1986b) Two-dimensional disturbance travel, growth and spreading in boundary layers. *J. Fluid Mech.* **169** 353–377.

[36] Smith F.T. (1987) Breakup in unsteady separation. *Trans. of the ASME Conf. on unsteady separation.* Cincinnati, OH.

[37] Smith F.T. (1988) Finite-time breakup can occur in any unsteady interacting boundary layer. *Mathematika* **35** 256–273.

[38] Smith F.T. (1993) Theoretical aspects of transition and turbulence in boundary layers. *AIAA Journal* **31** No.2 December 1993.

[39] Smith F.T. (1995) On spikes and spots: strongly nonlinear theory and experimental comparisons. *Phil. Trans. R. Soc. Lond. A* **352** 405–424.

[40] Smith F.T., Bodonyi R.J. (1985) On short-scale inviscid instabilities in flow past surface-mounted obstacles and other non-parallel motions. *Aero. Jnl.* June/July 205–212.

[41] Smith F.T., Bowles R.I. (1992) Transition theory and experimental comparisons on (I) amplification into streets and (II) a strongly nonlinear breakup criterion. *Proc. R. Soc. Lond. A* **439** 163–175.

[42] Smith F.T., Brown S.N., Brown P.G. (1993) Initiation of three-dimensional nonlinear transition paths from an inflectional profile. *Eur. J. Mech., B/Fluids* **12** 447–473.

[43] Smith F.T., Sykes R.I., Brighton P.W. (1977) A two-dimensional boundary layer encountering a three-dimensional hump. *J. Fluid Mech.* **83** 163–176.

[44] Stewart P.A., Smith F.T. (1992) Three-dimensional nonlinear blow-up from a nearly planar initial disturbance in boundary layer transition: theory and experimental comparisons. *J. Fluid Mech.* **244** 79–100.

[45] Stewartson K. (1970) Is the singularity at separation removable? *J. Fluid Mech.* **44** 347–364.

[46] Stewartson K., Stuart J.T. (1971) A nonlinear instability theory for a wave system in plane Poiseuille flow. *J. Fluid Mech.* **48** 529–545.

[47] Stewartson K., Williams P.G. (1969) Self-induced separation. *Proc. R. Soc. Lond. A* **312** 181–206.

[48] Stuart J.T. (1963) Laminar Boundary Layers. (ed. Rosenhead L.) Chpt. 9. *Oxford University Press.*

[49] Stuart J.T., Watson A.G. (1960) On the non-linear mechanics of wave disturbances in stable and unstable parallel flows. Part 1: The basic behaviour in plane Poiseuille flow. *J. Fluid Mech.* **Vol. 9 Part 3** 353–370.

[50] Stuart J.T., Watson A.G. (1960) On the non-linear mechanics of wave disturbances in stable and unstable parallel flows. Part 2: The development of a solution for plane Poiseuille flow and for plane Couette flow. *J. Fluid Mech.* **Vol. 9 Part 3** 371–389.

[51] Timoshin S.N., Smith F.T. (1995). *J. Fluid Mech.* - submitted.

[52] Tollmien W. (1935) General stability criterion of laminar velocity disturbances. (translated from the German original) *Tech. Memor. Nat. Adv. Comm. Aero., Wash.* No. 792.

[53] Tutty O.R., Cowley S.J. (1986) On the stability and numerical solution of the unsteady interactive boundary-layer equation. *J. Fluid Mech.* **168** 431-456.

[54] Van Dyke M. (1982) An album of fluid motion. *Parabolic* Stanford, California.

[55] Vickers I.P., Smith F.T. (1994) Theory and computations for breakup of unsteady subsonic and supersonic separating flows. *J. Fluid Mech.* **268** 147–173.

[56] Walton A.G., Smith F.T. (1992) Properties of strongly nonlinear vortex/Tollmien-Schlichting waves interactions. *J. Fluid Mech.* **244** 649–676.

[57] Wu X. (1993) On critical-layer and diffusion-layer nonlinearity in the three-dimensional stage of boundary-layer transition. *Proc. R. Soc. London A* **443** 95–106.

[58] Wu X., Lee S.S., Cowley S.J. (1993) On the weakly nonlinear three-dimensional instability of shear layers to pairs of oblique waves: the Stokes layer as a paradigm. *J. Fluid Mech.* **253** 681–721.